# DISSECTING THE ROLE OF QSEC IN MEDIATING QSEBC-PMRAB SIGNALING IN UROPATHOGENIC *ESCHERICHIA COLI*

By

Erin Jenness Breland

Dissertation

Submitted to the Faculty of the

Graduate School of Vanderbilt University

in partial fulfillment of the requirements

for the degree of

DOCTOR OF PHILOSOPHY

in

Pharmacology

August 11, 2017

Nashville, Tennessee

Approved:

Tina M. Iverson, Ph.D. - Chair

Terry P. Lybrand, Ph.D.

Eric P. Skaar, Ph.D., MPH

Benjamin W. Spiller, Ph.D.

Maria Hadjifrangiskou, Ph.D.

I dedicate this work to my biological and laboratory families. My grandmother Brenda: without her I would not be in the position I am today. My parents: Reed and Cynthia Breland, who required of me good grades and encouraged me to reach for the stars. My siblings: Shelby and Nick, who taught and continue to teach me to be myself. Finally, I dedicate this work to Dr. RoxAnn Karkhoff-Schweizer: it was my training at Colorado State that led me to microbiology, and it was Dr. RoxAnn who helped me fall in love with it.

ACKNOWLEDGEMENTS

There are many people, family, friends, and acquaintances I would like to thank for making all of this work possible. I would like to start by acknowledging the time and effort my mentor, Dr. Maria Hadjifrangiskou, poured into me over the last five years. I appreciate her dedication to UPEC and her fearless search for the truth. I would like to acknowledge the people who tolerated my dance moves and helped me navigate through graduate school. My lab siblings: Dr. Carrie Shaffer, my soul diamond and dancing partner; Dr. Kyle Floyd, the master baker and late night therapist; Dr. Kirsten Guckes, my sounding board and partner in QseBC crime; Head Coach Allison Eberly, the organized enforcer who needs to know, "This work was done to show her that she could do it too!"; Ellisa Zhang, our magical unicorn, without whom I would be eternally lost. Bradley "Lee" Steiner, the intellectual who constantly had me reevaluating my hypotheses; Dr. John Brannon who was always at the ready with a "bad dad joke"; and Melanie Hurst who braved the crazy and is keeping the legacy alive. The mighty Hadjis have survived infancy, best of luck during the preteen years!

I would like to thank my family, Reed, Cynthia, Shelby, and Nick, for supporting me and visiting me when I could not make it home. I recognize now that I did not call home often enough, but I will forever be grateful for the love and support that you constantly provided me throughout this entire process.

I would like to acknowledge both of the departments that I called home, the Departments of Pharmacology and Pathology, Microbiology and Immunology. I had an atypical graduate experience in that I was an active member in two diverse departments. None of this work would have been possible without funding from the T-32 Pharmacology Training Grant, the NSF Graduate Research Fellowship Program, and funds awarded to Dr. Hadjifrangiskou from

Vanderbilt and the NIH. I owe my success especially to Dr. Joey Barnett, Karen Gieg, Helen Chomicki, and Pradeep Srivastava. To my friends and peers in both departments, I cannot thank you enough for helping me both emotionally and scientifically. I would like to thank my committee for constantly challenging me to be better. Thank you Drs. Tina Iverson, Terry Lybrand, Eric Skaar, and Ben Spiller for helping me navigate the alphabet soup and driving the project ever forward.

Graduate school is not possible without friends to laugh and cry with you. I would like to thank the friends I made in IGP for supporting me, listening to me, and challenging me.

Most recently and importantly, I would like to thank my fiancé, Chris. Thank you for the comedic, emotional, and mental relief. Thank you for always believing in me and "forcing" me to live my dreams.

TABLE OF CONTENTS

Page

LIST OF TABLES

LIST OF FIGURES

# LIST OF ABBREVIATIONS

| | |
|---|---|
| ~P | phosphorylated |
| A | alanine |
| Amp | ampicillin |
| ANOVA | analysis of variance |
| APEC | avian pathogenic *Escherichia coli* |
| ASB | asymptomatic bacteriuria |
| ATP | adenosine triphosphate |
| B. | *Bacillus* |
| bp | base pairs |
| °C | degrees Celsius |
| cAMP | adenosine 3′,5′ monophosphate |
| CA-UTI | catheter-associated urinary tract infection |
| cDNA | complimentary deoxyribonucleic acid |
| CFU | colony forming units |
| CNF | cytotoxic necrotizing factor |
| c.p.m. | counts per minute |
| CRE | carbapenem-resistance Enterobacteriacea |
| $C_T$ | threshold cycle |
| $Cu^{2+}$ | copper |
| D | aspartic acid |
| DAEC | diffusely adherent *Escherichia coli* |
| DHp | histidine phosphotransfer domain |
| DNA | deoxyribonucleic acid |
| DMSO | dimethyl sulfoxide |
| DQC | dequalinium chloride |
| DTT | dithiothreitol |
| E | glutamic acid |
| E. | *Escherichia* |
| EAEC | enteroaggregative *Escherichia coli* |
| EHEC | enterohemorrhagic *Escherichia coli* |
| EIEC | enteroinvasive *Escherichia coli* |
| *EMSA* | electrophoretic mobility shift assay |
| EPEC | enteropathogenic *Escherichia coli* |
| ESCMID | European Society for Microbiology and Infectious Diseases |
| ETEC | enterotoxigenic *Escherichia coli* |
| ExPEC | extraintestinal pathogenic *Escherichia coli* |
| et al. | and others |

| | |
|---|---|
| $Fe^{3+}$ | ferric iron |
| fmol | femtomole |
| FRT | Flp Recombinase Target |
| FUTI | foodborne urinary tract infection |
| | |
| G | glycine |
| gfp | green fluorescent protein |
| h | hour(s) |
| H | histidine |
| HK | histidine kinase |
| HPK | histidine protein kinase |
| | |
| IBC | intracellular bacterial communities |
| IDSA | Infectious Diseases Society of America |
| IL | interleukin |
| IPTG | isopropyl-1-thio-β-D-galactopyranoside |
| | |
| K | lysine |
| KCl | potassium chloride |
| | |
| L | leucine |
| LB | Lysogeny Broth |
| LPS | lipopolysaccharide |
| | |
| MAEC | meningitis associated *Escherichia coli* |
| MFS | major facilitator superfamily |
| mg | milligram |
| MGB | minor groove binder |
| $MgCl_2$ | magnesium chloride |
| µg | microgram |
| MIC | minimum inhibitory concentration |
| mL | milliliter |
| µL | microliter |
| mM | millimolar |
| µm | micrometer |
| | |
| NMEC | neonatal meningitis causing *Escherichia coli* |
| | |
| OCS | one-component system |
| OD | optical density |
| | |
| P | proline |
| PCR | polymerase chain reaction |
| pH | potential hydrogen |
| PMB | polymyxin B |

| | |
|---|---|
| pmol | picomole |
| PmrAB | polymyxin resistant system AB |
| ppGpp | guanosine-3,5-bis(pyrophosphate) |
| p.s.i. | pounds per square inch |
| | |
| Q | glutamine |
| QIR | quiescent intracellular reservoir |
| qRT-PCR | quantitative reverse transcriptase/real time polymerase chain reaction |
| QseBC | quorum sensing Escherichia coli system BC |
| | |
| R | arginine |
| RNA | ribonucleic acid |
| RNA-seq | ribonucleic acid sequencing |
| RR | response regulator |
| rUTI | recurrent urinary tract infection |
| | |
| s | seconds |
| S | serine |
| S. | *Salmonella* |
| SDS | sodium dodecyl sulfate |
| SDS-PAGE | sodium dodecyl sulfate polyacrylamide gel electrophoresis |
| SEM | standard error of the mean |
| ST | sequence type |
| | |
| TCS | two-component system |
| Tris-HCl | tris hydrochloric acid |
| | |
| UPEC | uropathogenic *Escherichia coli* |
| UTI(s) | Urinary Tract Infection(s) |
| | |
| V | valine |
| VUTI | Vanderbilt urinary tract isolate |
| | |
| WT | wild-type |
| | |
| $Zn^{2+}$ | Zinc |

# DISSERTATION HYPOTHESIS, AIMS, AND PREVIEW OF CHAPTERS

The overarching goal of this research is to Identify signals and mechanisms of regulation to "break" the virulence cascade and attenuate uropathogenic *Escherichia coli* (UPEC) infections in *vivo.* This dissertation aims to address the following questions: What is the mechanism of regulation between two, non-cognate two-component systems (TCSs)? What are the signals and what are the responses that activate the TCSs PmrAB and QseBC? How can we take advantage of this system to decrease virulence and/or attenuate infection?

## *Hypothesis*

Non-cognate partner signaling is necessary for signal integration and response expansion in uropathogenic *Escherichia coli* and that the sensor kinase QseC is physically required to control these interactions; either by physically sequestering QseB or by controlling the PmrB sensor on the protein level.

## *Aims*

In this thesis, we look at the interactions of PmrAB and QseBC in the *E. coli* strain UTI89 (1). to address the following aims: **Aim 1. Identify molecular level determinants of QseB specificity and regulation:** Cognate partner specificity is, in part, dictated by a co-evolving, sensor/responder interacting surface. PmrB activates its cognate partner PmrA and non-cognate partner QseB similarly, but is unable to de-phosphorylate QseB in a physiologically relevant timeframe. This indicates that molecular determinants allowing for QseC-mediated bi-directional regulation of QseB are absent in PmrB. Herein, I describe how we: **A.1.a. Determined the role**

**of co-evolving residues in regulating QseB activation** by swapping the co-evolving residues of PmrB and QseC and evaluating the interactions of the resulting variants with QseB using *in vitro* phosphotransfer approaches. PmrB and QseC harboring alanines or the co-evolving residues of an unrelated sensor kinase will be tested as controls. **A.1.b. Dissected the role of known, critical, QseC residues**. Three independently isolated QseC variants, with mutations changing the conserved phospho-accepting histidine 246, complemented the *qseC* deletion mutant *in vivo*, despite loosing their phospho-activity. I will**:** (i) test how K205E and H246A/D/L QseC variants regulate QseB activity in the presence and absence of $Fe^{3+}$, using qPCR and Phos-tag gels, and (ii) probe *in vivo* variant interactions with other proteins by cross-linking/co-immunoprecipitation experiments. (iii) Parallel studies will assess the expression of *flhDC*, which is a target of QseB to evaluate how each QseC variant influences target gene expression. *In silico* sequencing revealed additional clade specific residues that may alter PmrAB-QseBC signaling. Future studies will elucidate residues that dictate specificity and identify cross-interaction specific regulation.

**Aim 2. Delineate the mechanism of signal-mediated responses within and between QseBC and PmrAB:** Studies in **e**ntero**h**emorrhagic ***E. coli*** (**EHEC**) identified epinephrine, norepinephrine, and bacterial autoinducer-3 as signals that activate QseC. However, these putative ligands do not elicit a QseC mediated response in UPEC under several conditions tested. Thus, the UPEC QseC ligand remains unknown. To further probe the difference in QseC response and identify ligands and growth conditions that activate UPEC QseC we: **A.2.a. Identified a role of QseB in biofilm formation on solid agar.** Future studies will elucidate niche and environmental specific stimuli that alters QseBC-PmrAB regulation of colony biofilm morphology. **A.2.b. Dissected the integrative outputs of QseBC and PmrAB in response to multiple input signals**. I tested the effects of identified QseC and PmrB signals ($Fe^{3+}$ and $Zn^{2+}$)

Future studies will focus on identifying signals that directly activate QseBC. Combined, we show here the importance of cross interaction between two two-component systems that regulate virulence and transient resistance to polymyxin B. We will continue to identify ways to test and target the mechanism of regulation within the four-component system to attenuate UPEC as an alternative therapeutic to antibiotics.

*Preview of the Chapters*

Chapter I provides a background on *Escherichia coli*, focuses on pathogenic *E. coli* with an emphasis on extraintestinal pathogenic *E. coli*. Chapter II introduces two-component signal transduction systems and describes a four-component interaction between the two-component systems PmrAB and QseBC. Chapter III discusses the interaction of PmrAB and QseBC with respect to ferric iron and polymyxin B resistance. Chapter IV discusses the role of the conserved histidine in UPEC QseC with respect to regulating the four-component system. Chapter V introduces the role of co-evolving residues in mediating interactions between cognate and non-cognate proteins in our four-component system. Chapter VI outlines potential future directions for this work.

# CHAPTER I

## INTRODUCTION TO THE DIVERSITY OF *ESCHERICHIA COLI* AND RELATED INFECTIONS WITH AN EMPHASIS ON EXTRAINESTINAL INFECTIONS

Portions of this introduction have been adapted from Breland *et al.* "An overview of two-component signal transduction systems implicated in extra-intestinal pathogenic *E. coli* infections". Review in *Frontiers in Cellular and Infection Microbiology. (2017).* PMID: 28536675

*Escherichia coli,* discovered in 1885 by Theodor Escherich, is perhaps one of the most well characterized, genetically tractable organisms. The species belongs to the Gammaproteobacteria class and the *Enterobacteriaceae* family and was named *E. coli* for its location in the colon. *E. coli* colonize the gastrointestinal (GI) tracts of humans, other warm-blooded mammals, and birds and in this context, they comprise part of the organism's normal flora (2, 3), or microbiome. To date, over 3,600 *E. coli* genomes have been sequenced in part or in full, revealing seven major phylogenetic groups—A, B1, B2, C, D, E, and F—with the remaining unclassified subtypes placed in an eighth group, *Escherichia* cryptic clade I (4, 5). The acquisition of genetic elements, primarily through horizontal gene transfer, gives rise to the several different clades including pathogenic *E. coli* with distinct virulence strategies. Figure one shows the phylogeny of 49 sequenced *E. coli* strains in the 5 major clades in which they cluster (**Fig. 1**). Pathogenic *E. coli* involved in food intoxication and infection separated from a K-12 ancestor more than 4.5 million years ago (6). Gastrointestinal or diarrheagenic *E. coli* pathotypes include diffusely adherent (DAEC), enteroaggregative (EAEC), enterohemorrhagic (EHEC),

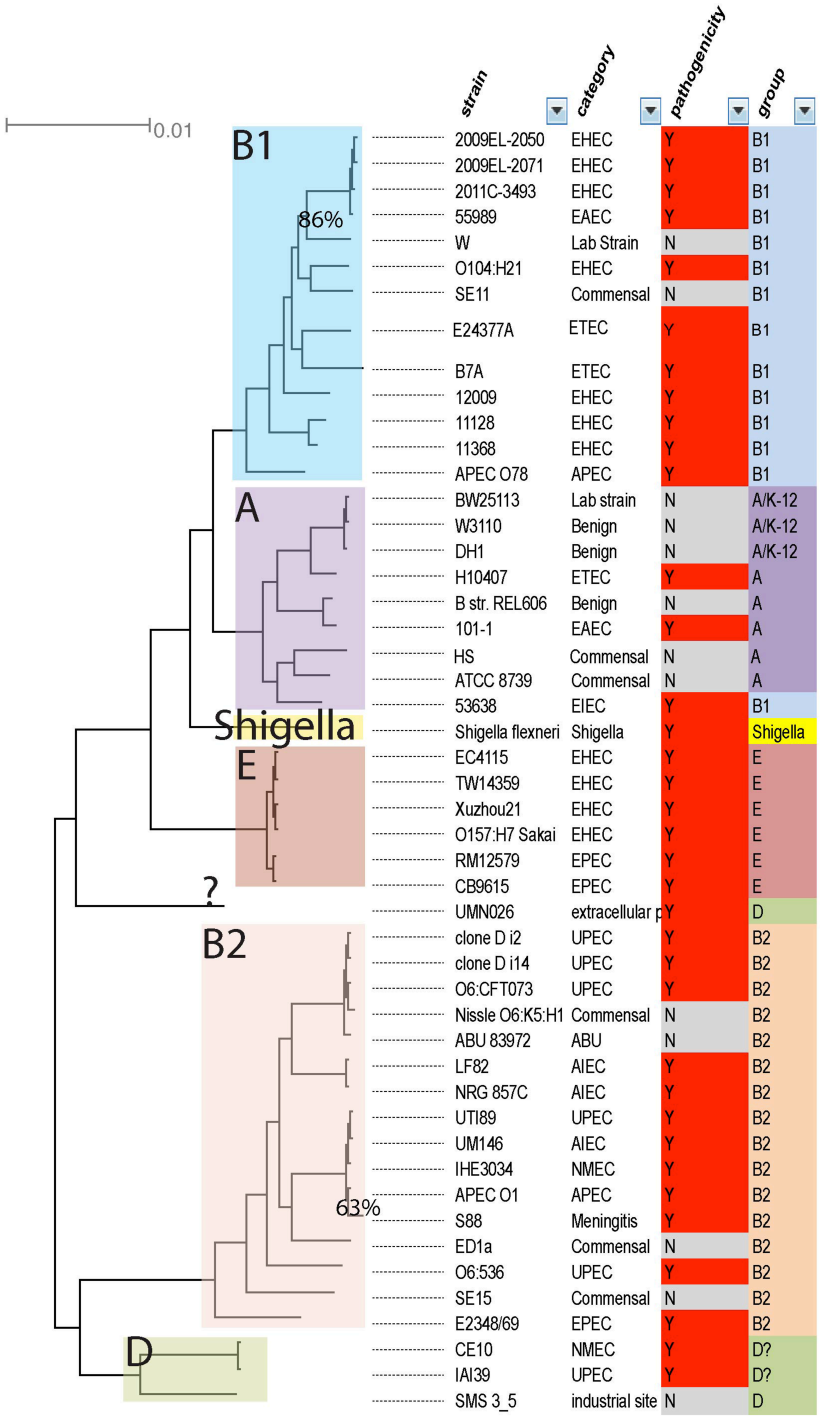


**Figure 1: Phylogenetic tree of 49 *E. coli* strains.** Figure depicts a phylogenetic tree of *E. coli* strains by clade. The phylogeny was based on alignments of 2679 single-copy core orthogroups, constructed using Fasttree with the mid-point rooted. Bootstrap values for all nodes were >90%, except for the nodes with values indicated on the tree. This figure was provided by Ashlee Earl and Abigail Manson from the Broad Institute of MIT and Harvard.

enteroinvasive (EIEC), enteropathogenic (EPEC), and enterotoxigenic (ETEC), which primarily cluster in clade E and B1. However, extra-intestinal pathogenic *E. coli* (ExPEC) pathotypes, which emerged 32 million generations ago (7, 8), primarily include avian pathogenic *E. coli* (APEC), neonatal meningitis causing or meningitis-associated *E. coli* (NMEC/MAEC), and uropathogenic *E. coli* (UPEC), and cluster in clades B2 and D.

### 1.1 ExPEC and related diseases

The human ExPEC strains predominantly cluster in the B2 and D phylogenetic groups and typically infect the nervous system and urinary tract; while APEC strains have also expanded into C and F groups and primarily infect the avian respiratory system (**Fig. 2,** (9-12). Infections by emerging avian pathogenic *E. coli* (APEC) strains (13) cause high morbidity and mortality in flocks of birds and account for considerable economic losses in the poultry industry (14). Interestingly, recent studies show that human consumption of infected poultry meat or eggs can result in food-borne extra-intestinal diseases in humans (15), which adds an additional concern for the poultry industry regarding food safety. APEC are the etiologic agent associated with colibacillosis, however severity of disease increases with co-morbid viral infections, such as Newcastle virus and avian infectious bronchitis virus, as well as with bacterial infections by *Mycoplasma gallisepticum* (16). Disease manifestations include colibacillosis, an infection that includes acute fatal septicemia or colisepticemia, sub-acute pericarditis, airsacculitis, salpingitis, and peritonitis (14). Current treatment relies on the use of antibiotics, as well as some commercially available heat-killed vaccines (16).

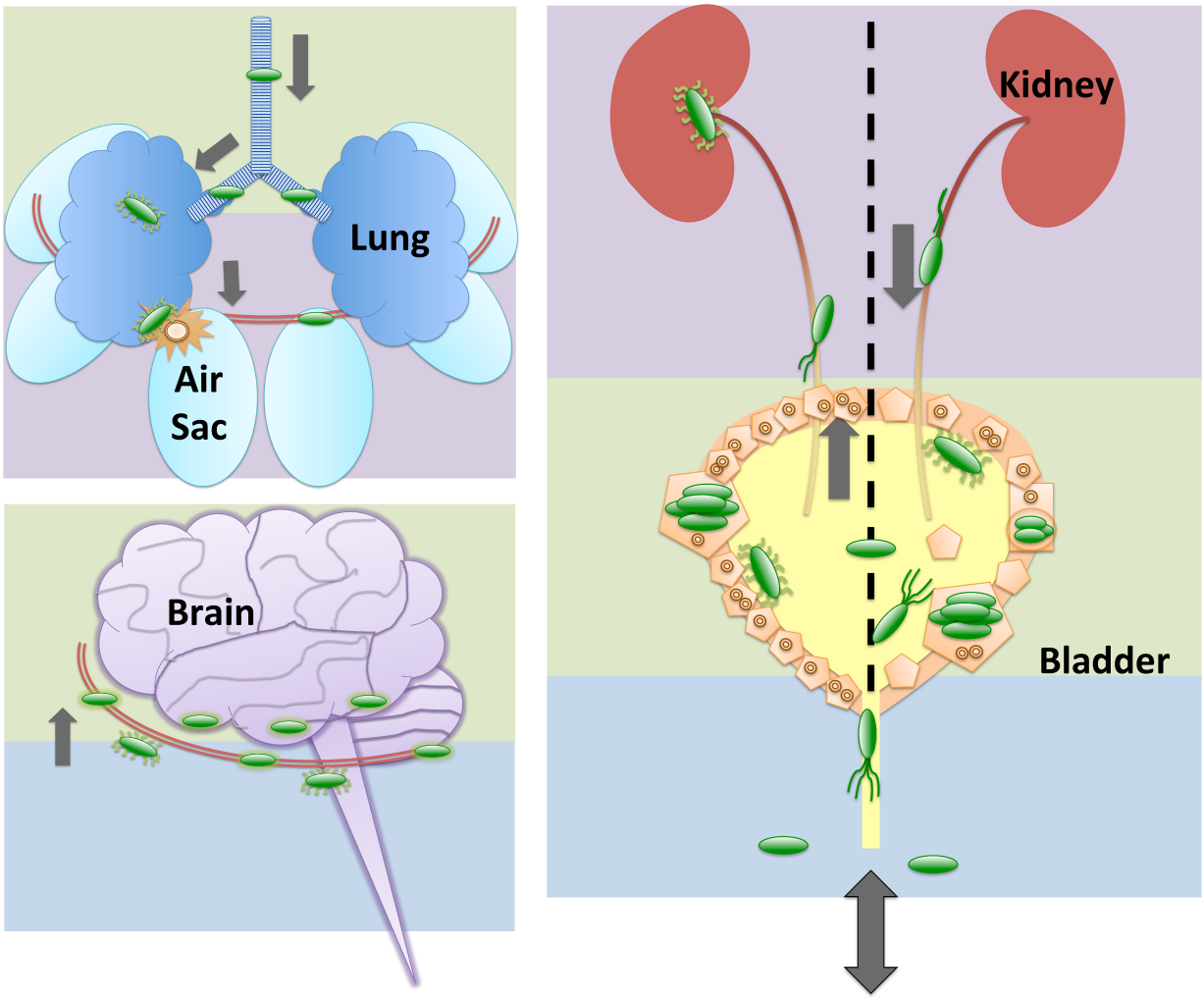


**Figure 2: Schematic of typical ExPEC pathogeneses.** Schematics depict a generalized view of the route of infection for APEC (top left) infecting an avian respiratory tract, MAEC/NMEC (bottom left) infecting the human meninges, and UPEC (right) infecting a human urinary tract. In the different panels, the infection progresses from green to purple (top left), blue to green (bottom left), and blue to green to purple (right).

Cats and dogs are susceptible to urinary tract infections (UTIs) and recurrent UTIs (rUTIs) (17, 18). In dogs, ExPEC strains are most commonly associated with uncomplicated UTIs, but have also been the cause of pyometra, mastitis, otitis, prostatitis, bacteremia, skin diseases, cholecystitis, and pneumonia (19, 20). Interestingly, while cats experience idiopathic lower UTI symptoms, no known association with UPEC or UPEC-like strains has been established to date (21). However, bronchopneumonia caused by *E. coli* harboring α-hemolysin and cytotoxic necrotizing factor (CNF) has been reported in cats and dogs (22, 23). Finally, recent reports have documented UTIs in big cats such as snow- and black-leopards, indicating that animals in captivity (such as zoo animals), and potentially in the wild, are susceptible to infections by ExPEC (24).

Studies have shown that calves and cows are both likely to develop UTIs, and *E. coli* is the most predominant etiologic agent (25). UTI symptoms in cattle include depression, muscle wasting and weakness, reduced feed intake, reduced milk production, and weight loss (25), all of which impact the dairy and meat industries. Additionally, cows are frequently catheterized to collect total urine for nutritional analyses. This repetitive catheterization results in increased risk for ascending UTIs (26). In addition to UTIs, another costly disease in cows is clinical mastitis (27). Clinical mastitis is an inflammation of the udders due to blockage or infection that results in visually abnormal milk production (28). The mammary pathogenic *E. coli* or MPEC are the predominant bacteria in clinical mastitis (29).

Horses have been reported to have both hemorrhagic pneumonia and soft tissue ExPEC infections (20, 30). Clinical symptoms of infection include animals lying on their side, abdominal breathing, shaking, convulsion, lameness, and death (31). Recently, Liu *et al*. (31) performed the first genomic analyses of a porcine-specific ExPEC, PCN033, isolated from the brain of a pig

(suggesting a meningitis-causing isolate; (32)). The genomic data placed PCN033 in the D phylogeny group and studies using an ear vein piglet (4–5 weeks) infection model demonstrated the pathogenic potential of this strain (31).

The steady, yet up until recently under-appreciated, rise in antimicrobial resistant *E. coli* in farming practices has played a significant role in the increasing incidence and lethality of extra-intestinal *E. coli* infections (33). Zoonotic transmission of ExPEC from animals to humans through the consumption of infected animal products is a newly identified route of transmission (34). One such example is the zoonotic potential of foodborne UTIs (FUTIs) in humans. A study published in 2015 shows that 129 out of 282 *E. coli* isolates sequence-typed as ExPEC strains. Status was determined by isolates containing two or more of the following ExPEC-associated genes: adhesins (*afaE8, bmaE, fimH, gafD, hra, papA, papC, papEF, papG, sfa,* and/or *focDE, sfaS*), toxins (*cdtB, cnf1, astA, hlyA, hlF, pic, tsh, sat*), siderophores (*fyuA, ireA, iroN, iutA*), protectins (*cvaC, iss, kpsM* K1, K2, and/or K100, *kfiC* K5, *rfc, traT*), and miscellaneous genes typically associated with extraintestinal *E. coli* (H7 *fliC, ibeA, ompT, malX, usp*; (15)). The *mcr*-1 gene has also been isolated from *E. coli* found in pigs and chicken raised for retail meat consumption (35). Increased antibiotic use in feed or antibiotic misuse in treating bacterial disease in farm animals will increase the likelihood of transmission of antibiotic resistant *E. coli (36)*. While not harmful in the human intestine, these ExPEC may cause subsequent infections if they enter different niches.

The most common diseases caused by ExPEC in humans include neonatal meningitis, UTIs, sepsis, pneumonia, and surgical site infections (37-40). NMEC is the leading Gram-negative cause of neonatal meningitis cases (41), while UPEC strains are the leading cause of both uncomplicated and catheter-associated UTIs, responsible for up to 80% community acquired

and 65% hospital acquired UTIs (42, 43). In addition, UTIs are a leading cause of *E. coli* bacteremia (44, 45). UTIs encompass infection anywhere in the urinary tract, urethra, bladder, ureters, or kidneys. Infections can range from asymptomatic bacteriuria (ASB) to systemic bacteremia. The timeline of infection ranges from self-limiting to chronic infection. The most common clinical symptoms for UTIs, as is reported in college age women, include increased frequency and urgency of urination, abdominal discomfort, dysuria, nocturia, and hematuria (46). Infections of the bladder are called cystitis. The most common symptoms include frequency, urgency, dysuria and less frequently suprapubic pressure, malaise, nocturia, and incontinence in children and the elderly (42). Pyelonephritis is an infection of the kidneys. In a UTI, this occurs as the infection ascends to the kidneys. The most common symptoms including frequency, urgency, dysuria, back pain, flank pain, fever, chills, malaise, nausea, vomiting, anorexia, abdominal pain (42). When bacteria are introduced into the urinary tract by a urinary catheter, these UTIs are considered catheter-associated (CA-UTI). These infections result in fever, chills, altered mental state, malaise or lethargy with no other identified cause, flank pain, costovertebral angle tenderness, acute hematuria, and pelvic discomfort. However if the catheter has been removed, the signs and symptoms will mirror those of cystitis or pyelonephritis (42). While multiple exposures to different strains do occur, UTIs caused by the same strain, can recur. This is the result of re-exposure to the same strain or more commonly a resurgence of an unresolved infection within the urinary tract (see section 1.2 UPEC transient intracellular lifecycle). Within 6 months of initial infection, there is a 20-30% chance women will experience a rUTI (47).

### 1.2 UPEC transient intracellular lifecycle

As a component of the human gut microbiome, UPEC typically cause ascending infections, exiting through the anus, entering the urinary tract through the urethra, and colonizing the bladder and kidneys (**Figs. 2 and 3**). In addition to emerging fUTI, direct person-to-person transmission results from fecal oral spread or sexual activity (42), and catheterization introduces periurethral bacteria into the urinary tract.

In order to cause infection in the bladder, there are many obstacles that UPEC must overcome **(Fig. 3**) (48). After exiting the colon, UPEC must first transverse to the urethra. From here, UPEC must ascend the urethra and resist the mucous barrier and the bladder's natural defense of urination, and antimicrobial factors (48, 49). UPEC able to bind uroplakin and resist being washed out must then overcome the host innate immune response including Toll-like receptor 4 (TLR4), which senses LPS and results in upregulation of proinflammatory interleukin 6 (IL-6) in response to UTI (50, 51). Nutrient acquisition and intracellular survival is imperative for successful infection. To bypass these bottlenecks of infection, the transurethral model of inoculating $10^7$ CFU of bacteria directly into the bladder allows for researchers to identify additional aspects that are important during UTI (52).

Studies utilizing human bladder cell lines and the murine infection models have revealed that during the initial stages of infection, UPEC use type 1 pili to bind to uroplakin and integrins on superficial umbrella cells that line the bladder (53-59). These same pili are subsequently utilized to form intracellular bacterial communities (IBCs), which are biofilm-like structures within the bladder cell during early and middle stages of infection (**Figs. 2 and 4**), between 2 and 8 hours in the C3H/HeN and C3H/HeJ mouse models (48, 60, 61). Responding to yet

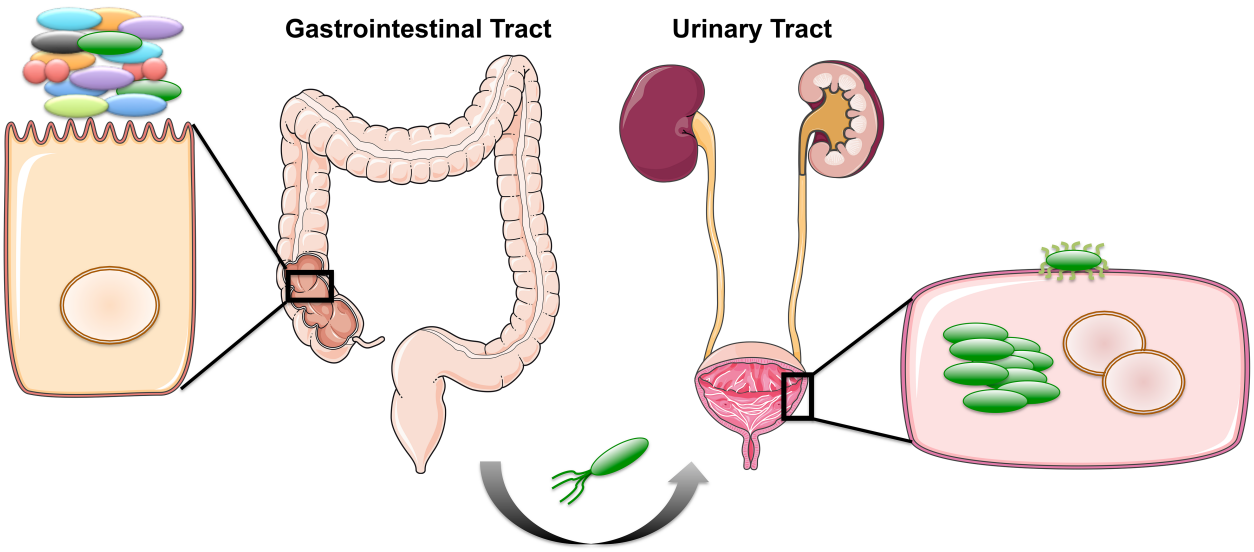


**Figure 3**: **Schematic following UPEC from colonization of the colon to urinary tract infection**. *E. coli,* including UPEC, exists as part of the microbiome in the gastrointestinal (GI) tract shown as green rod-shaped bacteria. Additional members of the microbiome are depicted in different colors and shapes. The first bottleneck to infection is transversal from the anus to the periurethral space. The second bottleneck is ascension of the urethra. Subsequent bottlenecks include resisting urination, antimicrobial agents, and exfoliation of bladder cells. Intracellular escape from fusiform vesicles and survival are imperative for acute cystitis. Once established in the urothelial cells, UPEC is able to colonize and infect the bladder.

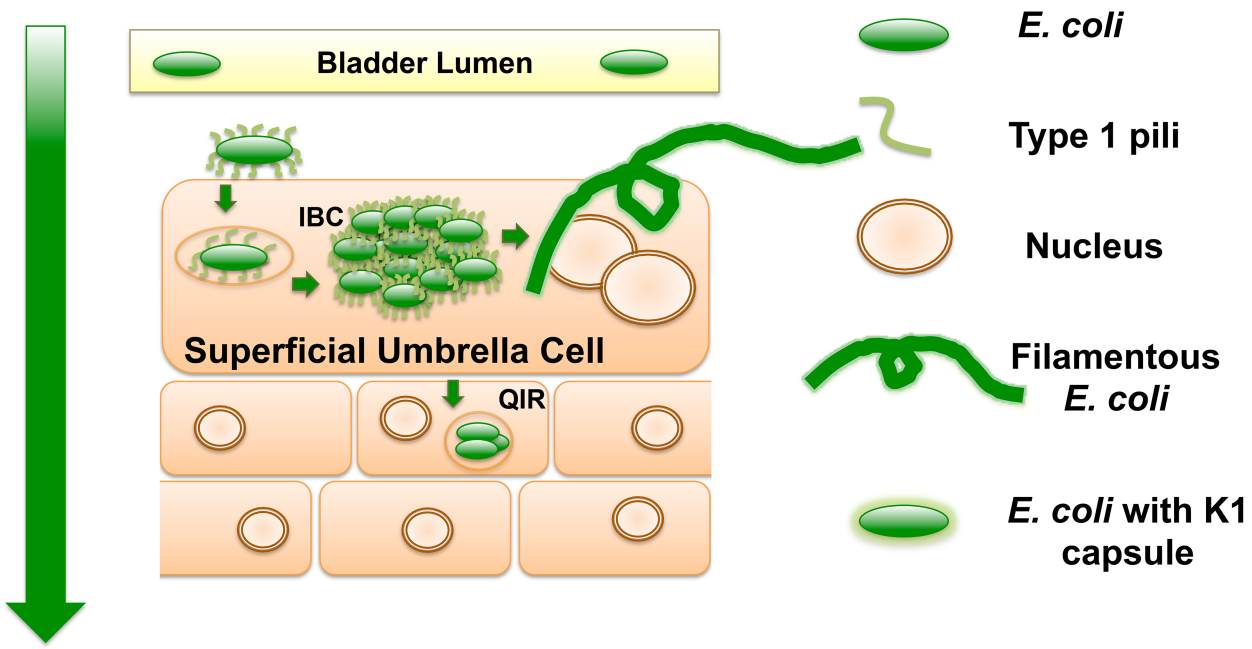


**Figure 4: UPEC infection strategy.** Diagram depicts a generalized schematic of the UPEC bacterial lifecycle. The leftmost green arrow depicts the typical route of infection from point of entry. UPEC attach to urothelial cells in a type 1 pili-dependent manner. UPEC are then endocytosed and escape into the cytosol where they replicate into intracellular bacterial communities (IBC). UPEC escape the IBC state by filamenting and fluxing out of the infected host cell. Dispersing UPEC can infect neighboring or underlying transitional cells, and/or can ascend the ureters to colonize and infect the kidneys.

uncharacterized signals, UPEC can egress from the transient intracellular state by filamenting and fluxing out of the infected host cell (61). The bladder cell can alternatively trigger an apoptotic-like cell death (55, 62) and become exfoliated prior to UPEC filamentation, shedding the IBC into the bladder lumen. Bladder cell exfoliation exposes underlying host cell layers to invasion by UPEC that can remain quiescent for prolonged periods of time (1, 63, 64). Quiescent intracellular reservoirs (QIRs) can cause recurrent infections ((1), **Figs. 2 and 4**). UPEC cells egressing from non-exfoliated bladder cells can re-initiate infection by engaging neighboring, naïve bladder cells, or by ascending to and colonizing the kidney (**Figs. 2 and 4**). Studies with murine mouse models of UTI have also elucidated that UTI leads to urothelial remodeling and may fail to regenerate even weeks after treatment. Transcriptome sequencing (RNA-seq) revealed that immune-related pathways, as well as pathways pertaining to tissue morphology, cellular development, and cellular growth and proliferation were significantly enriched (48, 65).

### 1.3 Diagnosis and treatment in the human population

Traditional diagnosis of UTI relied on bacterial urine counts of $10^5$ colony-forming units (CFUs) of bacteria per milliliter of urine and positive bacterial culture (66). If bacteria are present along with clinical symptoms, it is labeled as a UTI. The immune system, in most cases, is effective at clearing UTI. There are many innate factors in place that eliminate bacteria such as, detection through toll-like receptors, exfoliation of epithelial cells, and secretion of antimicrobial factors (67). Home remedies including cranberry supplements are widely advertised, but as of yet show little efficiency.

Treatment relies predominantly on antibiotics. The Infectious Diseases Society of America (IDSA) and the European Society for Microbiology and Infectious Diseases (ESCMID)

established new treatment guidelines in 2010 (68). Nitrofurantoin monohydrate/macrocrystals, trimethoprim-sulfamethoxazole, fosfomycin and fluroquinolones, respectively, are the preferred methods of treatment for cystitis. In the last 10 years, an alarming rise in multi-drug resistant isolates has further complicated treatment strategies (12, 69, 70).

Currently, there are no approved human vaccines against ExPEC; however vaccines are used in farming practices against *E. coli* (71). ExPEC infections in all afflicted populations are typically treated with antibiotics. Although this practice has been effective for many years both in the healthcare setting and in the poultry/farm industry, overuse, and misuse of antibiotics in the twentieth century has led to the emergence of multi-drug resistant ExPEC strains that are extremely difficult to eradicate. A recently emerged antibiotic resistant ST131 isolate harbors the blaCTX−M−15 gene producing extended spectrum beta-lactamases. ST131 isolates also harbor H4 serotype flagellar antigen, which augments adherence and invasion of bladder cells, and stimulation of IL-10 (72). In addition to the multi-drug resistant ST131 isolates, cases of colistin-resistant uropathogenic and avian pathogenic *E. coli* are also emerging (73, 74). The first United States report of a colistin-resistant *E. coli* was released in early 2016, with a ST457 urine isolate from a Pennsylvanian woman with a UTI (73). In the farm/poultry industry, a classic example of antibiotic resistance emergence is highlighted in the Yeruham study (25): a short 3-day antibiotic treatment resulted in many recurrent cases of UTIs in cattle, indicating the presence or the emergence of a resistant ExPEC population (25). In addition, the administration of antibiotics to farm animals increases the likelihood for asymptomatic colonization of animals by multidrug resistant ExPEC that can then colonize humans who come into contact with the cattle. Finally, thought-provoking studies by the Blaser group and colleagues are beginning to elucidate

possible correlations between antibiotic use in farm animals and increasing obesity in humans (75), raising concerns about continued use of antibiotics in livestock.

### 1.4 In search of therapeutic targets: virulence factors are not conclusively predictive, expression patterns are

ExPEC colonize and infect a wide range of host species, using an armamentarium of virulence factors that are not restricted to the ExPEC pathotype (**Fig. 5**). The presence of certain combinations of virulence factors can result in extra-intestinal pathogenesis, but among the different ExPEC pathotypes, there is little or no distinct set of virulence factors that is specific to UPEC, APEC, or NMEC. Rather, differential regulation of common virulence factors may be a key driver in the hierarchical expression of specific gene sets that enable/enhance colonization in distinct extra-intestinal niches (**Fig. 5**).

The difference in host and infection environment between gastrointestinal *E. coli* and ExPEC, indicate that different virulence factors are required or utilized under different conditions. There are factors commonly associated with UTI including chaperone usher pathway pili, protein adhesins, toxins, iron acquisition systems, transport systems, and other non-essential factors (7). However, these virulence factors are subject to distinct regulation depending on the host niche that each ExPEC pathotype harbors. The sequence types associated with UTI are ST 69, 73, 95, and 131 (76), the serotypes commonly associated with UTI are O1, O2, O4, O6, O16, O18, O25, and O75 (77). Similarly to APEC and NMEC, the presence of K1 capsule plays a role in pathogenesis during IBC formation (78). Increased production of type 1 pili corresponded to an increase in bladder colonization (79). In addition to type 1 pili, curli amyloid fibers, and P pili are critical for pathogenesis (80-83), along with other potentially uncharacterized adhesive

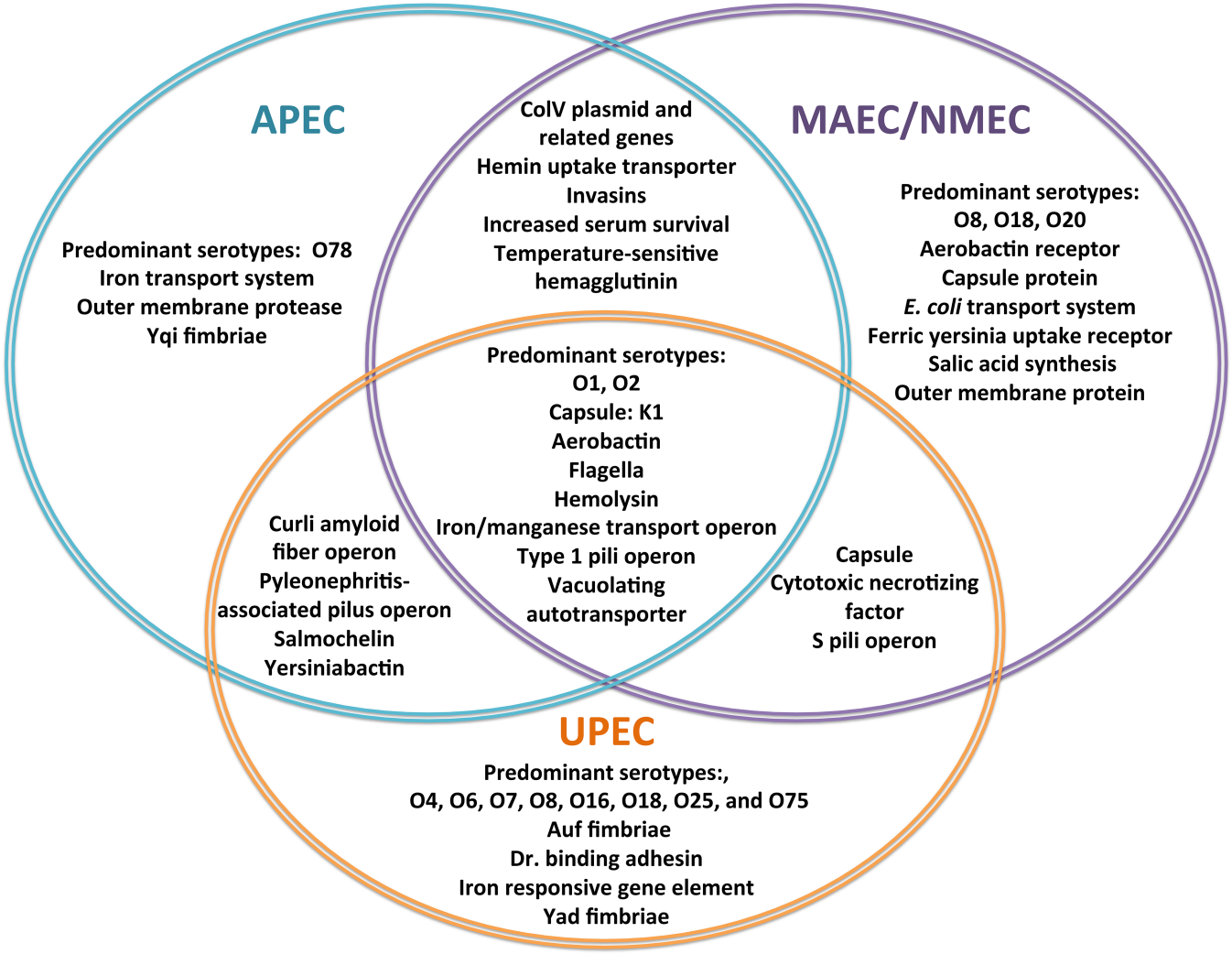


**Figure 5: Virulence Factors Involved in ExPEC Infections.** The Venn diagram represents the most commonly reported, virulence factors for APEC (blue), MAEC/NMEC (purple), and UPEC (orange). (84-95).

fibers. UPEC strains can harbor more than one dozen different types of CUP pili, each with distinct adhesion specificities and differential regulation patterns (90, 96, 97). The function and regulation of these fibers during UTIs are beginning to be elucidated (90). In addition to adherence factors, iron acquisition and acid tolerance and osmotic stress is critical for UPEC pathogenesis, as is for almost all bacterial infections (77, 98, 99). Several toxins, such as hemolysin A and vacuolating autotransporter toxin, have been associated with fine-tuning host cell exfoliation during infection (77). Several recent studies have revealed that despite being facultative anaerobes, UPEC require aerobic respiration during acute UTIs (100-103), indicating the presence of oxygen-sensing mechanisms that modulate virulence by production of type 1 pili, and possibly other factors, in response to altered oxygen levels. Furthermore, Shepherd *et al*. demonstrated that in addition to aerobic respiration, cytochrome *bd* oxidase is required for alleviating nitrosative stress during infection in the hypoxic bladder (104). There are putative urovirulence factors present in many strains of *E. coli*; however, it is expression of these genes that is associated with pathogenic risk and not carriage alone. In a study by Schreiber *et al.* (79) a phylogenetic comparison of 89 *E. coli* isolates showed that 60-75 % of the core genome was conserved. This left 25-40% of the genome to vary among strains. It may be non-traditional virulence factors including differential expression patterns of flagella, pili, maltose transport, and chemotaxis machinery for example (79) and regulatory factors such as two-component systems (described in the next chapter) that drive UPEC pathogenesis. Ultimately, the ability for UPEC to cause disease is a combination of the transcriptome, and ability to overcome host resistance.

Notably, numerous studies use laboratory strains of *E. coli* for comparative and analytical studies, sometimes over-simplifying the complexity and diversity of the *E. coli* species. Despite its frequent use in research, *E. coli* still possesses many secrets. Of the published research, most

studies have been done in decendents of a laboratory strain isolated from human feces (105). These strains are considered non-pathogenic, are in the A phylogenetic group, and are designated K-12. Studies reveal pathogenic *E. coli* deviate functionally and phenotypically from previously published K-12 results ((106-109) and unpublished data). The adaptation to host environments is eloquently nuanced, but allows for expansion of the limited core and pan genome.

### 1.5 A brief overview of targetable regulatory pathways

Current antibiotics used to treat UTIs target cell membrane synthesis, DNA replication, protein synthesis, and folic acid metabolism (110). Antibiotic exposure, overuse, misuse, or abuse, can result in antibiotic resistance; almost as quickly as new drugs are released resistance is identified (111). Current research focuses on finding new or alternative antibacterials as well as identifying new targets that reduce the likelihood of generating antibacterial resistance.

There are many regulatory processes within bacteria that result in virulence, targeting these pathways may alter the infectivity of the cell. Regulatory pathways such as: virulence gene regulation, quorum sensing, central metabolism, biofilm formation, DNA repair, stress response, and phosphorelay are all candidates for alternative therapeutics (112-116). The phosphorelay events of two-component systems described in the next chapter are an intriguing target for antibacterials, as there are many steps in the regulatory process that can be targeted in combination to change the infectious activity of a given bacterial population.

# CHAPTER II

## INTRODUCTION TO TWO-COMPONENT SIGNAL TRANSDUCTION SYSTEMS IN EXTRAINTESTINAL *ESCHERICHIA COLI*

Portions of this introduction have been adapted from Breland *et al.* "An overview of two-component signal transduction systems implicated in extra-intestinal pathogenic *E. coli* infections". Review in *Frontiers in Cellular and Infection Microbiology. (2017).* PMID: 28536675

### Bacterial signal transduction

Concerns about increased resistance are beginning to shift the focus of current research, not only to the development of new antibiotics, but also to the generation of agents that will have anti-virulence potential by targeting bacterial behavior as opposed to bacterial viability. For such agents to be effective, information about how bacteria, such as ExPEC, behave in response to environmental stimuli is crucial. Perhaps the most critical element in successful colonization and persistence in a specific niche is the ability of a pathogen to appropriately coordinate production of relevant virulence factors. This regulation must occur simultaneously with repression of other genes, the products of which are not needed in the particular environment. Bacteria are constantly bombarded with changing stimuli from within and outside the host. Within the host, these stimuli may come from innate immune defenses such as bursts of reactive oxygen species (117), cationic polypeptides and metal sequestration (118, 119), as well as exogenous stressors such as antibiotics (117). In addition, the different stages of each infection cascade are accompanied by niche-specific changes in oxygen levels, nutrients, osmolality, and temperature (120). Each of these cues is sensed by one or more bacterial signaling systems that will then coordinate bacterial behavior.

As is true for all bacteria, ExPEC deftly sense environmental stimuli using several signaling pathways that elicit downstream responses. These include one- and two-component and phosphorelay signal transduction systems, extracytoplasmic sigma factors, and second messengers. This chapter focuses on two-component systems that contribute to the pathogenesis of UPEC and the cross interactions of two distinct signaling networks PmrAB and QseBC.

**2.1 Two-component signal transduction**

Although eukaryotic-like serine/threonine kinases (121) are found within bacterial species, the majority of two-component system (TCS) receptors are histidine kinases (122-124). Two-component systems regulate functions such as quorum sensing, chemotaxis, sporulation, biofilm formation, and membrane stress response (116, 125-127).

Prototypical TCSs comprise a membrane-embedded bacterial signaling receptor that is responsible for intercepting one or more specific stimuli or ligands. Signal transduction from the membrane-embedded receptor to the response regulator occurs via a phosphorelay event to a cognate partner protein, termed the response regulator, which carries out the response (123, 128-130). The response regulator almost always resides in the cytoplasm and, in the majority of documented examples, acts as a transcriptional regulator (122, 123).

The subfamilies of histidine protein kinases (HPK) include $HPK_{1-11}$ and were named for the variation in conserved homology boxes located in the kinase and catalytic domains. (**Table 1**) (131). Histidine kinases typically function as dimeric membrane receptors and consist of a sensing domain, a kinase domain, and a catalytic domain that binds and hydrolyzes ATP (131). Sensing domains can be extracellular, membrane embedded, or intracellular (132). The three main structural classes of extracellular sensing domains include, α-β folds, all α-periplasmic binding protein folds, and a non-structural all-β fold domain (132).

**Table 1: HPK subfamilies and commonly associated RR receiver and output domains (131)**

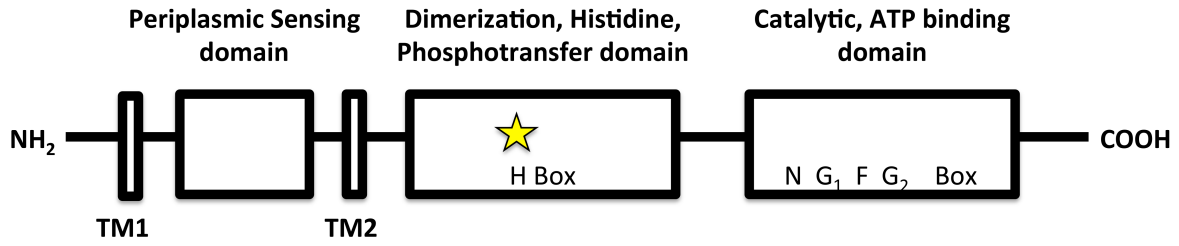


Schematic of HK domains with conserved homology H, N, G, F boxes and a star representing the conserved phosphor-accepting histidine

| HPK Subfamilies | Identifiable Features | Examples in *E. coli* | RR receiver domain | RR output domain |
|---|---|---|---|---|
| 1a | Most common type, Contains all homology box regions | BaeS<br>KdpD<br>PhoR | $R_A$ | Null<br>OmpR |
| 1b | Similar to 1a with an invariant KFT motif in the N box | **ArcB**<br>BarA<br>EvgS<br>RcsC<br>TorS | $R_B$ | Null<br>H2 |
| 2 | Alterations of residues in the H box, Diagnostic R downstream of conserved H box P | BasS (PmrB) (2a)<br>CopS (2a)<br>**CpxR(2b)**<br>**EnvZ (2b)**<br>RstB (2b)<br>**YgiY (QseC) (2a)** | $R_A$ | OmpR |
| 3a-i | Similar to 1 and 2 with slight changes in H box, Specific residues downstream of the conserved H and corresponding RR determine $3_{a\text{-}I}$ | CreC (3c) | $R_A$, $R_C$, $R_F$, $R_G$ and $R_H$ | OmpR<br>FixJ<br>H2<br>NtrC<br>Null |
| 4 | Slight variations in H box, Lacking KFT motif, PFX-TTK motif in F box | AtoS<br>HvdH<br>NtrB | $R_A$, $R_C$, and $R_F$ | Null<br>FixJ<br>NtrC<br>Null<br>ActR |
| 5 | H box lacks F and P, Alterations in N box, F box contains one F | DcuS<br>DpiB | $R_C$ | CitB |

| | | | | |
|---|---|---|---|---|
| 6 | Found in *Archaeoglobus* | Not represented in *E. coli* | Not represented in *E. coli* | Not represented in *E. coli* |
| 7 | Alterations to H box,<br>Negatively charged residue upstream H,<br>No H box P,<br>N box lacking one N,<br>F box missing | NarQ<br>NarX<br>UhpB | $R_C$ and $R_E$ | FixJ |
| 8 | P precedes H in H box,<br>Unusual N box sequence,<br>F box is not conserved | **YehU (BtsS)** | $R_C$ | LytR |
| 9 | No H box P,<br>DHG motif in N box,<br>Three residue spacer in F box | CheA | $R_A$ and $R_C$ | Null<br>Tandem<br>CheB |
| 10 | Kinases that regulate competence for genetic transfer in *Streptococcus* spp.,<br>No H box proline,<br>No D box | Not represented in *E. coli* | $R_D$ | ComE |
| 11 | Methanobacteria kinases | Not represented in *E. coli* | Not represented in *E. coli* | Not represented in *E. coli* |

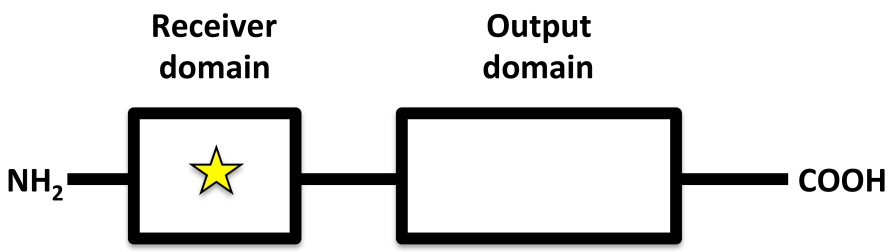


Schematic of RR domains with the star representing the conserved phosphor-accepting aspartic acid residue

*Bolded systems are discussed for their involvement in pathogenesis below.

Membrane-embedded sensors appear to rely on the transmembrane regions to sense and respond to signal (132). Finally, many cytoplasmic sensing domains exhibit conserved structural domains with five-stranded antiparallel β-sheet flanked by α-helices; others have a six-stranded antiparallel β-sheet; the third classical cytoplasmic sensing domain is found in phytochromes, these contain a phytochrome domain, which is similar in nature to the five stranded β-sheet domain (132).

Upon signal interception, the histidine kinase hydrolyzes ATP and undergoes auto-phosphorylation at a conserved histidine residue within the kinase domain (**Fig. 6**). Histidine kinase auto-phosphorylation stimulates the transfer of the phosphoryl group to a conserved aspartate residue on the cognate response regulator (**Fig. 6**), thus activating function. Many sensor kinases are bi-functional, having the ability to also act as phosphatases or reverse phosphotransferases, dephosphorylating the response regulator. Response regulator de-phosphorylation by the cognate sensor histidine kinase "resets" the signaling cascade, allowing the bacteria to respond again to the same stimulus upon re-exposure. Swift de-phosphorylation of the response regulator by the cognate histidine kinase also prevents aberrant activation of the response regulator by non-cognate kinases or other phosphor-donor molecules.

Response regulators belong to eight receiver domain subfamilies (133) and are typically categorized by the similarities of their output domain to well characterized RRs such as ActR, AmiR ArcB, CheB, CitB, ComE, OmpR, FixJ, LemA, LytR and NtrC (131, 134, 135). The majority of RR output domains are helix-turn-helix DNA binding domains; however, a subset of output domains bind RNA, ligands, or proteins, some are enzymatic in nature, while others have output domains of unknown functions (DUF) (135).

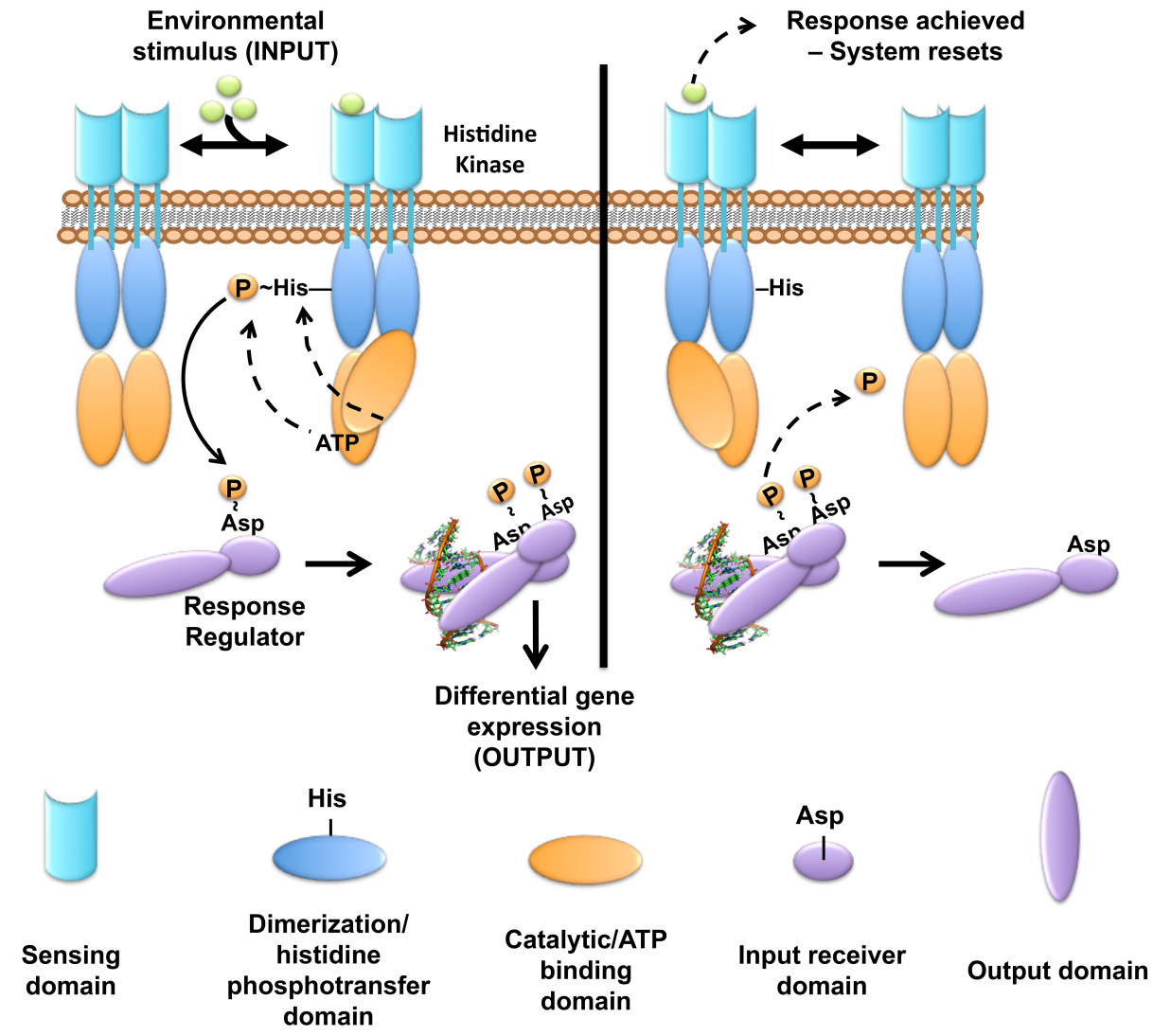


**Figure 6: Two-component system transduction schematic.** In most cases studied to date, the sensor histidine kinase is membrane-embedded. The sensor kinase detects signals or stimuli and undergoes auto-phosphorylation at a conserved histidine residue. The phosphoryl-group is then transferred to the cognate cytoplasmic response regulator at a conserved aspartate residue. Phosphorylated response regulators form an active dimer that can then regulate gene transcription. Following the appropriate cellular response, the sensor exhibits phosphatase or reverse phosphotransferase activity removing the phosphoryl-group from the response regulator to "reset" the system. While most kinases are found as a dimer in the membrane, dynamic interactions between the mono- and di-meric states may occur.

RRs catalyze the phosphotransfer to the conserved residue, this allows for some RRs to obtain a phosphoryl-group from additional sources like acetyl-phosphate (136). Table 1 shows a general relationship between HPK and RR receiver and output domains (131).

Of the 62 conserved TCSs genes harbored by *E. coli* strains (137), only a handful have been studied in the context of pathogenesis. Notably, there also are strain-specific TCSs, harbored only by certain strains or pathotypes, which are of particular interest, such as the KguRS TCS (138). Key TCSs that have been shown experimentally to be important for UPEC pathogenesis are discussed below.

### 2.2 Two-component system signaling networks involved in ExPEC pathogenesis

*ArcA/B*

When deleted for *arcA* and *arcB E. coli* are sensitive to hydrogen peroxide stress and exhibit compromised respiratory activity in low oxygen compared to wild-type strains (139, 140). The aerobic respiratory control system, or ArcA/B TCS, is a global regulator that facilitates adaptation from anoxic to aerobic conditions and mediates defense against reactive oxygen species (139). Unlike other TCSs, *arcB*, and *arcA* are not co-transcribed; ArcB is a tripartite sensor kinase that undergoes a phosphorelay event under anaerobic conditions. ArcA represses expression of many genes involved in aerobic respiration. In most cases, ArcA acts as a transcriptional repressor of enzymes involved in aerobic carbon metabolism. ArcA is a positive regulator of cytochrome *d* and pyruvate formate lyase involved in fermentation (141, 142). Oxidation of cytosolic cysteine residues found within the ArcB histidine kinase, results in the formation of disulfide bonds, resulting in reverse phosphotransfer under aerobic conditions, de-activating ArcA (142, 143). While most TCSs contain a large periplasmic sensing domain for the detection of stimuli, the

short sensing domain of ArcB is necessary for detection of the physiological redox state of quinones in the electron transport chain in the cytoplasmic membrane (142). In APEC, loss of the ArcA response regulator severely attenuates virulence, due to loss of flagellar motility, chemotaxis, and proper metabolic function (144).

*BarA-UvrY*

Deletion of *barA* or *uvrY* results in a similar hydrogen peroxide hypersensitivity (145, 146). The BarA-UvrY TCS regulates the expression of the carbon storage regulation system, a master regulator between glycolysis and gluconeogenesis, which is necessary for bacterial function and long-term survival (146). The BarA (bacterial adaptive response) tripartite sensor is involved in protection from hydrogen peroxide stress through the activation of RpoS sigma factor. Functioning slightly differently from typical TCSs, tripartite sensors undergo a phosphorelay event: the phosphate group is transferred from the histidine residue to an aspartate residue to a second histidine residue, all of which are located in different domains of BarA, before transferring the phosphoryl-group to UvrY, the cognate partner (147). UvrY, while part of the *uvrYAC* operon has no apparent role in DNA repair (147). UvrY does, however, activate the CsrB protein, which increases biofilms formation. Similarly to ArcA/B the genes coding for BarA-UvrY are not located on the same operon (145). In a macaque cystitis model, competition profiles between wild-type (WT) *E. coli* strain *DS17* and a *uvrY*::Kan$^{R}$ deletion strain suggest that the BarA-UvrY TCS is crucial for the switch between different carbon sources present in the urine (148). In both chicken embryos and a murine model of acute UTI, UPEC strain CFT073 with a *barA* or *uvrY* deletion displayed reduced virulence through decreased production of hemolysin and LPS (149).

*CpxAR*

CpxAR system was one of the three TCSs shown to be indispensable for *E. coli* fitness in the murine gut (150). The CpxAR system is comprised of the sensor kinase CpxA and the response regulator CpxR and is one of the *E. coli* systems responsible for sensing and coordinating the response to cell envelope stress (151, 152). In UPEC, CpxAR has been shown to play multiple roles in pathogenesis. Originally identified by the Silhavy group, CpxAR activation was shown to occur upon binding of commensal *E. coli* to hydrophobic surfaces (153). CpxAR activation was shown to depend on the presence of the outer membrane lipoprotein NlpE, and this was the first demonstration of a function for NlpE (153). A follow-up study revealed that activation of the Cpx system can occur in an NlpE-independent manner by inducing cues other than surface attachment (154). CpxAR was also shown to sense and respond to misfolded pilin subunits during the assembly of P pili, which are adorned with the adhesin protein PapG that binds glycolipid receptors on urothelial cells lining the kidney (155, 156). Joint collaborations from the Silhavy and Hultgren groups showed that the N-terminal extension of the PapE pilin subunit activated CpxAR (156). Misfolded PapE and PapG also activate the CpxAR system; upon activation, the periplasmic protein CpxP is upregulated to alleviate membrane stress by guiding mis-folded proteins to be degraded by proteolysis (154, 157). Most recently, the CpxAR system has been implicated in responding to antibiotics by altering the membrane integrity and increasing antimicrobial resistance (158). CpxA has also been shown to sense high osmolality conditions and result in the repression of curli expression, an important component in the production of biofilms (159). In UPEC, deletion of *cpxAR* impairs UPEC colonization of the murine bladder (160). More recent studies demonstrated that CpxAR regulates expression of α-hemolysin (HlyA), though only about 50% of UPEC isolates encode this pore-forming toxin. HlyA causes cytotoxicity in

urothelial cells (62). Nagamatsu *et al*. showed that loss of CpxR unleashes expression of HlyA and increases exfoliation of the host urothelium during infection, suggesting that CpxAR exerts a negative effect on *hlyA* expression, possibly fine-tuning cytotoxicity in urothelial cells for HlyA-harboring UPEC strains (62).

*EnvZ-OmpR*

In a murine model of UTI, deletion of *ompR* in the UPEC clinical isolate NU149 had a significant, two-log reduction in colony forming units in both the bladder and kidney, indicating a role of EnvZ-OmpR in pathogenesis (161). EnvZ-OmpR has been coined the "prototypical" TCS, owing to its early characterization (162). The sensor kinase EnvZ is phosphorylated under hypo-osmotic conditions and phosphotransfers to the response regulator OmpR. Activation of OmpR leads to upregulation of outer membrane porin proteins, such as OmpF or OmpC (163-165). OmpR has been shown to influence the expression of type 1 pili through transcriptional regulation of *fimB*, one of the site-specific recombinases that control the orientation of the type 1 pili promoter (166). UPEC encounter a significant change in extracellular osmolality as they exit the gut and ascend the urethra, so one can extrapolate that EnvZ-OmpR function is important during the early stages of infection (161).

*KguRS*

In a mouse model, deletion a CFT073 mutant deleted for *kguRS* colonized the urinary tract less efficiently (138). A more recently discovered, primarily UPEC-encoded system is KguRS. The KguS sensor kinase was reported to sense the presence of α-ketoglutarate in the UPEC strain CFT073 (138). Given that α-ketoglutarate is primarily utilized in the tubules of the kidneys, the studies by Cai *et al*. implied that utilization of α-ketoglutarate enhances the ability of UPEC to adapt to the urinary tract environment (138).

*PmrAB (BasRS)*

Originally named for the polymyxin resistance phenotype observed in *Salmonella enterica* Typhimurium (167, 168), the PmrAB system has been shown to be involved in antibiotic resistance. The PmrB sensor is known to directly bind ferric iron ($Fe^{3+}$) and mediates alterations to the lipopolysaccharide (LPS) layer of the outer membrane to protect the cell against cationic polypeptide stress (169-171). A constitutively active PmrA variant showed intrinsic resistance to polymyxin B (PMB) yet, conferred susceptibility to an anionic compound deoxycholic acid (172). PmrAB is required for virulence in a murine model of infection (173, 174). PmrAB is also indirectly involved in altering LPS in response to low levels of magnesium ($Mg^{2+}$). PhoQ, a HK from the PhoPQ system, directly senses the extracellular decrease of $Mg^{2+}$ and activates the accessory protein PmrD which binds and stabilizes PmrA~P, in addition to PhoP the cognate partner, that activates expression of *pmrAB (175)*. The PmrD protein in *E. coli* however, does not activate PmrAB in response to PhoPQ activation (176).

*QseBC*

In UPEC, deletion of *qseC* results in severe attenuation of infection due to reduced expression of motility genes, several CUP systems including type 1 pili, curli fibers, and several metabolic pathways (101, 177). This misregulation of virulence factors occurs only in the absence of QseC, but not in the absence of QseB or the entire QseBC system (177). The QseBC system, comprised of the sensor kinase QseC and the response regulator QseB, was reported to be involved in quorum sensing in enterohemorrhagic *E. coli* (EHEC; (178)). EHEC QseC was shown to respond to norepinephrine, epinephrine, and autoinducer-3 (179) and this deletion severely attenuates EHEC virulence (180). *In vitro* studies show phosphotransfer and desphosphorylation of QseB by QseC (177), the underlying mechanism of this regulation is unknown.

### 2.3 Evidence of cross interaction between closely related systems

Gene duplication of TCS may result in overlapping recognition of signals, phosphor-relay events, and outputs (**Fig. 7**). Cross interactions between two-component systems are thought to occur infrequently. Cross-talk is described to result in negative effect for the bacterium, while cross-regulation is said to enhance physiologic function (181). There are several cases where cross-regulation has been identified between TCSs. These include the nitrogen sensing pathways NarLX-NarPQ in K-12 *E. coli* (182), CpxAR-EnvZOmpR in *E. coli* (183), PhoPQ-PmrAB in *Salmonella enterica (184)*, HssRS-HitRS in *B. anthraces* (185), and now PmrAB-QseBC in UPEC (186). Understanding how these bacterial networks communicate during infection will elucidate new avenues for targeting bacterial virulence without applying selective pressure.

*BtsS/R (YehU/T) and YpdA/B*

Originally referred to as YehUT, this two-component system was recently renamed due to its role in metabolite sensing. Named Bts for Brentztraubensäure, the original name given to pyruvic acid when it was first synthesized in 1835, BtsS has been shown to directly bind extracellular pyruvate (107). This HK also detects changes in external L-serine and is repressed in the presence of high levels of extracellular serine (≥ 50 μM) (107). The RR, BtsR has been shown to activate the only known target YjiY, a transmembrane protein with putative peptide transport activity (187). Expression of the sole target steady state transcript *yjiY* was elevated during the acute and chromic murine model of UTI (107). It is presumed that the role of BtsS/R in sensing extracellular concentrations of serine and pyruvate may play a role in the infection process (107).

The YpdA/B TCS is reported to respond to high levels of extracellular pyruvate and augment activation of BtsRS (188). The only known downstream target of the RR, YpdB, is *yhjX*, a putative transporter in major facilitator superfamily (188). Like for the BtsRS system, during

chronic and acute infection, the steady state transcript for *yhjX* is increased in the murine model of UTI (unpublished).

*QseBC and PmrAB*

Recent studies have uncovered non-partner interactions that occur between the QseB response regulator and another TCS, PmrAB (186). PmrB constitutively phosphotransfers to QseB in the absence of the QseC sensor (**Fig. 7C**, (186)). This constitutive activation leads to aberrant gene repression by QseB and attenuation of virulence, making the QseBC system an excellent target for anti-virulence strategy development. QseC and PmrB are both classified as class I, HPK2a histidine kinases (131, 189). The response regulators QseB and PmrA both have an $R_{AI}$ receiver domain and are categorized to have OmpR like-output domains (131). There is 33.53% protein sequence identity between the kinases and a 45.21% sequence identity between the response regulators. This similarity is presumed to be the result of a genetic duplication event.

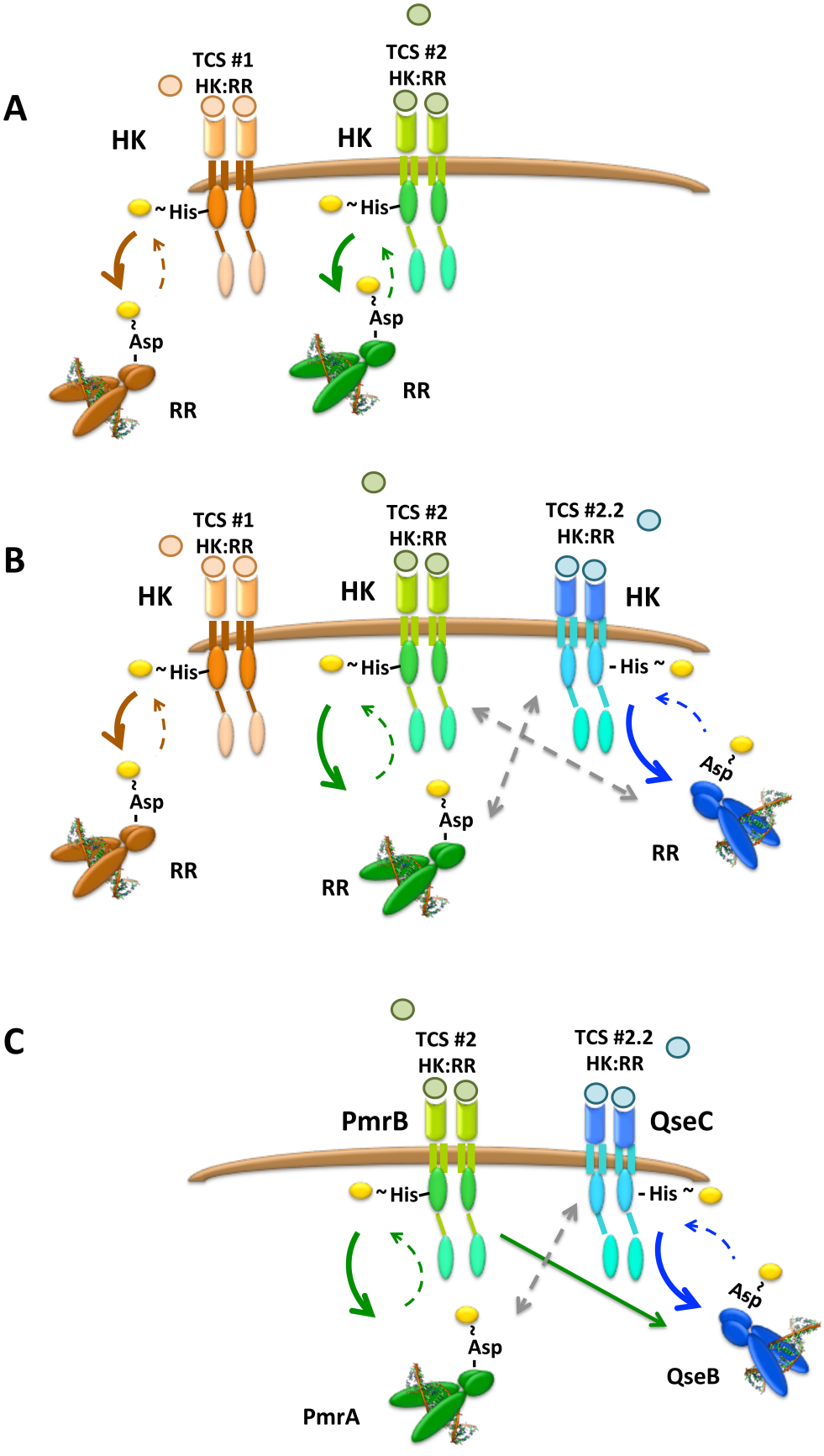
A
TCS #1
HK:RR
HK
~ His
Asp
RR
TCS #2
HK:RR
HK
~ His
Asp
RR
B
TCS #1
HK:RR
HK
~ His
Asp
RR
TCS #2
HK:RR
HK
~ His
Asp
RR
TCS #2.2
HK:RR
HK
- His ~
Asp
RR
C
TCS #2
HK:RR
PmrB
~ His
Asp
PmrA
TCS #2.2
HK:RR
QseC
- His ~
Asp
QseB

**Figure 7: Schematic depicting two-component system duplication and cross-interaction.** (**A**) Represents two independent (orange and green) cognate two-component systems sensing and responding independently. (**B**) When gene duplication occurs (blue from green) a new two-component system arises (blue) that may have cross-interaction prior to divergence (gray arrows). Following divergence, these systems will no longer recognize one another and the cross-talk or cross-regulation will disappear (gray arrows). (**C**) In UPEC, the PmrAB (green) and QseBC (blue) are still shown to cross-interact under physiologic conditions.

The interactions between QseBC and PmrAB were described by Kostakioti and Hadjifrangiskout *et al.* and Guckes *et al*. (177, 186). These data show that deletion of *qseC* results in global changes in UPEC cystitis isolate strain UTI89 (1). Microarray analysis revealed 443 genes are significantly altered in the absence of QseC, which is equivalent to almost 8% of the genome (101). These genes fall into ten primary categories, metabolism, membrane transport, genetic information processing, translation, regulators, signal transduction, fimbriae, stress response, plasmid, as well as hypothetical proteins and others (101). Deletion of *qseC* results in decrease in biofilm formation, IBC formation, curli production, and motility (177). This suppression of virulence traits was discovered to be a result of the constitutive phosphorylation of QseB by non-cognate partner PmrB in the absence of QseC regulation (186). It was also shown that PmrA is involved in inducing *qseBC* expression in the presence of ferric iron (186). Under non-inducing conditions PmrB acts as a delayed phosphotransferase to QseB with no *in vitro* phosphatase activity (186). While it is known that these two TCSs interact, the amount of cross-regulation is unknown. The relationships between the sensors, the responders, and non-cognate partners are still to be elucidated.

# CHAPTER III

## PMRAB-QSEBC NON-COGNATE PARTNERS PROMOTE TRANSIENT POLYMYXIN B RESISTANCE IN UPEC

This chapter has been adapted from Guckes* and Breland* *et al.* "Signaling by two-component system noncognate partners promotes intrinsic tolerance to polymyxin B in uropathogenic *Escherichia coli*". *Science Signaling. (2017).* PMID: 28074004

*Both authors contributed equally to this work

Typical TCSs include a sensor histidine kinase (HK) that acts as a receptor coupled to a partner response regulator (RR) that coordinates changes in bacterial behavior, often through its activity as a transcriptional regulator. HK:RR interactions are typically confined to cognate pairs. This work describes how two distinct TCSs in uropathogenic *Escherichia coli* (UPEC) interact to mediate a cellular response to ferric iron, which results in transient resistance to polymyxin B.

### 3.1 Introduction

Constant sensing of the environment via the use of TCSs affords bacteria the ability to quickly adapt to change. In all reported cases, TCSs become activated in response to specific signals, which may act as ligands that activate the histidine kinase receptor either via direct binding (190, 191) or via indirect and oftentimes uncharacterized mechanisms (192-195). Upon signal detection, the histidine kinase dimer auto- phosphorylates at a conserved histidine residue located in the cytoplasmic portion of the protein (123, 196). The histidine kinase then transduces the signal by transferring this phosphoryl group to a conserved aspartate residue on its cognate response regulator (122, 196, 197). Phosphorylation of the response regulator typically results in a conformational change, leading to dimerization and a change in the activity of the response

regulator (123, 125, 196, 198, 199). Most response regulators mediate output by acting as transcription factors (123, 125, 196). Thus, in response to an incoming stimulus, there is a rapid phosphotransfer event, leading to maximal phosphorylation of the cognate response regulator within 5 to 10 min. For TCSs that autoregulate the expression of the genes that encode them, the phosphorylated response regulator can act as an activator of transcription, and this series of events is referred to as an activation surge (200, 201). In contrast to mammalian kinases, bacterial histidine kinases can be bifunctional, exhibiting both kinase and phosphatase activities toward the cognate response regulator (196, 199). The inherent phosphatase function of histidine kinases prevents aberrant activation by non-cognate histidine kinases or other phospho-donor molecules, which in turn ensures proper regulation of downstream targets.

Few examples of TCS non-cognate partner interactions have been described in the literature (202-206). A review by Laub and Goulian has categorized non-partner TCS interactions as beneficial or detrimental to the bacterium, defining these as cross-regulation or cross-talk, respectively (181). In all reported cases of detrimental cross-talk to date, the non-cognate interactions occur in the absence of one cognate partner, which is an artificial condition (129, 177, 183, 185, 186, 207). Very few studies have reported naturally occurring, beneficial, cross-regulation (202-204). Previous studies in uropathogenic *Escherichia coli* (UPEC) determined that cross-talk between the QseBC and PmrAB TCSs occurs in the absence of the sensor kinase QseC (**Fig. 8**, (177, 186)). Specifically, deletion of *qseC* leads to deregulation of gene expression and attenuation of virulence, due to an accumulation of phosphorylated QseB (QseB~P) as a result of cross-activation from PmrB (Chapter II, **Figs. 7, and Fig. 8)** (101, 186). Consequently, deletion of the *pmrB* gene in the *qseC*

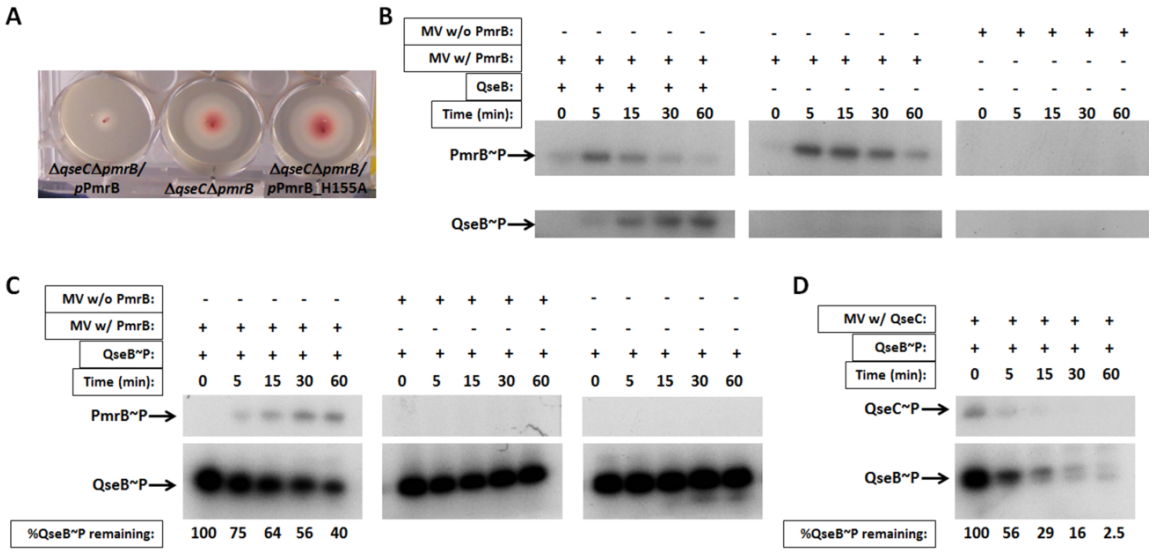


**Figure 8: PmrB phosphorylates QseB in the absence of QseC** (reprinted with permission (186)) **(A)** Effects of inactivating PmrB kinase activity on the motility of UTI89Δ*qseC*Δ*pmrB*/pPmrB, UTI89Δ*qseC*Δ*pmrB* and UTI89Δ*qseC*Δ*pmrB*/pPmrB_H155A. Motility diameters were measured after a 7h of incubation at 37°C. (**B**) Phosphotransfer assays with PmrB-enriched membrane vesicles (MV) and purified QseB. Middle panel demonstrates PmrB autokinase activity in the absence of QseB. The last panel depicts a mock phosphotransfer assay using MV without PmrB to verify that phosphotransfer to QseB occurs specifically by PmrB. A representative of 3 independent experiments is shown. (**C-D**) *In vitro* phosphatase assays with PmrB-enriched membrane vesicles (MV) and *in vitro* phosphorylated QseB~P. Percent QseB~P was calculated based on peak intensity analysis of each band normalized to the sample at t=0, using the ImageJ software. A representative of 3 independent experiments is shown.

Deletion mutant suppresses all the adverse phenotypes associated with the absence of QseC (**Fig. 8,** (101, 177, 208, 209)), leading to the hypothesis that QseC phosphatase function is critical to the ability of this sensor to control QseB.

*In vitro* kinetic profiling revealed the availability of PmrB to phosphorylate QseB in a cognate-partner fashion, which is unlike other cases of reported cross-talk. The rapid kinetic phosphotransfer activity of PmrB to QseB also suggests that the interacting surface of the QseC and PmrB must be very similar indicating recent evolutionary divergence. Indeed, studies by Wu *et al*. show that QseB diverged from PmrAB based on their hierarchical classification of evolution (210). Here, we present evidence that PmrB and QseB physiologically interact in response to the activating signal of PmrB. This cross-interaction leads to the upregulation of genes involved in LPS modification, conferring transient resistance to polymyxin B, one of the last resort antibiotics for treating multi-drug resistant *E. coli* (211).

### 3.2 Materials and methods

*Bacterial strains and growth conditions*

All bacterial strains are listed in Table 2. Cultures were grown in Lysogeny broth (Fisher) or N-minimal broth (177) with or without 100 μM ferric iron (Fisher) or 100 μM epinephrine (Sigma) at 37 °C with shaking. UTI89Δ*qseC*, UTI89Δ*pmrB*Δ*qseC*, and the corresponding pQseC, pQseC-mycHis, pPmrB, and pQseC-mycHis plasmid constructs harboring the corresponding wild-type *qseC* and *pmrB* gene sequences were created previously (177, 186) and are listed in Table 3. Deletion constructs were generated using the lambda-red recombination method as described by (212). Promoter activity for the *qseBC* operon was measured using a previously constructed plasmid (177, 186), listed in table 3, in which the *qseBC* promoter region is fused to *gfp*.

**Table 2: Bacterial strains used in this chapter**

| Strain | Source |
|---|---|
| *Salmonella enterica* Typhimurium 14028 | Mark Goulian |
| UTI89 | (1) |
| UTI89Δ*qseC* | (177) |
| UTI89Δ*qseB* | (177) |
| UTI89Δ*qseBC* | (177) |
| UTI89Δ*pmrB* | (186) |
| UTI89Δ*pmrA* | (186) |
| UTI89Δ*pmrAB* | (186) |
| UTI89Δ*qseB*Δ*pmrA* | This study |
| UTI89Δ*qseC*Δ*pmrA* | This study |
| UTI89Δ*qseBC*Δ*pmrA* | This study |
| UTI89Δ*phoPQ* | This study |
| UTI89Δ*qseC*Δ*pmrA*Δ*phoPQ* | This study |

**Table 3: Plasmids used in this chapter**

| Plasmid | Source |
|---|---|
| pTrc99A_pQseC | (177) |
| pTrc99A_pPmrB | (177) |
| pBADmycHisA_QseC | (186) |
| pBADmycHisA_QseB | (177) |
| pBADmycHisA_PmrB | (186) |
| pBADmycHisA_PmrA | (186) |
| P*qse*::*gfp* | (186) |

*Phosphotransfer assays*

Membranes enriched for UTI89-derived PmrB or QseC (7 μg) were incubated with purified QseB (14 μg), at protein concentrations of 25 μM and 0.7 μCi ($\gamma$-$^{32}$P)ATP, in the absence or presence of signal. Each reaction solution includes 1 × tris-buffered saline (TBS), 0.5 mM dithiothreitol (DTT), and 0.5 mM $MgCl_2$. Aliquots (10 μl) were withdrawn from a 7 × master reaction mix at different time points, mixed in a 1:1 ratio with 2 × SDS loading buffer, and kept on ice until SDS–polyacrylamide gel electrophoresis (SDS-PAGE) analysis. Gels were dried and exposed to x-ray film for 48 hours at −80 °C. Band intensities corresponding to QseB~P over time were quantified using ImageJ software and normalized to QseB~P at t = 0. All experiments were repeated two to four times.

*Phosphatase assays*

Glutathione Sepharose beads (GE Healthcare Life Sciences) bound to the cytosolic portion of PmrB, as described previously (181), were prepared and used to *in vitro* phosphorylate QseB as described in (184). QseB~P (0.2 nmol) was incubated at room temperature with 7 μg of membrane vesicles in the presence or absence of 100 μM $Fe^{3+}$ with 1× TBS, 0.5 mM DTT, and 0.5 mM $MgCl_2$. Aliquots (10 μl) were withdrawn from the reaction at different time points, mixed in a 1:1 ratio with 2 × SDS loading buffer, and kept on ice until SDS-PAGE analysis. Gels were dried and exposed to x-ray film at −80 °C. Band intensities corresponding to QseB~P over time were quantified using ImageJ software and normalized to QseB~P at t = 0.

*Preparation of HK-enriched membranes*

UTI89Δ*qseC*/pQseC-mycHis and all UTI89Δ*pmrB*/pPmrB_mycHis were grown to an $OD_{600}$ =

0.6, in LB with shaking at 37°C and induced with 0.02% arabinose for 2 h. Cells were broken by French Press (1000 p.s.i.) and total membranes were isolated by 1 h ultra-centrifugation at >1,000,000 × *g*, re-suspended in 20 mM Tris pH 8.0/1 mM $MgCl_2$ as we previously described (177, 186).

*Purification of tagged QseB and PmrA*

The pQseB-mycHisA and pPmrA-mycHisA plasmid constructs used for expression and purification of tagged QseB and PmrA, respectively, were previously described (177). QseB or PmrA expression was induced with 0.1% arabinose, and the tagged proteins were affinity-purified using a TALON column (Clontech) followed by anion exchange chromatography through a Mono Q column (GE Healthcare), as described (177).

*Electrophoretic mobility shift assays*

Purified QseB-mycHisA and PmrA-mycHisA were phosphorylated *in vitro* using glutathione Sepharose beads fused to the cytosolic portion of PmrB, as described (186). Phosphorylated QseB-mycHisA or PmrA-mycHisA (0 to 250 pmol per reaction) was incubated with about 6 fmol of a 105-bp fragment of the *yibD* promoter region in binding buffer (final concentration: 20 mM tris-HCl, 5 mM $MgCl_2$, 5 mM KCl, 10% glycerol) for 20 min at room temperature. Reactions were loaded onto a 5% acrylamide nondenaturing gel, and electrophoresis was performed for 2.5 hours at 50 V. Gels were dried at 80 °C for 2 hours before they were exposed to X-ray film at −80 °C for 2 hours to overnight.

*qRT-PCR expression analysis*

Cultures were grown to log phase at 37 °C with shaking, and samples were collected and flash-frozen using dry ice and ethanol until RNA extraction. RNA was extracted using the RNeasy kit

(Qiagen), deoxyribonuclease (DNase)–treated using TURBO DNase I (Ambion), and reverse-transcribed using SuperScript II Reverse Transcriptase (Invitrogen). DNase-treated RNA samples not subjected to reverse transcription were used as negative controls. Complementary DNA (cDNA) was amplified using the *gfp*- and *rrsH*-specific primers listed in Table A1. qRT- PCR was performed, using an ABI StepOne Plus Real-Time PCR machine and multiplexed TaqMan MGB chemistry, in triplicate with two different amounts of cDNA (50 or 25 ng per reaction). Relative fold change was determined by the $\Delta\Delta C_T$ method where transcript abundances were normalized to *rrsH* abundance.

*PMB sensitivity assay*

Bacteria were grown overnight at 37 °C with shaking. Overnight cultures were then subcultured into N-minimal medium with or without 100 μM ferric chloride ($FeCl_3$). Once N-minimal cultures reached mid-logarithmic phase of growth, cultures were normalized to an $OD_{600}$ (optical density at 600 nm) of 0.3 in phosphate-buffered saline (PBS) and incubated with or without PMB (2.5 μg/ml) at 37 °C for 1.5 hours. Cells were plated on LB agar to determine colony-forming units per milliliter. Percent survival was calculated by dividing the number of bacteria that grew after exposure to PMB by the number of bacteria that grew after incubation in PBS alone and multiplying the quotient by 100. The MICs for PMB without pretreatment of bacteria with ferric iron were calculated using Etest strips (BioMérieux).

*Statistics*

All statistical analyses were performed using GraphPad Prism software. When calculating the survival ratio in the PMB sensitivity assay, pre-conditioned and non-conditioned bacteria were compared pairwise between strains and were shown to be statistically significant between the

indicated strains using a nonparametric one-way ANOVA by the Kruskal-Wallis test, $P < 0.01$.

### 3.3 Results

*All components of the QseBC and PmrAB TCSs are required for proper response to ferric iron*

Previous studies had shown that when activated, QseB auto-regulates the *qseBC* regulon (213). We therefore assessed *qseBC* auto-regulation to determine whether there is beneficial cross-regulation between pmrB and QseB in response to a PmrB stimulus. Bacteria were grown in N-minimal medium that contains low-levels of ferric iron ($Fe^{3+}$) (214) and were spiked with $Fe^{3+}$ during logarithmic growth. Samples were obtained at various time points from 0 to 60 min after exposure to $Fe^{3+}$, and qRT-PCR analysis was performed to measure the transcriptional surge of the *qseBC* promoter over time (**Fig. 9**). In the UPEC strain UTI89, a robust surge in steady-state transcript was observed at 15 min after the addition of iron (**Fig. 9**). These results indicated that expression of the *qseBC* system is induced in response to activation of the PmrB sensor. In strains lacking QseB, QseC, PmrB, or PmrA the transcriptional surge was abolished (**Fig. 9**), implying that the components of both TCSs are required to drive the expression of *qseBC* in response to the $Fe^{3+}$ stimulus.

In *Salmonella*, PmrB binding to ferric iron promotes the expression of genes involved in lipopolysaccharide (LPS) modification (170, 215). Other reported activators of PmrB include $Al^{3+}$and mildly acidic pH (216, 217). Low concentrations of $Mg^{2+}$ as well as polymyxin B (PMB) and other anti- microbial peptides activate PmrAB indirectly through the PhoPQ TCS (218-220). Previous studies indicated that QseC kinase activity is enhanced in response to epinephrine, norepinephrine, and autoinducer 3, a secreted bacterial signaling molecule of unknown structure

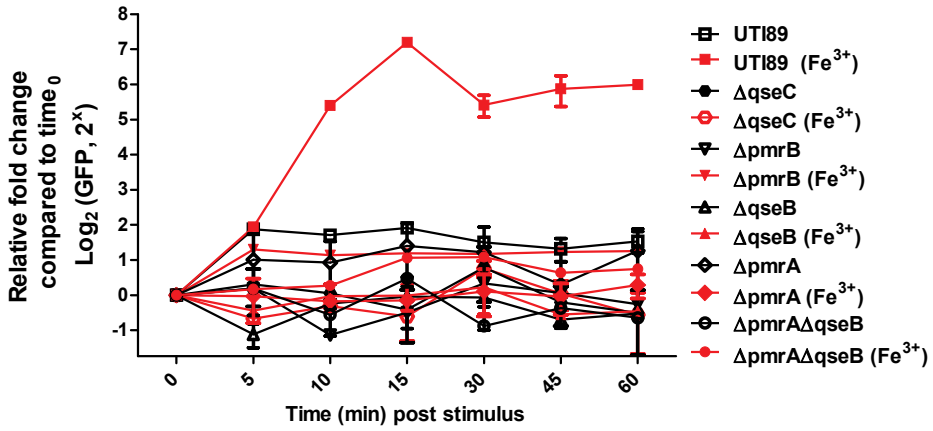


**Figure 9: All components of both PmrAB and QseBC are required for the *qseBC* transcriptional surge in response to ferric iron.** The abundance of green fluorescent protein (*gfp*) transcripts from the P*qse*::*gfp* fusion construct in UTI89 and in UTI89 deletion strains lacking components of the PmrAB and QseBC TCSs was determined by qRT-PCR analysis. Analysis was performed both in the absence and in the presence of ferric iron ($Fe^{3+}$). Fold changes were calculated using the $\Delta\Delta C_T$ method, with *rrsH* as an endogenous control, and samples were normalized to time 0. Error bars indicate SEM, $n \geq 3$ for each mutant strain.

(179). We have demonstrated that in the absence of signal, QseC readily autophosphorylates and phosphotransfers to QseB (**Fig. 10**) (177, 186). *In vitro* phosphotransfer assays indicated that the presence of epinephrine (**Fig. 10**), norepinephrine, or spent UPEC supernatant fractions (221) did not increase the rate of QseC-mediated phosphotransfer under the conditions tested. On the basis of the quantification of QseB~P (fig. S1, A and B), it appears that epinephrine either decreases the rate of phosphotransfer to QseB or increases the rate of dephosphorylation of QseB by QseC (**Fig. 10, A to C**). Subsequent qRT-PCR analyses probing for changes in *qseB* transcript abundance in the presence of epinephrine indicated no differences in *qseB* steady-state expression in the presence or absence of epinephrine in the UPEC strain UTI89 or in UTI89 lacking the *qseC* gene (**Fig. 10**). The *qseC* deletion mutant UTI89Δ*qseC* showed constitutively high amounts of *qseB* transcript, which is the result of unregulated PmrB phosphotransfer to QseB (186). Together, these results indicated that, in UPEC, epinephrine and norepinephrine do not stimulate the kinase activity of the QseC histidine kinase and that QseBC is involved in proper stimulus response to ferric iron in conjunction with PmrAB.

We then probed whether the activation surge we observed (**Fig. 9**) was specific to stimulation with ferric iron or whether other cations would elicit the same response. To test the specificity of the coordinated response to ferric iron, we used $ZnCl_2$ and $CuSO_4$ as sources $Zn^{2+}$ and $Cu^{2+}$. These metal cations were chosen on the basis of previous studies identifying high concentrations of extracellular $Zn^{2+}$ as a putative signal for *E. coli* PmrB (222) and hypersensitivity to toxic ions, such as $Cs^{+}$, $Co^{2+}$, $Cu^{2+}$, $Ni^{2+}$, and $Ru^{3+}$, in *E. coli* strains lacking QseBC (223). We tested the steady-state transcript abundance of *qseB* using a qRT-PCR approach similar to that which we used to measure the responses to $Fe^{3+}$ (**Fig. 11**). Only the presence of $Fe^{3+}$ resulted in a typical transcriptional surge (**Fig. 9**), whereas $Zn^{2+}$ caused a modest and

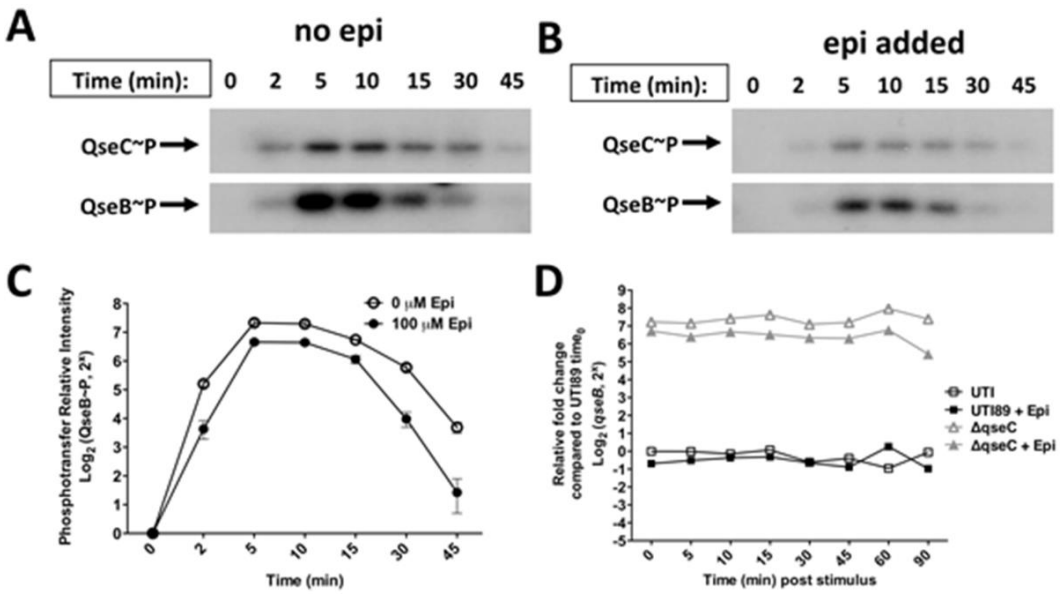


**Figure 10: QseC activity is not enhanced in the presence of epinephrine. (A-B)** Panels show radiographs that track autophosphorylation and subsequent phosphotransfer of $^{32}$P-γATP to QseB by QseC in UTI89 membrane fractions in the absence (**A**) and presence (**B**) of epinephrine (Epi). n = 3 biological replicates. (**C**) Representative quantification of phosphorylated QseB (QseB~P) in the presence (filled circle) or absence (open circle) of epinephrine using ImageJ. (**D**) Representative qRT- PCR analysis tracking the relative fold change of *qseB* transcript in wild-type UTI89 (squares) and UTI89Δ*qseC* (triangles) in the presence (filled shape) or absence (open shape) of epinephrine. Fold changes are graphed on a $Log_2$ scale. n = 2

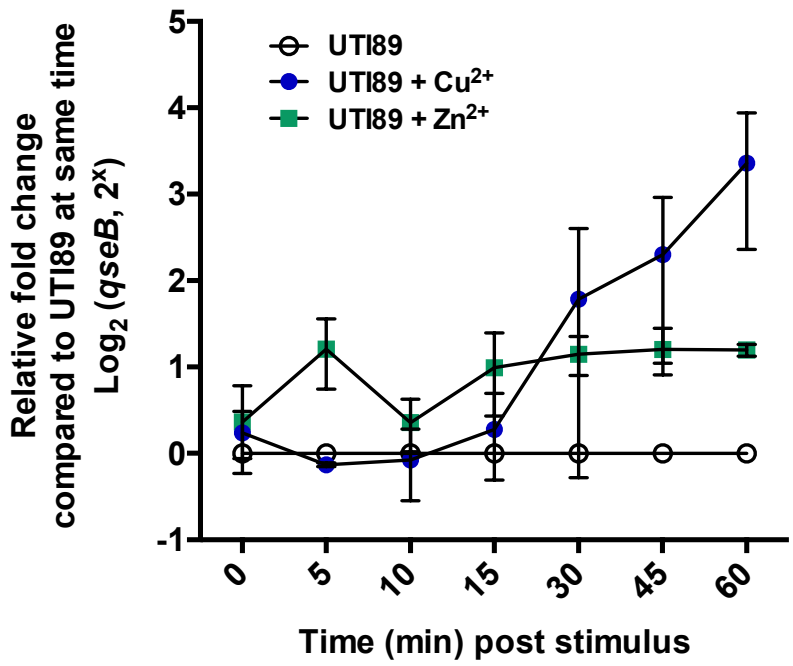


**Figure 11: The *qseBC* transcriptional surge is specific to ferric iron.** The graph depicts qRT-PCR analysis of *qseB* transcript abundance in UTI89 in N- minimal medium (open circles), UTI89 in the presence of $Cu^{2+}$ (blue circles), and UTI89 in the presence of $Zn^{2+}$ (green squares). Fold changes were calculated using the $\Delta\Delta C_T$ method, where *rrsH* was used as an endogenous control and samples were normalized to matching time points of UTI89 in the absence of added metal cations. Fold changes are graphed on a $Log_2$ scale. Error bars indicate standard error of the mean (SEM), n = 3 biological replicates.

consistent increase in the abundance of *qseB* transcripts, which was maintained over time and did not return to baseline (**Fig. 11**). Addition of copper $Cu^{2+}$ cations steadily increased the amount of *qseB* transcript over time, reaching maximal transcription at 60 min after stimulation (**Fig. 11**), suggesting that increased *qseBC* transcription in response to $Cu^{2+}$ may be due to a different copper-responsive regulator and not QseB. On the basis of these observations, we evaluated protein-protein interactions and downstream regulatory events in response to $Fe^{3+}$.

*PmrB phosphotransfers to PmrA and QseB upon stimulation with ferric iron*

The above experiments indicate a strong surge in *qseBC* transcript in response to $Fe^{3+}$ that only occurs when the QseBC and PmrAB systems are intact. These studies also suggested that PmrB, and not QseC, mediates the response to $Fe^{3+}$ by phosphorylating both PmrA and QseB. We thus evaluated the kinase activity of PmrB toward PmrA and QseB, all isolated from strain UTI89, in the presence and absence of ferric iron (216). For our studies, we used membrane fractions enriched with PmrB from strain UTI89, which harbors 98% nucleotide identity and 99% protein sequence identity to previously tested, non- pathogenic *E. coli* strain K12 (**Table 5**) (224). In the absence of signal, UPEC PmrB exhibited strong phosphatase activity toward PmrA isolated from UTI89 (**Fig. 12A**). This observation was consistent with previous reports evaluating PmrB activity in nonpathogenic *E. coli* (224). PmrB indiscriminately phosphorylated QseB, isolated from UTI89, in the absence of signal (**Fig. 12B**).

When the phosphotransfer assays were repeated with 100 μM $Fe^{3+}$ added to the reaction buffer, PmrB phosphotransfer to both PmrA and QseB increased (**Fig. 2, C and D**). On average, maximal phosphorylation of the response regulators was observed 10 min after addition of the stimulus, with the highest rate of phosphotransfer occurring within the first 2 min of the reaction

**Table 4: QseB and QseC protein sequence identity among *E. coli* strains and other enteric bacteria.** Clustal Omega was used to align and compare sequence. The percent identity was reported from the percent identity matrix following alignment.

| Clade | Strain | QseB protein sequence identity (%) | GenBank accession number | QseC protein sequence identity (%) | GenBank accession number |
|---|---|---|---|---|---|
| | ***E. coli*** | | | | |
| **B2** | **UPEC str. UTI89** | 100 | ABE08897.1 | 100 | ABE08898.1 |
| **B2** | **APEC O1K1 str. O1** | 100.00 | ABJ02530.1 | 100.00 | ABJ02531.1 |
| **B2** | **B2 phylogenetic group: O83:H1** | 100.00 | YP_006121348.1 | 98.89 | YP_006121349.1 |
| **D1** | **D1 phylogenetic group: UMN026** | 100.00 | YP_002414171.1 | 98.89 | YP_002414172.1 |
| **D2** | **D2 phylogenetic group: IAI39** | 100.00 | YP_002409426.1 | 98.22 | YP_002409427.1 |
| **B2** | **UPEC str. CFT073** | 99.54 | AAN82208.1 | 98.89 | AAN82209.1 |
| **A** | **K12 str. MG1655** | 99.54 | NP_417497.1 | 98.89 | NP_417498.1 |
| **B1** | **B1 phylogenetic group: O104:H4** | 99.54 | AFS72693.1 | 98.22 | AFS72692.1 |
| **B1** | **EAEC str. E55989** | 99.54 | CAU99558.1 | 98.22 | CAU99560. |

| | | | | | |
|---|---|---|---|---|---|
| **E** | **EHEC str. EDL933** | 99.54 | AIG70396.1 | 98.22 | AIG70397.1 |
| **E** | **EPEC O55:H7 str. CB9615** | 99.54 | ADD58237.1 | 98.22 | ADD58238.1 |
| **E** | **O157:H7 str. Sakai*** | 99.54 | NP_311934.1 | 97.13 / 98.55 | NP_3909913-3910437 NP_3910431-3911261 |
| **B1** | **ETEC O139:H28 str. E24377A** | 99.07 | ABV19769.1 | 98.22 | ABV17955.1 |
| | **Additional enteric bacteria** | | | | |
| | ***Shigella sonnei* str. Mosely** | 100.00 | EJL13232.1 | 99.11 | EJL13233.1 |
| | ***Salmonella enterica* Typhimurium str. LT2** | 87.67 | NP_462092.1 | 79.29 | NP_462093.1 |
| | ***Salmonella enterica* Typhimurium str. 14028S** | 87.67 | ACY90252.1 | 79.29 | ACY90253.1 |
| | ***Klebsiella pneumoniae* str. 342** | 83.11 | ACI08570.1 | 67.04 | ACI08526.1 |
| | ***Edwardsiella tarda*** | 74.89 | ADO13165.1 | 56.35 | ADO24152.1 |

***Sakai has a stop codon in the middle of this putative QseC sequence rendering QseC non-functional in this strain.**

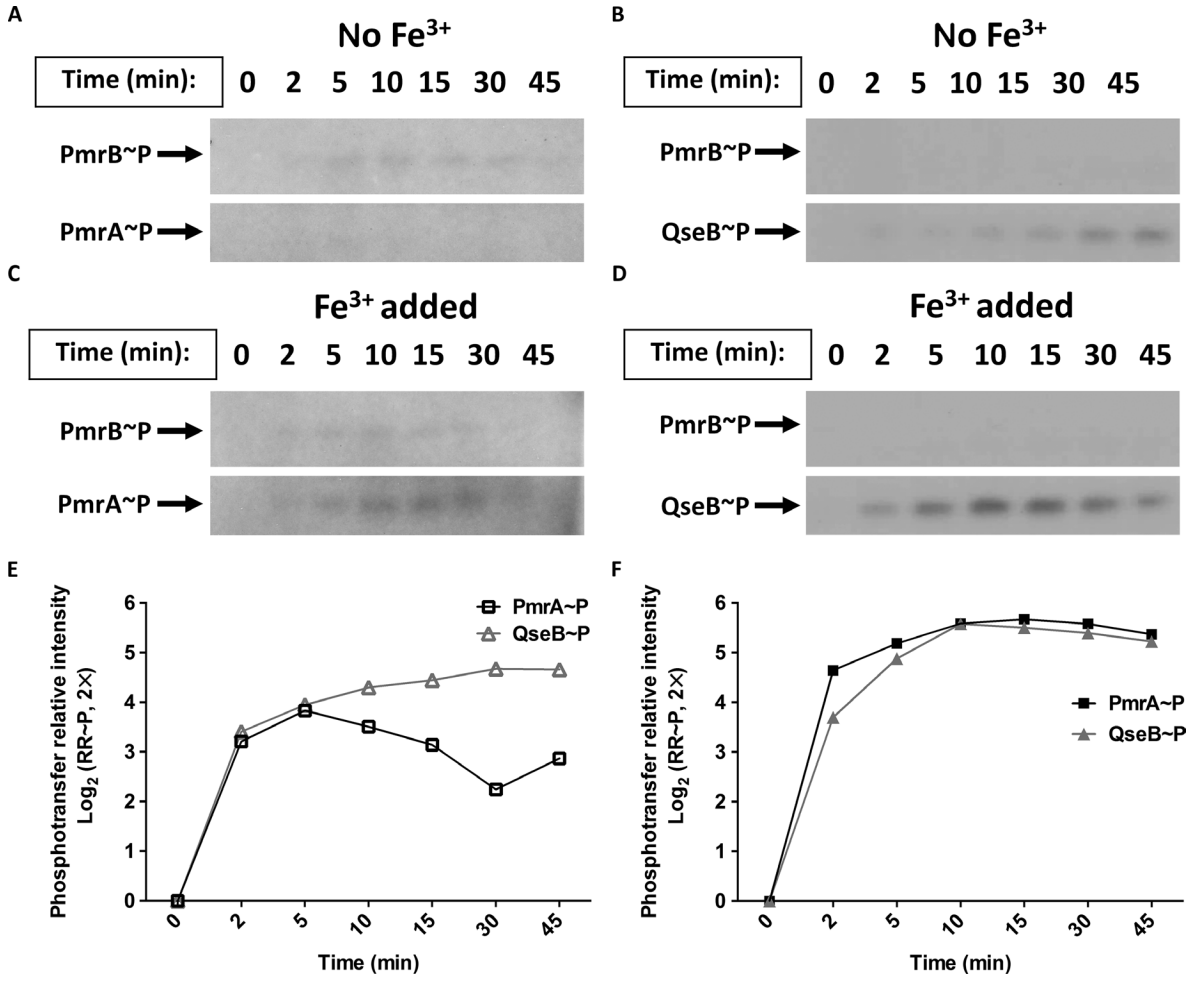


**Figure 12: Ferric iron enhances PmrB phosphotransfer activity.** (**A** and **B**) Representative radiographs tracking the autophosphorylation of PmrB in membrane fractions from UTI89 cells and subsequent phosphotransfer of radiolabeled adenosine triphosphate (ATP) from PmrB to PmrA (**A**) and QseB (**B**) in the absence of $Fe^{3+}$, n = 3. (**C** and **D**) Representative radiographs tracking the autophosphorylation of PmrB and the subsequent phosphotransfer of radiolabeled ATP from PmrB to PmrA (**C**) and QseB (**D**) in the presence of $Fe^{3+}$, n = 3. (**E** and **F**) Representative quantification of phosphorylated forms of the response regulators (RR~P) PmrA (PmrA~P, squares) and QseB (QseB~P, triangles) over time in the absence (**E**) or presence (**F**) of $Fe^{3+}$. Abundance was normalized relative to abundance at t = 0.

(**Fig. 12, E and F**). These data indicate that the presence of $Fe^{3+}$ changed the kinetic behavior of PmrB toward both cognate (PmrA) and non-cognate (QseB) partners.

*QseB and PmrA cooperatively control the expression of ferric iron–regulated targets*

Given the activation of PmrA and QseB in response to $Fe^{3+}$ *in vitro*, we assessed whether PmrA and QseB were both required for optimal induction of $Fe^{3+}$–stimulated transcripts. YibD is a glycosyltransferase, and *PmrA* stimulates *yibD* expression in response to ferric iron in *Salmonella enterica* (225-227). The promoter of UPEC *yibD* also contains a PmrA binding consensus site and is bound by PmrA in *in vitro* assays (186). Whereas ferric iron induced a surge of *yibD* expression in the UPEC strain UTI89, this surge was abolished in UTI89Δ*pmrA* and reduced by fivefold in UTI89Δ*qseB* (**Fig. 13A**). Subsequent electrophoretic mobility shift assays (EMSAs) indicated that PmrA and QseB each bound to the *yibD* promoter, albeit at different pmol concentrations (**Fig. 13, B and C**). Addition of *in vitro* phosphorylated PmrA (PmrA~P) caused a discernable mobility shift of DNA corresponding to a portion of the *yibD* promoter at a concentration of 30 pmol of purified protein per reaction, whereas *in vitro* QseB~P (177) caused a mobility shift only when present at a concentration of 100 pmol per reaction (**Fig. 13, B and C**).

*PmrA and QseB mediate UPEC transient resistance to polymyxin B*

Studies in *Salmonella enterica* established that the PmrAB TCS induces LPS modifications to buffer against damage caused by antimicrobial peptides such as polymyxin B (225). In *Salmonella,* the PhoPQ TCS cooperates with PmrAB to control LPS modifications in response to increased ferric iron and decreased magnesium, as well as in response to cationic polypeptide assault (215). However, the same coordination of the response to ions has not been demonstrated

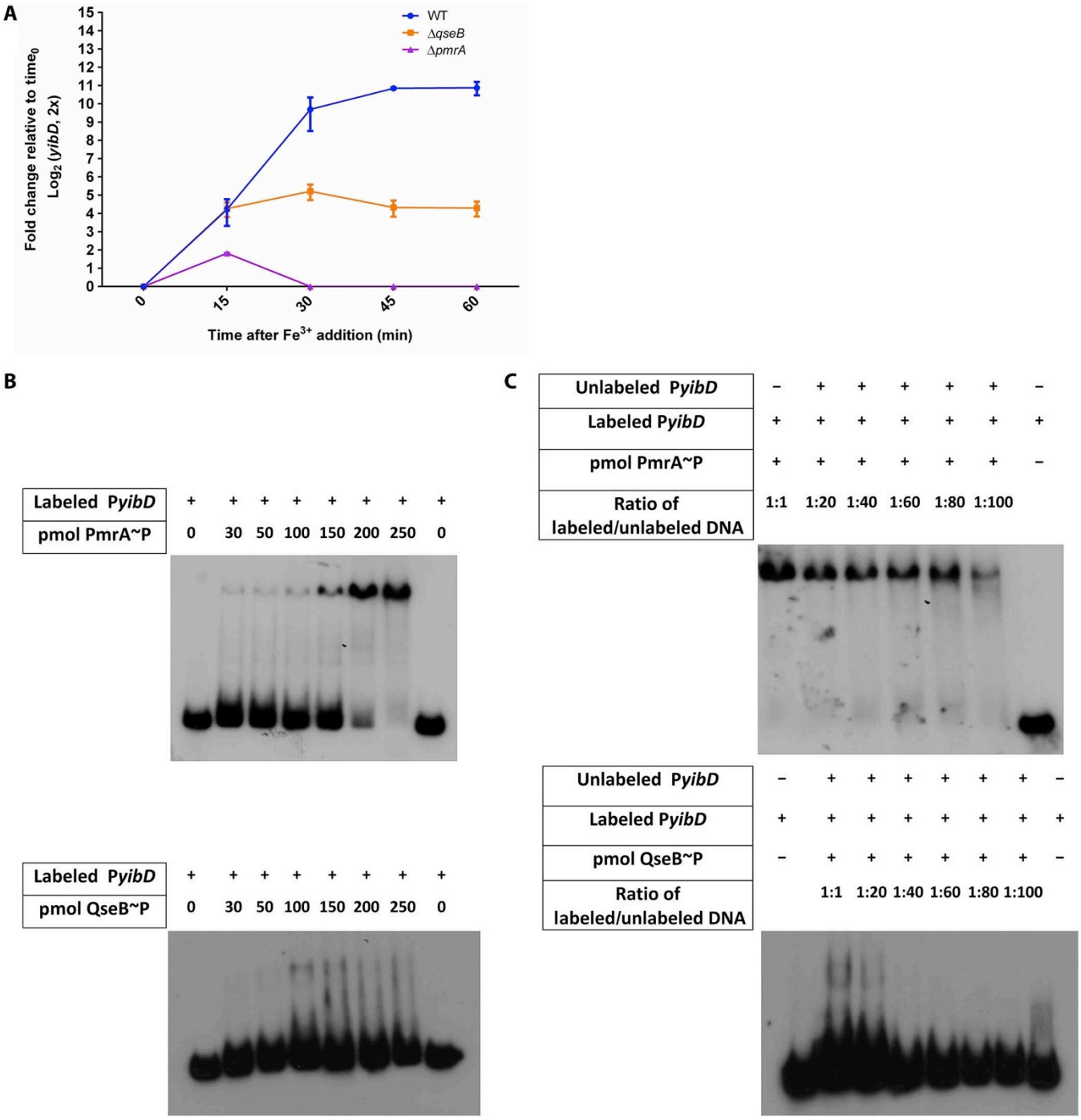


**<u>Figure 13</u>: Additional targets directly controlled by both PmrA and QseB in response to ferric iron.** (**A**) *yibD* expression in response to $Fe^{3+}$ was measured in UTI89, UTI89Δ*pmrA*, and UTI89Δ*qseB* using qRT-PCR. The abundance of *yibD* at each time point was normalized to the abundance in each strain at t = 0, using *gyrB* as an endogenous control to calculate $\Delta\Delta C_T$ values. Error bars indicate SEM, n = 3. WT, wild type. (**B**) EMSA using a radiolabeled 105–base pair (bp) fragment of the *yibD* promoter incubated with indicated amounts of *in vitro* PmrA~P or QseB~P. (**C**) Mobility shift of radiolabeled *yibD* promoter induced by incubation with PmrA~P

for PmrAB and PhoPQ in *E. coli* where pretreatment of *E. coli* with polymyxin B or similar cationic polypeptides does not induce resistance (176). However, pretreatment with ferric iron does. On the basis of the observation that QseB and PmrA co-stimulate the expression of *yibD* (**Fig. 13A**), a target associated with LPS modifications, we tested the UPEC strain UTI89 and UTI89 mutants harboring deletions of QseBC, PmrAB, and PhoPQ components for PMB resistance after pretreatment with ferric iron. We grew the UPEC strain UTI89 and isogenic *pmr* and *qse* deletion mutants in the presence or absence of ferric iron for 2 hours and then exposed the cells to PMB (2.5 μg/ml) and subsequently assessed survival. As a control, *S. enterica* serovar Typhimurium strain 14028 was included in the experiments because it has previously been shown that *Salmonella* tolerance to PMB increases after incubation with ferric iron in a manner that is dependent on PmrAB and PhoPQ (176). Consistent with previous observations, *Salmonella* exhibited a higher overall tolerance to PMB, even in the absence of ferric iron conditioning. Conditioning with ferric iron before exposure to PMB resulted in comparable survival for the UPEC strain UTI89 and *Salmonella*, at about 75% (**Fig. 14A**). In UPEC, percent survival after preconditioning was statistically significantly decreased in the absence of PmrA, declining to 20%. Strikingly, the Δ*qseB* mutant exhibited even greater reduction in survival after PMB treatment despite ferric iron preconditioning, declining to about 10% compared to the pretreated UPEC strain UTI89. The mutants lacking both *pmrA* and *qseB* exhibited survival comparable to that of the Δ*pmrB* mutant. Unlike what has been reported for Salmonella (176, 228), deletion of *phoPQ* did not statistically significantly alter UTI89 survival, indicating that preconditioning with ferric iron increases UPEC tolerance to PMB through coordinated regulation of downstream targets by PmrAB and QseBC.

Examination of PMB MICs without pretreatment indicated overall sensitivity of WT and

deletion strains, except for UTI89Δ*qseC*Δ*pmrA* in which the PmrB to QseB reaction is favored (**Fig. 14A**) To determine whether this phenotype was strain-specific, we tested various other strains of extraintestinal pathogenic *E. coli* (ExPEC), including the well-characterized strains EC958 and CFT073, as well as urinary isolates collected from the Vanderbilt University Hospital. PMB tolerance after ferric iron preconditioning varied among the different strains. Vanderbilt urinary tract isolates (VUTIs) 39, 47, 61, and 77 and CFT073 exhibited increases in PMB tolerance after ferric iron pretreatment, with VUTI77 and CFT073 having the highest tolerance (**Fig. 15**). However, VUTI61 and EC958 exhibited no difference in PMB susceptibility with or without ferric iron pretreatment, suggesting that the observed effects with PMB are neither strain-specific nor universally shared among all urinary *E. coli* isolates. Such differences could be attributed to the differential interactions between the TCSs driven by SNPs within key protein interaction surfaces, differences in the carriage of genes dedicated to LPS modifications, or variability in LPS constitution. Increase in *mcr-1* carriage, a plasmid encoded colistin resistance gene, and the idea that cross-regulation between PmrAB and QseBC increases UPEC tolerance to PMB transiently, indicates need for better testing and alternative therapeutics. These differences in LPS modification following pretreatment with ferric iron may lead us to better diagnostic assessments of resistance to the last resort drugs such as colistin (211).

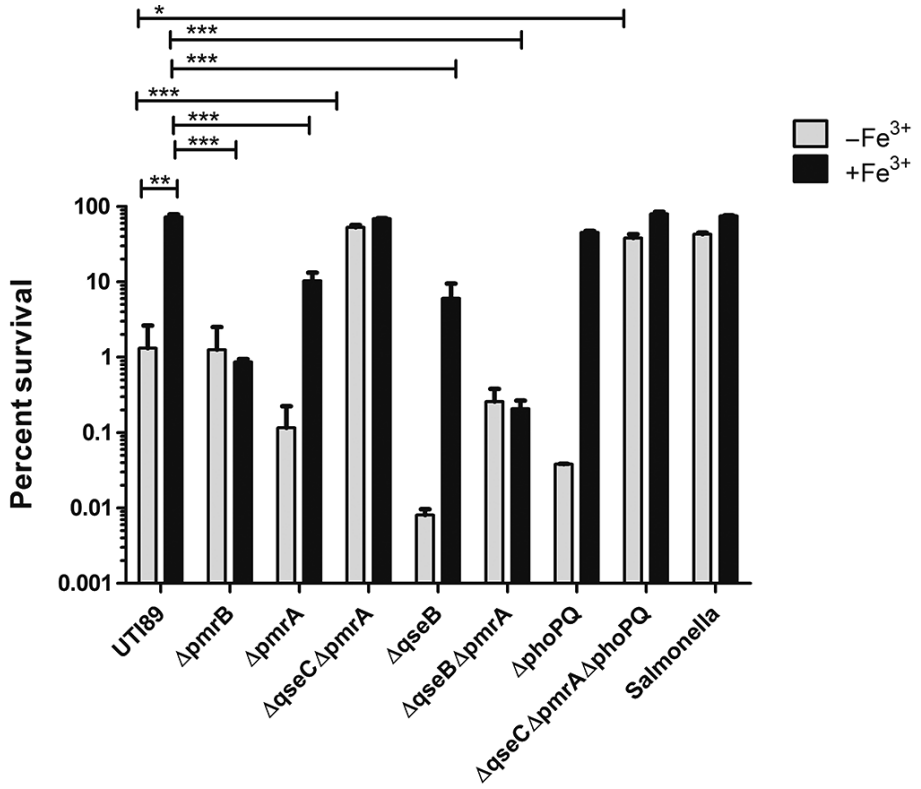


**Figure 14: Ferric iron enhances resistance to PMB in a manner that depends on both PmrA and QseB.** Tolerance of UTI89, indicated UTI89 deletion strains, and *S. enterica* Typhimurium 14028 to PMB with or without $Fe^{3+}$ preconditioning. Error bars represent SEM, n = 3; *$p < 0.05$, **$p \leq 0.01$, ***$p \leq 0.001$.

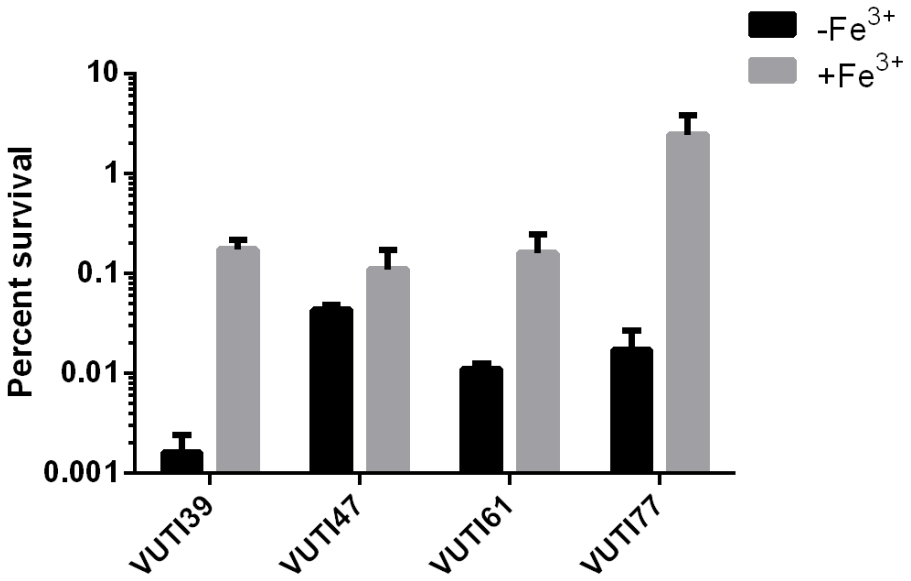


**Figure 15: PMB tolerance after ferric iron preconditioning varies between clinical urinary isolates.** Graph depicts tolerance of various clinically isolated *E. coli* strains to 2.5 μg/mL polymyxin B with or without ferric iron preconditioning. "-$Fe^{3+}$" indicates cells grown in N-minimal media without additional ferric iron before exposure to polymyxin B. "+$Fe^{3+}$" indicates cells grown in N-minimal media with ferric iron before exposure to polymyxin B. Survival was calculated by dividing the number of colony forming units (CFUs) recovered after polymyxin B incubation by the number of CFUs recovered after incubation in PBS alone, and multiplying by 100. Error bars represent standard error of the mean (SEM), n=3 biological replicates.

### 3.4 Discussion

A handful of previous studies have described histidine kinases that are capable of phosphorylating both their cognate partner and a non-cognate response regulator in bacterial cells (202, 204-206). These examples can be found in multiple bacterial species, including cross-phosphorylation of YycF by PhoR in *Bacillus subtilis* (203) and interactions between ArcB and OmpR in *E. coli* (202). In these examples, cross-regulation between TCSs is critical for mediating appropriate responses to environmental stress. However, in these cases, the presence of the two interacting non-cognate partners is sufficient for the proper response, unlike the QseBC and PmrAB systems, where all four components are required for appropriate responses to signal (**Fig. 9**).

In *Rhodobacter capsulatus*, interacting TCSs NtrBC and NtrXY have been reported to mediate nitrogen responses. Bacteria lacking the NtrC response regulator, or both the NtrY and NtrB histidine kinases, cannot properly use molecular nitrogen ($N_2$) or urea as a nitrogen source. This suggests interactions between non-cognate partners NtrY and NtrC in wild-type cells (205). However, unlike the PmrB non-cognate interaction described in this study, no specific signal that initiates NtrY-NtrC interactions has been identified. NarPQ and NarLX are interacting TCSs that control nitrate metabolism in the nonpathogenic *E. coli* strain K12. The histidine kinases NarQ and NarX can phosphorylate both response regulators NarL and NarP both during *in vitro* assays and under physiologic conditions within the bacterium. NarX preferentially senses nitrate, but NarQ senses both nitrate and nitrite. To fine-tune responses to these stimuli, there is a kinetic bias toward the different response regulators (182, 204). Whereas NarQ has a slight kinetic preference for NarL, NarX has a very strong kinetic preference for NarL, which allows NarX to de-phosphorylate NarL when nitrate is absent (182, 204, 229). In contrast, the QseBC-PmrAB interactions described appear to be coordinated in response to a single stimulus, which culminates

in the kinetically equivalent phosphorylation of two response regulators, at least based on *in vitro* phosphotransfer assays (**Fig. 12**).

Although our transcriptional studies focused mostly on the *qseBC* operon, we observed similar interactions for an additional shared transcriptional target, *yibD*. This target was previously reported to be part of the extensive PmrAB regulon in *Salmonella* (225-227). To date, the only direct transcriptional targets reported for QseB have been *qseBC* and *flhDC* (178, 213). Deletion of either *pmrA* or *qseB* diminished the *yibD* and *qseBC* transcriptional surge in response to ferric iron (**Fig. 13A**), suggesting that both *yibD* and the *qseBC* operon are part of the QseBC-PmrAB regulon in *E. coli* and that QseB augments transcription of *yibD* in the presence of PmrA. In other reports, mutation of *pmrA* decreases the survival of *E. coli* MG1655 in the presence of PMB by several orders of magnitude (176). Here, we show that the decrease in survival caused by PMB is smaller for UTI89 than that reported for MG1655. This could be differences in the QseBC/PmrAB residues important for this interaction; the expression carriage of genes that are critical for LPS modification. Notably, differences in tolerance to antimicrobial agents were highly variable in the VUTI strains we analyzed; this too supports the possibility that single-nucleotide polymorphisms or other genomic variations in these strains, may be responsible for altered stimulus response.

The involvement of QseC in mediating the proper surge and decline of the transcriptional responses to ferric iron is not yet clear; when QseC is absent, any *qseBC* transcriptional surge is obscured by constitutively high *qseB* expression (**Fig. 12E**). *In silico* sequence scanning reveals that PmrB and QseC share 33.53% sequence identity. Other sensors with similarly high identity, such as NarX and NarQ (28.5% identity) and AtoS and ZraS (27.6% identity), are known to cross-regulate to allow cells to adjust to environmental stress (205, 224). The increase in PMB

tolerance seen in UTI89 after ferric iron conditioning (**Fig. 16**) suggests that the cross-interactions between QseBC and PmrAB may aid the bacteria in fine-tuning responses to stress imposed by cationic stress such as the last line of defense drug, colistin, which exhibits the same mechanism of action as PMB.

One possible mechanism for QseC-mediated control of the ferric iron response is heterodimerization of QseC with PmrB, which would prevent aberrant phosphotransfer between PmrB and QseB until the presence of ferric iron favors the formation of homodimers. Alternatively, QseC could sequester QseB and prevent QseB from interacting with and being phosphorylated by PmrB in the absence of signal. Future studies will focus on delineating the potential protein-protein interactions that could be contributing to the tight control of QseBC-PmrAB responses to ferric iron. This hypothesis was tested as described in Chapter IV.

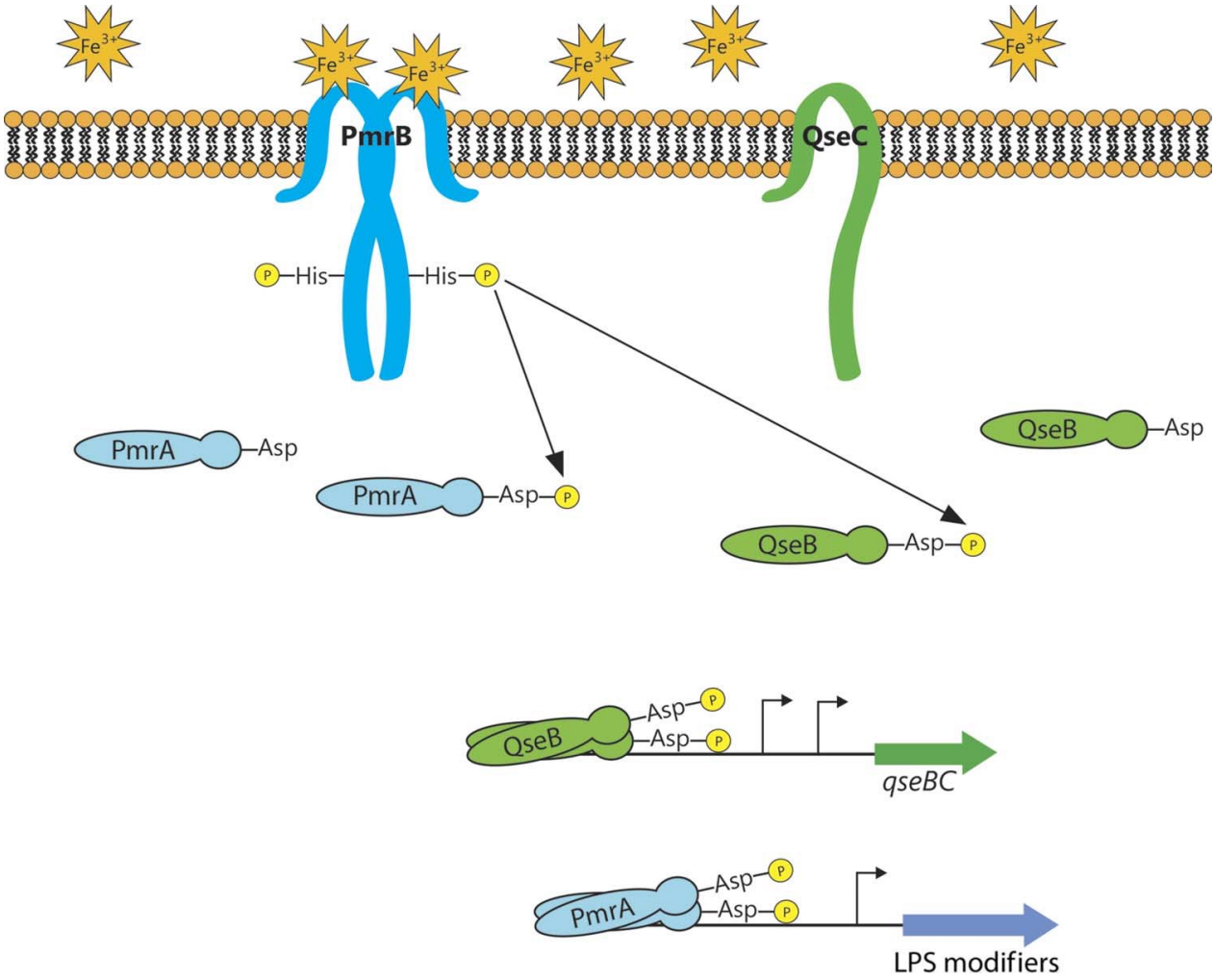


**Figure 16: Model of PmrAB and QseBC signal transduction in response to ferric iron.** Ferric iron is sensed by the sensor kinase PmrB, which, in turn, phosphorylates both the cognate response regulator PmrA and the non-cognate response regulator QseB. The phosphorylated response regulators stimulate transcription from the *qseBC* promoter and alter the expression of genes involved in modifying LPS. The role of QseC is ambiguous in the signaling cascade but is required for physiologically relevant signaling in the UPEC strain UTI89.

CHAPTER IV

# THE QSEC HISTIDINE KINASE CONTROLS PMRB-QSEB INTERACTIONS BY SEQUESTERING QSEB AWAY FROM THE NON-COGNATE PARTNER

This chapter has adapted from Breland *et al.* "The histidine residue of QseC is required for canonical signaling between QseB and PmrB in uropathogenic *Escherichia coli*" in the *Journal of Bacteriology*. (2017). PMID: 28396353

Our previous work demonstrated that response of uropathogenic *E. coli* to ferric iron requires cross-regulation between QseBC and PmrAB (Chapter III, **Fig. 16,** (230)). The same studies assigned a role for PmrB as the signal receiver/transducer and established that the bacterial output response is coordinated via the action of both PmrA and QseB. However the contribution of QseC was not elucidated. In this work, we present evidence indicating that QseC relies on reverse-phosphotransfer to catalyze the de-phosphorylation of its cognate partner, QseB. This function is essential for the proper stimulus response to ferric iron.

## 4.1 Introduction

As discussed in chapter II, bacterial histidine kinases comprise multiple domains, including diverse extracellular sensing domains, a semi-conserved dimerization and histidine phosphotransfer domain (DHp), and a well-conserved catalytic ATP-binding domain (Chapter II, **Table 1**) (123, 137). Conserved sequence motifs, or homology boxes, exist among all histidine kinases and are termed the H, N, G1, F, and G2 boxes (**Fig. 17**, Chapter II, **Table 1** (137, 231)). Auto-phosphorylation, in response to signal, occurs on a conserved histidine residue located in the "H box" of the cytoplasmic kinase domain (123). The C-terminal conserved catalytic domain, common in ATPases, is a distinct α/β sandwich fold (137). The N, G1, F, and G2 boxes

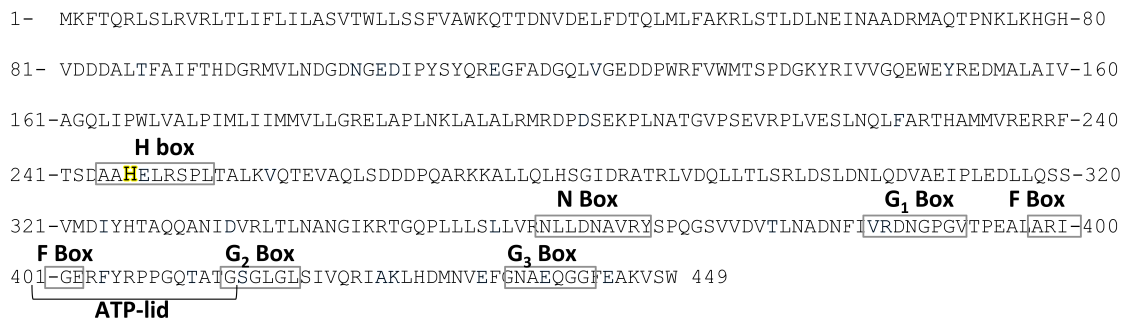


**Figure 17: QseC amino acid sequence and defined domains.** The QseC (UTI89_C3451) amino acid sequence from UPEC strain UTI89. In gray boxes are well-defined domains, common to many sensor histidine kinases. The H box is harboring the conserved phosphorylated histidine residue (yellow).

comprise a conserved ATP binding cavity and between the F and G2 boxes, a linker region can adopt different conformations based on differential nucleotide binding; this linker is termed the ATP lid (137). In most cases to date, the response regulator associated with a bacterial TCS serves as a transcriptional regulator (232), the phosphorylation of which leads to dimerization and exposure of a DNA binding domain that, in turn, leads to engagement of target promoters and alteration of gene transcription (122, 123, 181, 196, 199).

Even though the structures of the catalytic and regulatory domains of histidine kinases and response regulators are largely conserved across TCSs (233), numerous studies have revealed distinct mechanisms by which TCS partners communicate to carry out proper stimulus responses. Recent studies have also elucidated examples in which protein-protein interactions occur across two TCSs, like in the case of the QseBC and PmrAB (230). Previous studies with several bacterial pathogens identified that deletion of the *qseC* gene, which codes for the QseC histidine kinase, attenuates bacterial virulence (101, 177, 221). Studies in uropathogenic *E. coli* (UPEC) investigating the basis of bacterial attenuation in the Δ*qseC* mutant uncovered that loss of QseC leads to a high abundance of phosphorylated response regulator (QseB~P), that aberrantly regulates metabolic and virulence determinants (101, 177). Subsequent studies identified that increased levels of QseB~P in the *qseC* deletion mutant were due to the interaction of QseB with the PmrB sensor kinase of the PmrAB TCS (186). *In vivo* and biochemical studies demonstrated that PmrB could indiscriminately phosphorylate QseB at rates comparable to QseC and that deletion of the *pmrB* gene in the *qseC* deletion strain suppressed all the defective phenotypes associated with the absence of QseC (101, 177, 186, 208, 209). The observation that PmrB - QseB protein-protein interactions are nearly as robust as QseC – QseB interactions (186), raised the hypothesis that PmrB and QseB physiologically interact to mediate stimulus responses in

wild-type (WT) UPEC. Subsequent studies investigating the hypothesized PmrB-QseB interaction in UPEC, revealed that presence of the PmrB-activating $Fe^{3+}$ leads to phosphorylation of both PmrA and QseB by PmrB and results in elevated tolerance of UPEC to polymyxin B (230). The same studies also elucidated that phosphorylated PmrA (PmrA~P) and QseB (QseB~P) co-regulate downstream targets, that in *Salmonella* spp. are exclusively controlled by PmrA (230). Together, these studies provided evidence of two TCSs, whose partner proteins interact to mediate a particular response. However, while these previous studies established a clear role for PmrB in its molecular interaction with QseB, the precise molecular function of QseC in the PmrAB-QseBC signal transduction circuitry remains elusive. Given that deletion of the *qseC* gene leads to a constitutive interaction between PmrB and QseB that, in turn, leads to high abundance of QseB~P, it was hypothesized that QseC acts as a bi-functional sensor that maintains QseB in the de-phosphorylated, "OFF", state in the absence of signal by mediating QseB de-phosphorylation (177, 186). The mechanism by which QseC de-phosphorylates QseB~P is unknown. In this work, we present evidence indicating that QseC-mediated de-phosphorylation of QseB occurs via reverse phosphotransfer and that the conserved H246 residue on QseC is required for proper stimulus response to $Fe^{3+}$.

## 4.2 Materials and Methods

*Strains and constructs*

UTI89Δ*qseC*, UTI89Δ*pmrB*Δ*qseC*, and the corresponding, pQseC, and pQseC-mycHis plasmid constructs harboring the corresponding wild-type *qseC* gene sequences were described previously (177, 186). QseC single-point mutation variants were constructed using site-directed mutagenesis as described in the relevant section below. Recombination of constructs into the *qseC*

chromosomal locus was performed following the protocol previously described (234).

*Site-directed mutagenesis*

Site-directed mutagenesis was performed on pQseC and pQseC-mycHis as we previously described (177, 186) and using the primer sets listed in Table A1. Constructs were introduced into UTI89Δ*qseC* via electroporation (101, 177, 186) and validated by plasmid isolation and sequencing.

*Motility assays*

Motility assays were performed as previously described (235). Bacteria were picked from single colonies and inoculated in Lysogeny Broth (LB) for overnight (18 h) static incubation at 37 °C. Approximately 5 uL from each overnight were then stabbed into 0.25% LB agar supplemented with 0.001% 2,3,5-triphenyltetrazolium chloride. Plates were incubated at 37 °C for 7 h. Motility was evaluated by measuring the motility diameters. Experiments were performed a minimum of three times with triplicate plates/strain. Statistical analysis was performed using one-way ANOVA with a Dunnett's multiple comparisons correction.

*Preparation of QseC-enriched membranes*

UTI89Δ*qseC*/pQseC-mycHis and all UTI89Δ*qseC*/pQseC_mycHis_variants were grown to an $OD_{600}$ = 0.6, in LB with shaking at 37°C and induced with 0.02% arabinose for 2 h. Cells were broken by French Press (1000 p.s.i.) and total membranes were isolated by 1 h ultra-centrifugation at >1,000,000 × *g*, re-suspended in 20 mM Tris pH 8.0/1 mM $MgCl_2$ as we previously described (177, 186).

*Kinase and in vitro de-phosphorylation assays*

Membranes from each strain (7 μg) were incubated in the absence or presence of purified QseB (14 μg) with 0.7 μCi (γ-32P)-ATP, in 1 × TBS/0.5 mM DTT/0.5 mM $MgCl_2$ per reaction. A 7-15 reaction master-mix (depending on the extent of the time-course) was prepared and 10 μl aliquots were removed at different time points, mixed in a 1:1 ratio with 2 × SDS loading buffer and kept on ice until SDS-PAGE. For the phosphatase assays, beads were prepared and used to *in vitro* phosphorylate QseB according to (184). QseB~P (0.2 nmol, equal to 9,000 c.p.m) was incubated at room temperature with 7 μg of membrane vesicles in 1 × TBS/0.5 mM DTT/0.5 mM $MgCl_2$. Aliquots (10 μl) were withdrawn from the reaction master-mix and treated as described above. Gels were dried and exposed to X-ray film for 48 h at -80 °C. Band intensities corresponding to QseB~P over time were quantified using ImageJ software and normalized to QseB~P at t = 0. All experiments were repeated 2-4 times.

*QseB purification*

The pQseB-mycHisA construct used for QseB expression and purification was previously created (177). QseB expression was induced with 0.1% arabinose and QseB was affinity-purified using a Talon column (Clontech), followed by anion exchange chromatography through a MonoQ column (GE Healthcare), as described in (177).

*Quantitative real time PCR expression analysis*

Samples were collected at the specified time-points from cultures grown to exponential phase at 37 °C with shaking and samples were collected at the specified time-points. RNA was extracted from bacteria using the RNeasy kit (Qiagen), DNase-treated using Turbo DNase I (Ambion), and reverse transcribed using Superscript II Reverse Transcriptase (Invitrogen). DNAse-treated RNA

samples not subjected to reverse transcription were used as negative controls. qPCR was performed in triplicate using 50 ng cDNA per reaction. cDNA was amplified using *qseB* and *rrsH* specific primers listed in Table A1. Relative fold change was determined by the $\Delta\Delta C_T$ method where transcript abundances were normalized to *rrsH* abundance. Quantitative real time PCR was performed using an ABI StepOne Plus Real Time PCR machine, using multiplexed TaqMan MGB chemistry.

### 4.3 Results and Discussion

*QseC-mediated de-phosphorylation of QseB occurs via reverse phosphotransfer and requires the QseC H246 residue*

Phosphorylation of QseC is predicted to occur at the conserved H246 residue. To begin investigating the role of H246 in PmrAB-QseBC interactions, we performed site-directed mutagenesis on the *qseC* gene sequence to alter the H residue into alanine (H246A), aspartate (H246D), or leucine (H246L). These substitutions were selected so as to represent 1) non-charged (A), 2) oppositely charged (D), and 3) a non-polar (L) alterations. As expected, each QseC_H246 variant was abolished for auto-kinase and kinase activities (**Fig. 18**), indicating that no other residue is phosphorylated in QseC under the conditions tested. In UPEC, loss of QseC leads to accumulation of QseB~P due to the ability of the PmrB kinase to phosphorylate QseB indiscriminately (186). These past observations led to a model in which QseC is predicted to regulate the level of QseB~P via de-phosphorylation (177). Interestingly, testing of the kinase-inactive QseC_H246A/D/L variants for their ability to de-phosphorylate QseB~P *in vitro* revealed that the QseC_H246 variants were unable to de-phosphorylate QseB~P in the *in vitro*

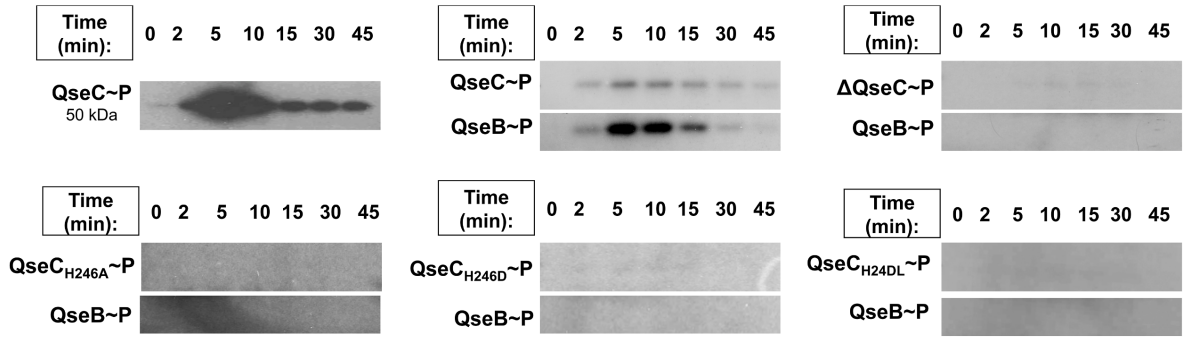


**Figure 18: QseC_H246 variants are kinase-inactive.** Panels depict radiographs tracking the kinase activity of QseC and QseC_H246A/D/L proteins. Top row, left: Purified QseC-enriched total membranes incubated with γ-$^{32}$P-ATP over a period of 45 minutes to track QseC autokinase activity. Samples were taken at the indicated time-points, quenched with the addition of 2 × SDS sample buffer and stored on ice prior to loading. Top row, middle: Control kinase reaction using purified QseC-enriched membranes and purified QseB protein. Reaction was set up as for the autokinase reaction, but with QseB included in the reaction prior to addition of γ-$^{32}$P-ATP. Top row, right: Control kinase reaction using purified QseB with total membranes from UTI89Δ*qseC* to verify that the phosphotransfer observed comes solely from the action of QseC. Bottom panel: Kinase reactions tracking the activity of QseC H246 variants. All images are representative of at least 3 biological replicates.

conditions used, with the exception of H246D, which facilitated partial QseB de-phosphorylation by 30-45 minutes of incubation (**Fig. 19**). These data suggest that, at least *in vitro*, QseC mediates de-phosphorylation of QseB~P via reverse phosphotransfer and not by exhibiting phosphatase activity as it is typical for other sensor histidine kinases. Indeed, the wild-type QseC protein begins dephosphorylating QseB~P as soon as the reaction is started (**Fig, 19**, top left panel) and the phosphoryl group appears to be returned onto the QseC protein over the period tested (**Fig, 19**, top left panel).

*The QseC_H246 variants rescue the qseC deletion phenotype of UTI89ΔqseC*

Deletion of the *qseC* gene in UPEC leads to repression of motility via the action of QseB~P on the expression of the *flhDC* gene pair that codes for the master flagella regulator (177). Based on the *in vitro* reaction observations, it is expected that the QseC_H246A/D/L variants would be unable to suppress the motility defect of the Δ*qseC* deletion mutant. Surprisingly, all variants rescued motility when introduced to UTI89Δ*qseC* (**Fig. 20A**). In order to eliminate the possibility that copy-number effects associated with using plasmid constructs may be influencing our observations, we employed a recently developed negative selection recombineering approach (234) to reinsert the corresponding mutated *qseC* sequences back into the UTI89 chromosomal locus. When tested, the resulting strains were as motile as wild-type UTI89 (**Fig. 20B**), indicating that the QseC_H246A/D/L variants can indeed rescue the motility defect of UTI89Δ*qseC*, despite their inability to de-phosphorylate QseB~P via reverse phosphotransfer. This finding suggested that QseC does not need to phosphor-transfer to and from QseBC in order to regulate its function. In the absence of QseC, QseB~P binds and induces the expression of *qseBC* resulting in increased levels of *qseB* steady-state transcript (101, 186, 230). qPCR analysis demonstrated that introduction of the mutated *qseC* sequences suppressed the aberrant expression of *qseB*

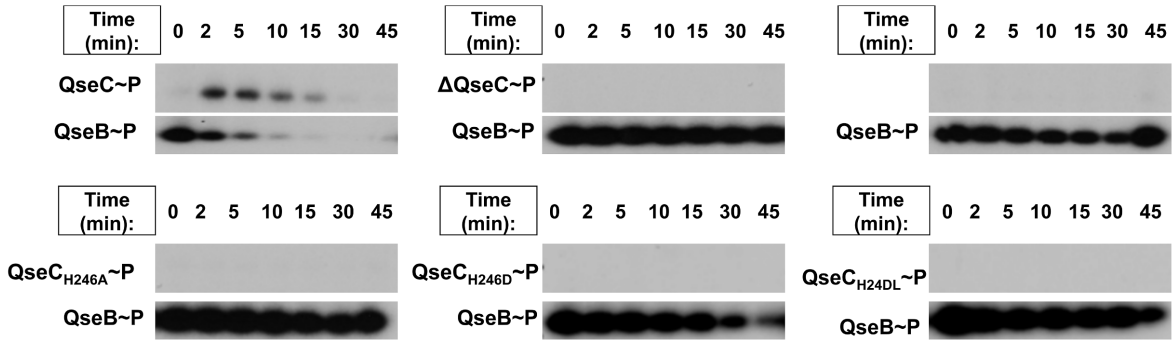


**Figure 19: QseC H246 variants cannot mediate de-phosphorylation of QseB~P.** Panels depict the result of *in vitro* de-phosphorylation assays comparing the ability of QseC_H246A/D/L variants to mediate the de-phosphorylation of previously *in vitro*-phosphorylated QseB (QseB~$^{32}$P). Top panel, left: Reaction containing purified, *in vitro* phosphorylated QseB~$^{32}$P and total membranes containing QseC. Samples were taken at the indicated time-points, quenched with the addition of 2 × SDS sample buffer and stored on ice prior to loading. Top panel, middle and right: Control reactions containing previously *in vitro*-phosphorylated QseB (QseB~$^{32}$P) incubated with total membrane fractions prepared from UTI89Δ*qseC* (to verify that QseC is the only protein in the reaction mediating the de-phosphorylation of QseB~P) or with no membranes (to indicate the extent of spontaneous loss of the phosphoryl group from QseB~$^{32}$P). Bottom panels: Reactions containing purified, *in vitro* phosphorylated QseB~$^{32}$P and total membranes containing each of the QseC_H246 variants. Images are representative of at least 3 biological replicates.

(**Fig. 20C**), indicating that each QseC_H246 variant has the ability to prevent QseB-mediated activation of the *qseBC* promoter. Attempts to measure *in vivo* QseB~P levels in the strains expressing the QseC_H246 variants using Phos-Tag were unsuccessful, therefore we were unable to directly determine whether there are differences in the levels of QseB~P in the different strains.

We next employed a genetics approach to further investigate how the QseC_H246A/D/L variants may be rescuing the motility defects of UTI89Δ*qseC*. We reasoned that, if QseC functions by sequestering QseB away from PmrB, then over-expression of QseB should eventually saturate QseC-QseB interactions in all strains and allow for PmrB-mediated activation of the extra QseB copies. If QseC functions by physically sequestering PmrB away from QseB, then over-expression of *qseB* will not have an appreciable phenotype, while over-expression of *pmrB* should eventually lead to activation of QseB. Finally, if QseC exhibits *in vivo* phosphatase activity that is independent of the H246 residue (and which may not have been captured *in vitro*), then over-expression of QseB in either the WT or the strains harboring QseC_H246A/D/L variants would not abolish motility. We thus introduced previously created and validated QseB and PmrB plasmid constructs (177, 186) into WT UTI89, UTI89Δ*qseC*::QseC$_{WT}$, UTI89Δ*qseC*::QseC_H246A, UTI89Δ*qseC*::QseC_H246D and UTI89Δ*qseC*::QseC_H246L and tested the resulting strains for their ability to swim. Consistent with our previous observation (**Fig. 20B**), UTI89Δ*qseC*::QseC$_{WT}$ exhibited wild type levels of motility, which was unaffected upon introduction of QseB or PmrB extra-chromosomally (**Fig. 20**D, dark blue bars). This demonstrated that QseC-mediated de-phosphorylation by reverse phosphotransfer is sufficient in controlling the levels of multiple copies of QseB. Introduction of pPmrB into each of the strains expressing QseC_H246-variants had little effect on motility, suggesting that QseC does not function by sequestering PmrB away from QseB in the absence of

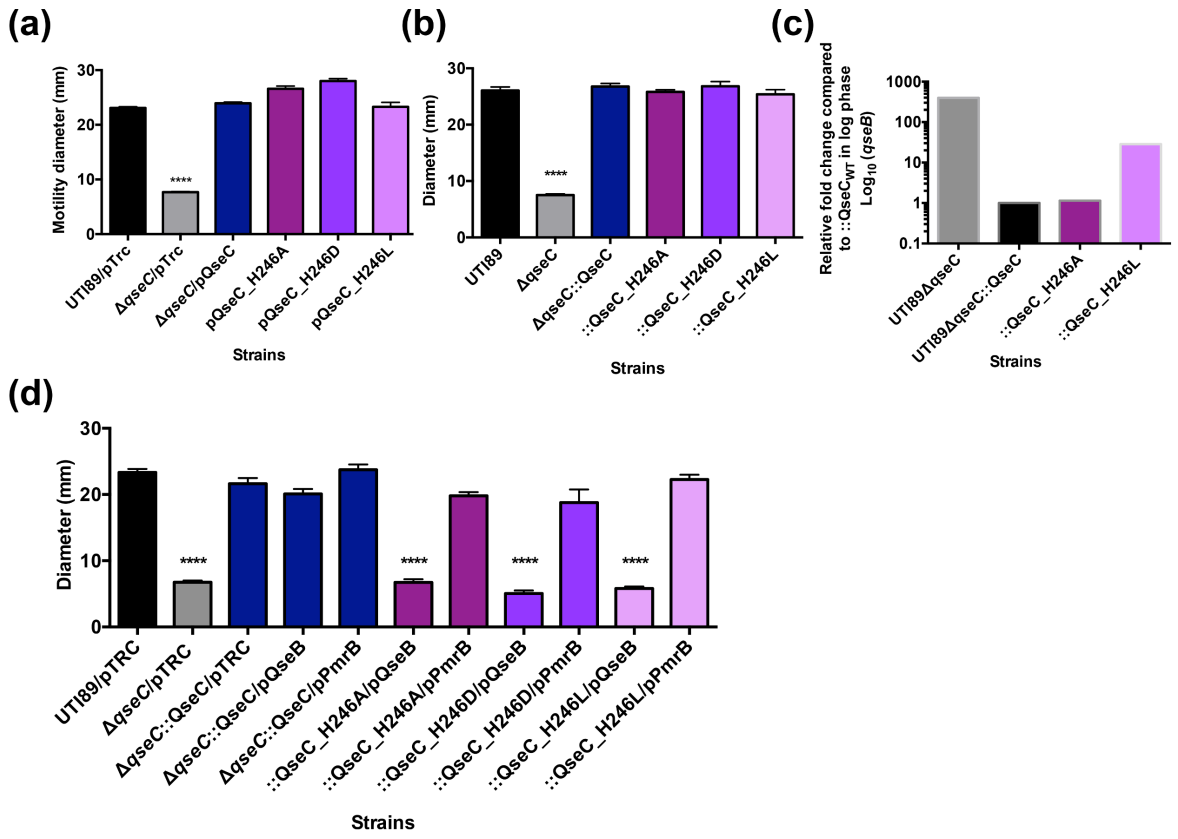


**Figure 20: The QseC-H246A/D/L variants rescue the motility defect of UTI89Δ*qseC* by sequestering QseB**. **A-B** and **D**) Graphs depict motility diameters of isogenic UTI89 strains expressing different QseC variants. Motility diameters were measured after bacteria were stabbed in soft agar supplemented with tetrazolium chloride and incubated at 37 °C for approximately 7 h. Graph depicts the average of at least 3 biological replicates. ***, $p<0.0001$ by one way ANOVA. (**A**) Motility of strains carrying empty vector (pTRC99A, designated as "pTRC"), or a vector that harbors the wild-type *qseC* (pQseC) or corresponding mutated *qseC* sequences (designated as pQseC_H246A, pQseC-H246D or pQseC-H246L. (**B**) Motility of strains in which the wild-type (WT) *qseC* allele or the mutated sequences encoding the QseC-H246 variants was recombineered into the chromosomal *qseC* locus. (**D**) Motility of strains in (**B**) harboring a plasmid that carries the wild-type *qseB* or *pmrB* genes under their native promoters. (**C**) Quantitative PCR analysis comparing *qseB* steady-state transcript in the strains expressing the QseC_H246A and QseC_H246L variants (designated as "::QseC_H246A" or "::QseC_H246L") to the *qseB* transcript levels in an isogenic *qseC* deletion strain (UTI89Δ*qseC*) and an isogenic strain harboring the wild-type *qseC* allele (UTI89Δ*qseC*::QseC). Relative fold change was determined by the $\Delta\Delta C_T$ method where transcript abundances were normalized to *rrsH* abundance. Quantitative real time PCR was performed using an ABI StepOne Plus Real Time PCR machine, using multiplexed TaqMan MGB chemistry.

signal. In contrast, introduction of pQseB in each of the QseC_H246 bearing strains led to significantly reduced motility (**Fig. 20D**). These data suggested that QseC_H246 variants rescue motility in the absence of signal by physically sequestering QseB away from PmrB.

*The QseC H246 residue is required for proper stimulus response by PmrAB-QseBC*

The *in vivo* motility results demonstrated that the phospho-inactive QseC_H246 variants rescue the *qseC* deletion phenotype in UPEC Δ*qseC* by sequestering QseB away from PmrB (**Fig. 20**). We have recently reported that in UPEC, there is coordinated regulation by QseB and PmrA to control the expression of targets involved in tolerance to polymyxin B (230). Specifically, activation of PmrB by $Fe^{3+}$ leads to a transient surge in *qseBC* transcription, which requires the activation of both PmrA and QseB (186). The presence of QseC is absolutely required for PmrB-QseB-PmrA-mediated stimulus response to $Fe^{3+}$ (230). To determine how the QseC_H246 variants would influence the $Fe^{3+}$ stimulus response we cultured UTI89Δ*qseC*::$QseC_{WT}$, UTI89Δ*qseC*::QseC_H246A, UTI89Δ*qseC*::QseC_H246D, and UTI89Δ*qseC*:: QseC_H246L in N-minimal media as previously described (200, 201, 230) in the presence and absence of $Fe^{3+}$ and monitored the *qseB* transcriptional surge using qPCR. UTI89Δ*qseC*::$QseC_{WT}$ exhibited a *qseBC* transcriptional surge in response to stimulation (**Fig. 21A**), as previously reported (230). However, *qseB* steady-state transcript in the strains expressing the QseC_H246 variants was delayed (H246A), or abolished altogether (H246L) (**Fig. 21B**), supporting the hypothesis that the QseC_H246 variants sequester QseB away from PmrB and this physical interaction is preventing canonical PmrB-QseB interactions in response to signal. To further validate that physical QseC_H246 – QseB interactions prevent canonical signaling by QseBC-PmrAB, we investigated

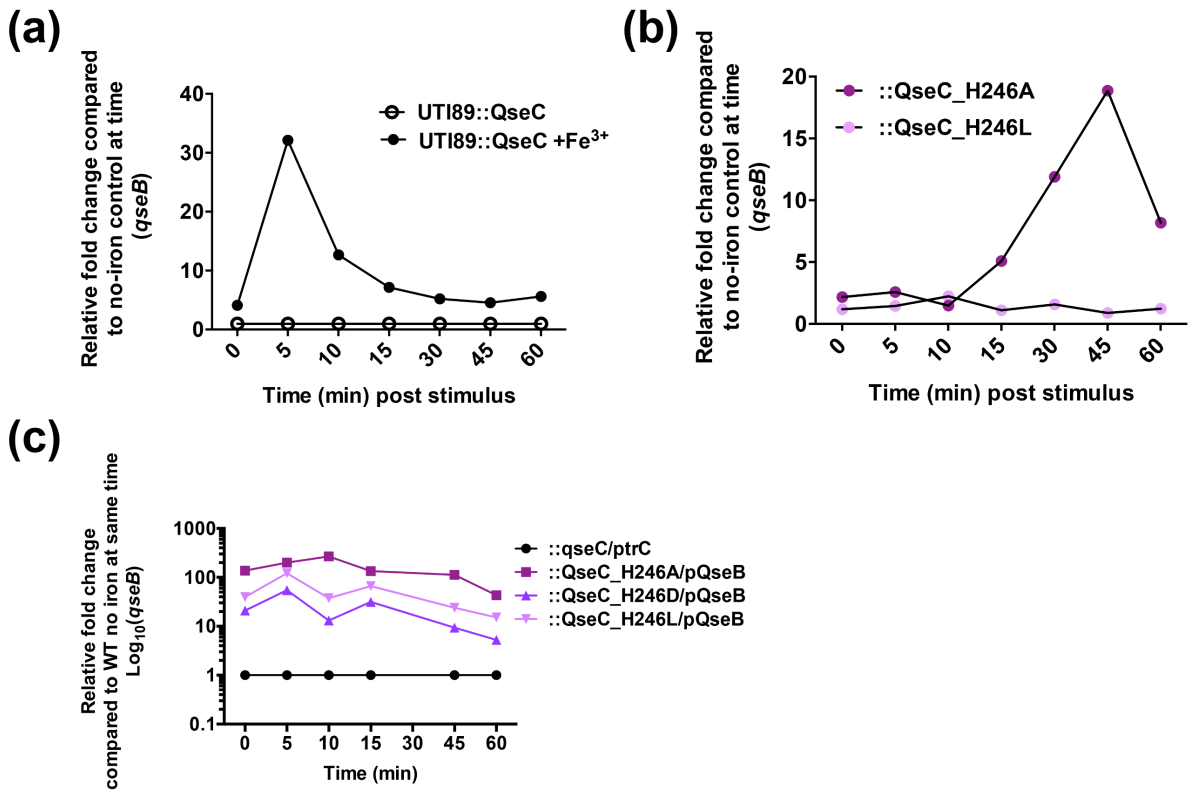


**Figure 21: The QseC H246 residue is required for canonical signaling through PmrB.** (**A**) qPCR analysis data depicting that wild-type UTI89 in which the wild-type *qseC* allele was removed and re-introduced via recombination, exhibits wild-type levels of *qseBC* induction surge in response to stimulation with $Fe^{3+}$. (**B**) Graph depicts steady-state *qseB* transcript levels in response to stimulation with $Fe^{3+}$in strains that express the QseC_H246A/L variants. Relative steady-state transcripts are normalized first to starting concentrations of each culture at t = 0 and then to the corresponding time-point of samples taken from the same strains without stimulation. (**C**) Graph depicts steady-state *qseB* transcript levels in response to stimulation with ferric iron in UTI89Δ*qseC* and in strains that express an extra copy of *qseB* in addition to expressing the QseC_H246A/L variants. Relative steady-state transcripts are normalized to cultures with no $Fe^{3+}$ at corresponding time points. Graphs are representative of the average of 2 biological replicates.

the effects of the QseC_H246 variants harboring the extra copy of *qseB* on the *qseBC* transcriptional surge in response to $Fe^{3+}$. We hypothesized that if the delay or abolishment of *qseBC* expression (**Fig. 21B**) were due to the ability of the QseC_H246 variants to better sequester QseB away from PmrB, then *qseB* expression levels in the *qseB* merodiploid strains would be similar to those of the *qseC* deletion strains once QseB levels exceed the native levels of QseC. qPCR analyses revealed that *qseB* transcription in the QseC_H246A/D/L strains harboring pQseB was constantly elevated (**Fig. 21C**), indicating that the inability of QseC to properly perform its kinase and reverse phosphotransferase activities has a deleterious effect on canonical PmrB signaling. Collectively, these data indicate that alteration of the H246 phospho-accepting residue of QseC abrogates the de-phosphorylating function of QseC and de-regulates the interaction between QseB and PmrB in response to $Fe^{3+}$.

### 4.4 Conclusions

Control of two-component system signaling is achieved via several means, including protein stability, sensor histidine kinase – response regulator protein – protein interactions, spatial tethering, as well as protein stoichiometry (224, 236-239). In phosphorelay systems, complexity is even higher, encompassing the use of accessory proteins that mediate phosphorylation/de-phosphorylation events in response to different cues (240, 241). In UPEC, the polymyxin resistance AB system, PmrAB, which is activated in response to high concentrations of $Fe^{3+}$(242), has been shown to interact under physiological conditions with the quorum sensing *E. coli* (Qse) BC system (186, 230) to mediate tolerance to PMB. In WT UPEC, addition of $Fe^{3+}$ in the media leads to increased expression of *qseBC* in a manner that is dependent on the response regulators PmrA and QseB (186). However, this interaction becomes uncontrolled in the absence of the

QseC sensor kinase, which led to the working model that the ability of QseC to de-phosphorylate QseB and "re-set" the system is essential for controlling the network (177) (**Fig. 22**). Here we present evidence of a mechanism in which QseC physically sequesters QseB away from PmrB in addition to serving as the primary controller of QseB via reverse phosphotransfer.

Notably, our studies have not yet evaluated how QseC interfaces with PmrA. Previous studies identified PmrA as a regulator of *qseBC* expression (186), where deletion of *pmrA* reduces expression of *qseBC* by 50% (186). Whether QseC contributes to phosphorylation of PmrA or QseB in response to $Fe^{3+}$ and how this action may be influencing the herein described observations, is unknown. Investigations are currently underway to determine whether QseC-PmrA interactions also occur and what their contribution is to this signaling network. Further dissection of the QseBC –PmrAB protein-protein interactions will provide insight into how this pathway is maintained and regulated.

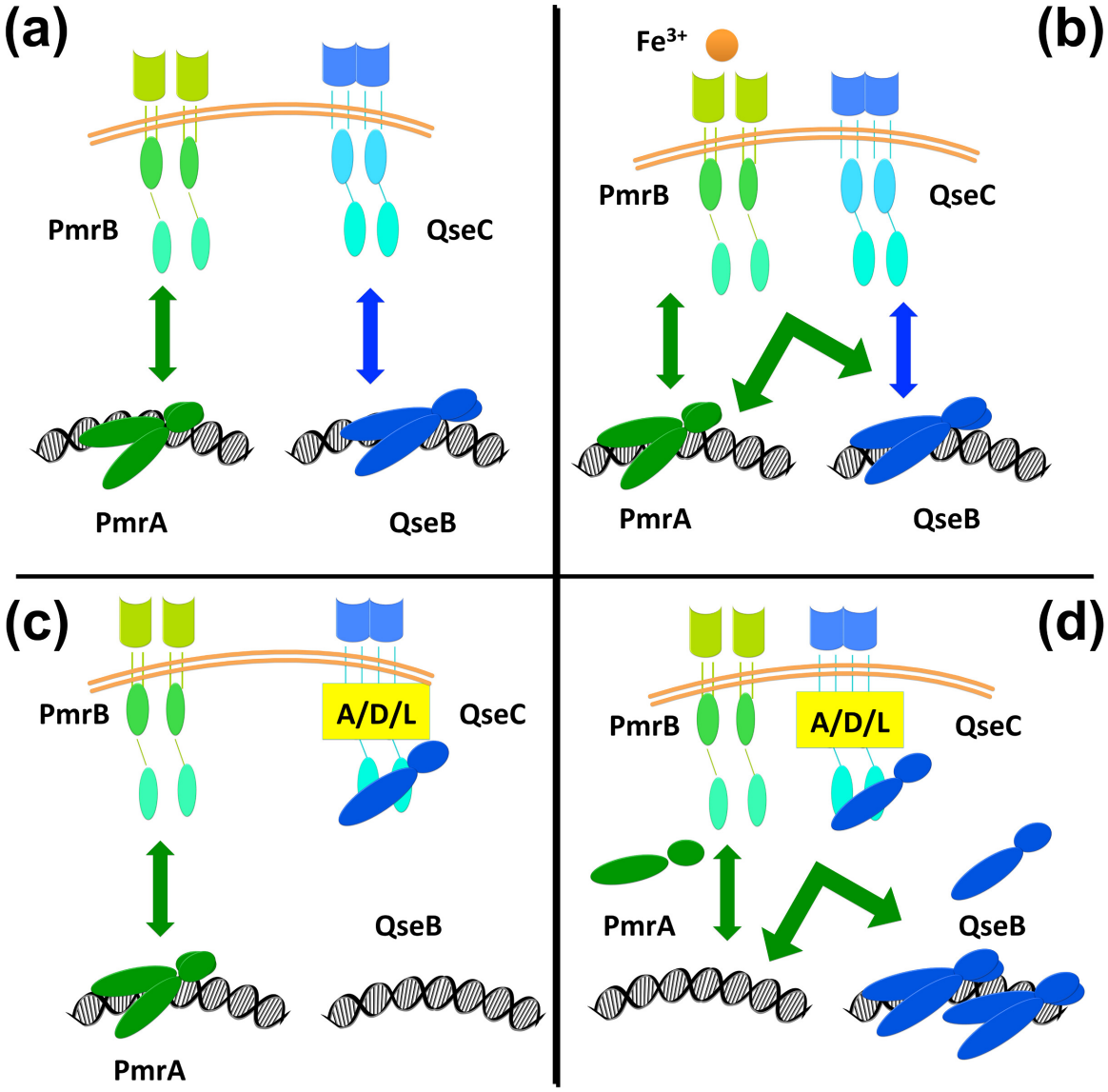


**Figure 22: The different interaction states of PmrAB and QseBC.** (**A**) Panel depicts WT PmrAB and QseBC interactions in the absence of signal. (**B**) Depicts WT PmrAB and QseBC interactions in the presence of the PmrB signal ferric iron ($Fe^{3+}$). (**C**) Depicts the presumed ability of the QseC_H246A/D/L variants to sequester QseB from PmrB in the absence of signal. (**D**) Depicts the inability of the QseC_H246A/D/L variants to sequester an overabundance of exogenous QseB in the absence of signal resulting in a *qseC* deletion phenotype.

# CHAPTER V

# ONGOING STUDIES, CONCLUDING REMARKS, AND FUTURE DIRECTIONS

Our previous studies uncovered a rare signaling phenomenon during which a specific signal induces a physiologic interaction between non-cognate, two-component system proteins. This interaction leads to a modified response to a cationic polypeptide. The increased tolerance to cationic stress offers a fitness advantage to the bacteria, allowing them to evade lysis and possibly predation. However, is this conserved over the diverse *E. coli* species?

## 5.1. Ongoing Studies:

*Co-evolution of a "four-component" signaling network in extra-intestinal E. coli*

Gene duplications, gene deletions, and horizontal gene transfer events are a few of the ways in which bacterial genomes are altered over time as a function of selective pressures Since a majority of TCSs exist in operons, they lend themselves to "gene block" duplication and retention of acquired genes (243). Gene duplication events in bacteria arise on the order of $10^{-3}$ to $10^{-7}$ (244, 245). The major outcomes that arise following gene duplication include the bacteria gaining a second system with conserved function, a second system with new or partial function compared to the parent system, a second system that is deleterious, or a non-functional system (246). If there is positive selective pressure, the new duplication will be maintained. If the duplication is deleterious or unnecessary, the duplication may be inactivated and subsequently deleted. These conserved duplication events can lead to an overlap in sequence space, a term coined by Michael Laub to indicate a set of conserved interacting networks (137). In parallel to gene duplication

events, the selective pressures imposed to each TCS may differ in response to environment and other genetic factors harbored by a strain.

Previously, we have shown that two paralogous TCS interact and respond to ferric iron ($Fe^{3+}$) and this interaction can lead to transient polymyxin B (PMB) resistance (Chapter III, (230)). It is therefore enticing to hypothesize that the interaction between PmrAB and QseBC is the result of co-evolution. Analysis of TCS ancestry revealed the origination of PmrAB to be ancestral to QseBC; this combined with homology suggests duplication (Chapter II, **Fig. 7**, (210)). Evidence of separate independent divergence from commensal *E. coli*, indicates that signaling networks while conserved, may be regulated differently in enteric and extra-intestinal pathogenic and commensal *E. coli* strains (6, 8). The response to ferric iron, based on selective pressures may result in different outcomes that are clade specific. PmrB has been shown to directly bind $Fe^{3+}$, however, the mechanism of detection is not well established. It is possible that proteins containing iron-sulfur clusters may also be detected. As EHEC has been previously reported to respond to epinephrine (178), this may be the case in which catecholamines chelates $Fe^{3+}$ (247) and this is what may be sensed for intestinal *E. coli*.

In our ongoing studies, we aim to identify if the signaling observed in UPEC strain UTI89 is conserved among all *E. coli* clades. Secondly, we want to determine the role of previously defined coevolving residues involved in the interaction surface in PmrAB-QseBC signaling in UPEC.

*In silico sequence comparisons reveal other potential coevolving residues*

In collaboration with Ashley Earl and Abigail Manson from the Broad Institute, 49 *E. coli* species from all 5 major clades of the *Escherichia* genera, spanning all the major pathotypes, were

compared for their differences and similarities in QseBC and PmrAB (Chapter I, **Fig. 1**). The strains were then characterized by their previously reported capsule (K), flagella (H), and oligosaccharide (O) serotypes (**Table 5**).

The promoter regions of *qseBC* and *pmrAB* were aligned to identify possible clade specific differences that would mediate differential physiologic responses (**Table 6**). Within the *qseBC* promoter, four nucleotides were identified that differed between strains with the third and fourth mutations varying by clade. There are five single nucleotide polymorphisms (SNPs) in the *pmrAB* promoter based on the strains tested. In this promoter the first and third mutations seemed to be conserved by clade. We are in the process of using site directed mutagenesis (SDM) to change the residues in the *qseBC* promoter that correlate to the third and fourth mutation alone and in combination. We will test the steady state transcription of *gfp,* driven by the altered promoters, to see if there are differences in the response to $Fe^{3+}$. We do not foresee these alterations in the *qseBC* promoter affecting the ability of UTI89 to respond normally to $Fe^{3+}$.

In parallel, the protein sequences for PmrB, QseC, PmrA, and QseB were compared to identify residues that may be important in maintaining proper physiologic interactions within and between the non-cognate partners (Chapter II, **Fig 7**) with respect to evolutionary clade. PmrA was the most conserved, followed by QseB with only a few residues varying between clades. PmrB and QseB have residues that appear to co-vary between clades. Notably, QseC has the most degenerate sequence with the most differences between clades (**Fig. 23, Table 7**).

**Table 5. Known serotypes for the strains compared *in silico* analysis**

| Clade | Pathotype | Strain Name | K antigen | O antigen | H antigen |
|---|---|---|---|---|---|
| A | EIEC | 53638 | | 144 | |
| A | EAEC | 101-1 | | X | 10 |
| A | Commensal | ATCC 8739 | | 146 | |
| A | Benign | B str. REL606 | | 7 | |
| A | Lab strain | BW25113 | | X | |
| A | Benign | DH1 | | 16 | |
| A | ETEC | H10407 | | 78 | 11 |
| A | Commensal | HS | | 8 | 4 |
| A | Benign | W3110 | | 16 | |
| B1 | EHEC | 11128 | | 111 | X |
| B1 | EHEC | 11368 | | 26 | 11 |
| B1 | EHEC | 12009 | | 103 | 2 |
| B1 | EAEC | 55989 | | 104 | 4 |
| B1 | EHEC | 2009EL-2050 | | 104 | 4 |
| B1 | EHEC | 2009EL-2071 | | 104 | 4 |
| B1 | APEC | APEC O78 | | 78 | |
| B1 | ETEC | B7A | | 148 | 28 |
| B1 | ETEC | E24377A | | 139 | 28 |
| B1 | EHEC | O104:H21 | X | 104 | 21 |
| B1 | Commensal | SE11 | | 152 | 28 |
| B1 | Lab strain | W | | | |
| B2 | ABU | ABU 83972 | 5 | | |
| B2 | APEC | APEC O1 | 1 | 1 or 12 | 7 |
| B2 | UPEC | Clone D i14 | | | |
| B2 | UPEC | Clone D i2 | | | |
| B2 | EPEC | E2348/69 | | 127 | 6 |
| B2 | Commensal | ED1a | | 81 | |
| B2 | NMEC | IHE3034 | 1 | 18 | 7 |
| B2 | AIEC | LF82 | | 83 | 1 |
| B2 | Commensal | Nissle O6:K5:H1 | 5 | 6 | 1 |
| B2 | AIEC | NRG 857C | | 83 | 1 |
| B2 | UPEC | O6: CFT073 | 2 | 6 | 1 |
| B2 | UPEC | O6:536 | 15 | 6 | 31 |
| B2 | Meningitis | S88 | 1 | 45 | 7 |
| B2 | Commensal | SE15 | | 150 | 5 |
| B2 | AIEC | UM146 | | | |
| B2 | UPEC | UTI89 | 1 | 18 | 7 |
| D | NMEC | CE10 | 1 | 7 | |

| | | | | | |
|---|---|---|---|---|---|
| D | UPEC | IAI39 | 1 | 7 | |
| D | Industrial site | SMS 3_5 | | | |
| E | EPEC | CB9615 | | 55 | 7 |
| E | EHEC | EC4115 | | 157 | 7 |
| E | EHEC | O157:H7 Sakai | 2 | 157 | 7 |
| E | EPEC | RM12579 | | 55 | 7 |
| E | EHEC | TW14359 | | 157 | 7 |
| E | EHEC | Xuzhou21 | | 157 | 7 |
| (248-250) | | | | | |

**Table 6: Variations in the nucleic acid residues in the promoter regions**

| | | Clade | | | | |
|---|---|---|---|---|---|---|
| **Promoter** | **Conserved nucleic acid residue** | **A** | **B1** | **B2** | **D** | **E** |
| ***qseBC*** (*upstream of qseB*) | -135A | | | | CE10, IAI39 -135G | |
| | -81A | | APEC_078 -81- | UM146 -81- | | |
| | -65G | | | -65A | -65A | |
| | -32G | | | | | -32A |
| ***pmrAB*** (upstream of *eptA/pmrC*) | -91C | | | -91A | -91A | |
| | -86A | | | | SMS3_5-86C | |
| | -84C | | | UTI89, UM146, IHE3034 -84T | | -84G |
| | -72c | | | | | RM12579 -72T |
| | -4C | | 12009 -4A | | | |

*Differences compared to promoter sequence from the other 48 *E. coli* sequences

The nucleic acid residues are numbered from the A+1 of the downstream gene either *qseB* or *eptA*/*pmrC*. For mutations that are conserved across the clade, no specific strains are identified. For the mutations that are strain specific, strains are listed with their change from the consensus sequence. Sequence alignments are shown in the appendix for all strains.

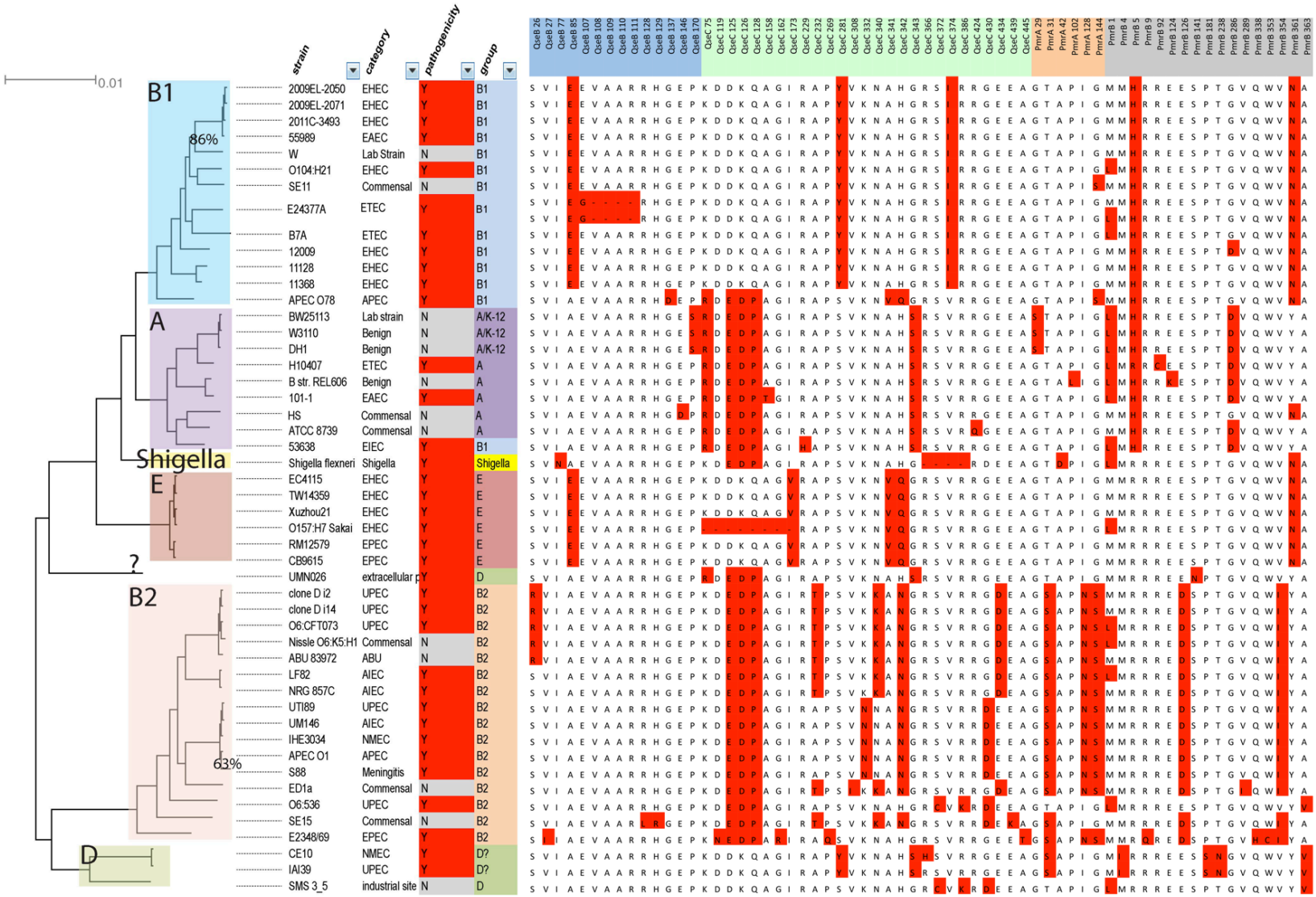


**Figure 23: Residues that differ among clades.** For the protein alignments, the residues that differed are listed mapped back to the phylogenetic tree depicting clade-specific sequence patterns. The 49 strains were compared and the residues that differ from all other strains for PmrB (blue column), QseC (green column), PmrA (orange column), and QseB (gray column) are marked in red.

**Table 7: Variations in protein residues of QseBC and PmrAB listed by clade**

| | Clade | | | | |
|---|---|---|---|---|---|
| **Protein** | **A** | **B1** | **B2** | **D** | **E** |
| **QseB** | | E85 | R/S26 | | E85 |
| **QseC** | R75<br>E125<br>D126<br>P128<br>S343 | Y281<br>I374 | E125<br>D126<br>P128<br>T/A 232<br>N/K 332<br>K/N 340<br>N342<br>D/G424<br>D/E430 | Y281<br>S343 | V173<br>V341<br>Q342 |
| **PmrA** | | | S31<br>N128<br>S144 | S31 | |
| **PmrB** | L1<br>H5<br>D286 | H5<br>N361 | D126<br>I354 | I4<br>S181<br>N238<br>V363 | N361 |

*Differences compared to protein sequence from the other 48 *E. coli* sequences

Protein sequence alignments were made for all of the strains listed in Table 5. QseC from stain Sakai was left out of the QseC alignment since this protein is disjointed and non-functional in strain Sakai. The amino acids reported in this table show deviations from the consensus protein sequence. Full sequence alignments are shown in the appendix.

This is intriguing given the observation that the EHEC signal epinephrine does not elicit a UPEC QseC response (Chapter III, (230)). To elucidate whether clade-specific residue differences are sufficient to alter signaling, non-partner interactions, and transient resistance to PMB, ongoing studies are focused on the testing the response of different *E. coli* strains spanning the five major clades for their steady state *qseB* transcript response to stimulus by $Fe^{3+}$. We predict that if there is a clade-specific response to the interactions between PmrAB and QseBC we should see differences in the transcriptional surge profiles by qPCR. We will also be swapping different components of the four-component systems between strains to identify which residues confer clade-specific functionality. Based on our results, we will start to identify which components are necessary and sufficient for the integrated response to $Fe^{3+}$. If there are clade specific results, we can start addressing the role of additional factors in antibiotic resistance such as the activity of additional axillary proteins, LPS modification and outer membrane rearrangement.

As part of these studies, the response of urine-associated *E. coli* (presumably ExPEC) to PMB following pretreatment of $Fe^{3+}$ was addressed. We have shown that pretreatment with $Fe^{3+}$ predisposes UPEC strain UTI89 to transient resistance to PMB (Chapter III, (230)). When pretreated with the same concentration of $Fe^{3+}$, the four clinical Vanderbilt urinary tract isolates (VUTIs) we tested had differences in intrinsic resistance and the percent survival when exposed to PMB (Chapter III, (230)). These differences may be attributed to variations in cell wall, capsule, or genetic variations in PmrAB and QseBC. To follow up on this hypothesis, we isolated the genomes of 300 clinical isolates with corresponding clinical data. Figure 24 shows the breakdown of the 300 strains. We are in the process of using *in silico* sequence comparisons

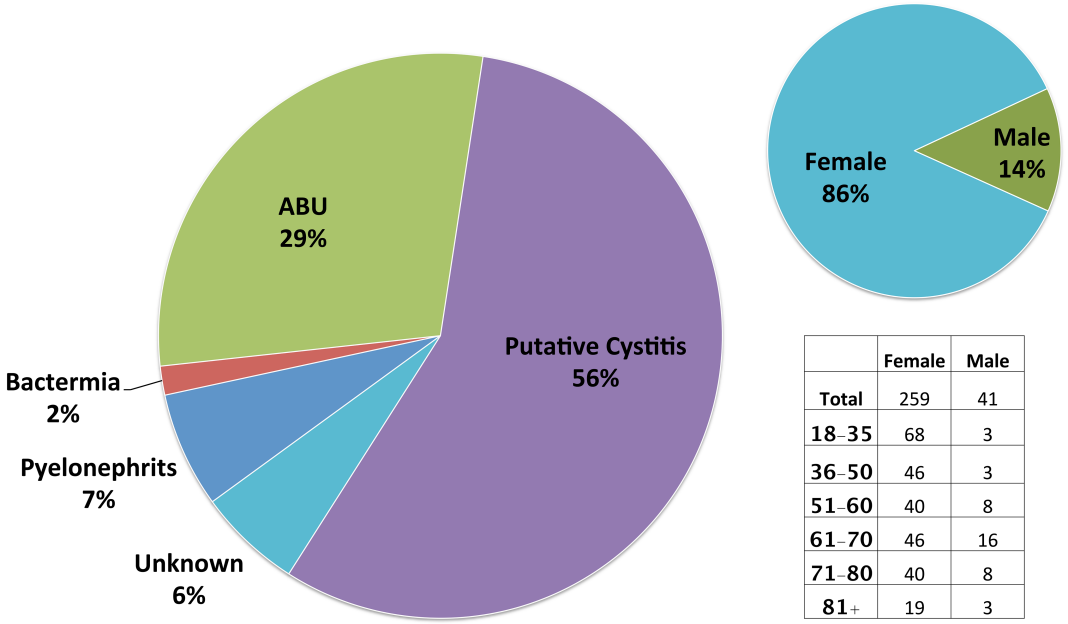


| | Female | Male |
|---|---|---|
| Total | 259 | 41 |
| 18-35 | 68 | 3 |
| 36-50 | 46 | 3 |
| 51-60 | 40 | 8 |
| 61-70 | 46 | 16 |
| 71-80 | 40 | 8 |
| 81+ | 19 | 3 |

**Figure 24. Distribution of urine associated *Escherichia coli* from the Vanderbilt clinic.** With known patient data for 300 Vanderbilt Urinary Tract Isolates (VUTIs), the distribution of confirmed and unknown infection is listed in the chart on the left with the gender breakdown shown in the chart and table on the right.

to identify relevant clinical differences between urinary isolates to see if these differences in the *pmrAB* and *qseBC* operons corresponded with disease severity. We predict that disease severity or intrinsic antibiotic resistance will be linked to specific SNPs located in the *pmrAB* and/or *qseBC* operons. Future studies will test these clinical samples for antibiotic resistance and presence of a capsule.

*Coevolving residues for the PmrAB and QseBC two-component systems*

The Laub group has extensively shown the residues important in TCS cognate partner interactions are six residues on the HK and RR respectively (239). Based on the similarities of the interacting surfaces (**Fig. 25**), we asked the question, does changing the PmrB residues to mirror those of QseC confer greater regulatory ability of PmrB toward QseB? The percent identities in the gene and protein sequences are 48.34% and 32.65% respectively for the kinases and 54.48% and 45.21% respectively for the response regulators.

*The PmrB co-evolving residues only dictate kinase activity towards QseB.*

Given that PmrB robustly phosphorylates QseB, but is significantly slower as a QseB-specific phosphatase, we first evaluated the contribution of the QseC co-evolving residues for their involvement in QseB de-phosphorylation. We tested whether "grafting" the QseC co-evolving residues onto the PmrB sequence would improve PmrB phosphatase function towards QseB. Using site-directed mutagenesis, the co-evolving

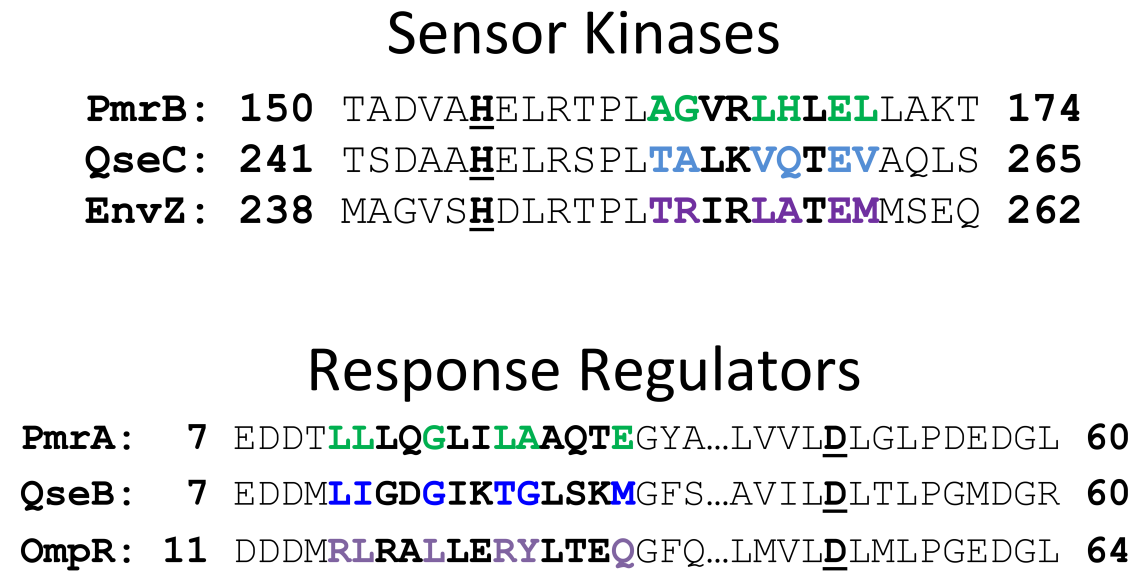


**Figure 25. Sequence alignment of the coevolving residues in PmrAB, QseBC, and EnvZ-OmpR.** The residues identified as co-evolving are colored and in the bold interacting surface. The conserved histidine (H) and aspartate (D) are underlined.

residues in PmrB (253-$AG_{VR}LH_{L}EL$-261) were sequentially changed to those of QseC (162-$TA_{LK}VQ_{T}EV$-170) (**Fig. 25**). We previously demonstrated that aberrant phosphorylation of QseB by PmrB in the *qseC* deletion mutant leads to QseB-mediated repression of flagellar motility (186). Consequently, a UPEC mutant deleted for both *qseC* and *pmrB* displays wild-type levels of motility (186). Using loss of motility as a proxy to PmrB-mediated activation of QseB in the absence of QseC, we tested the effects of each PmrB co-evolving residue mutation in the UTI89*ΔpmrBΔqseC* background, by introducing each *pmrB* variant on a plasmid under its own promoter. We found that, when at least four PmrB co-evolving residues were replaced with the co-evolving residues of QseC, motility in the corresponding mutants was abolished (**Fig. 26**).

*QseC residues grafted onto PmrB alter the in vitro phosphorylation phenotypes*

We have previously shown that QseC functions as a reverse-phosphotransferase to regulate the PmrAB-QseBC interactions (Chapter IV, (251)). Using *in vitro* phosphorylation assays to test the ability of PmrB variants to phosphotransfer to QseB we see that when 3 resides are altered to mirror QseC, we see a sustained phosphotransfer from 2-10 min with subsequent dephosphorylation from 10-45 min in the absence of QseC; with 5 altered resides, there is a rapid phosphotransfer 5-10 min and dephosphorylation 15-30 min (**Fig. 26**). This second phenotype mirrors that of WT QseC phospho-transferring to QseB in the absence of signal (Chapter IV, (251)). However, in the presence of $Fe^{3+}$, there is sustained phosphotransfer with 3 QseC residues and gradual phosphotransfer when PmrB harbors 5 of the QseC coevolving residues (**Fig. 26**).

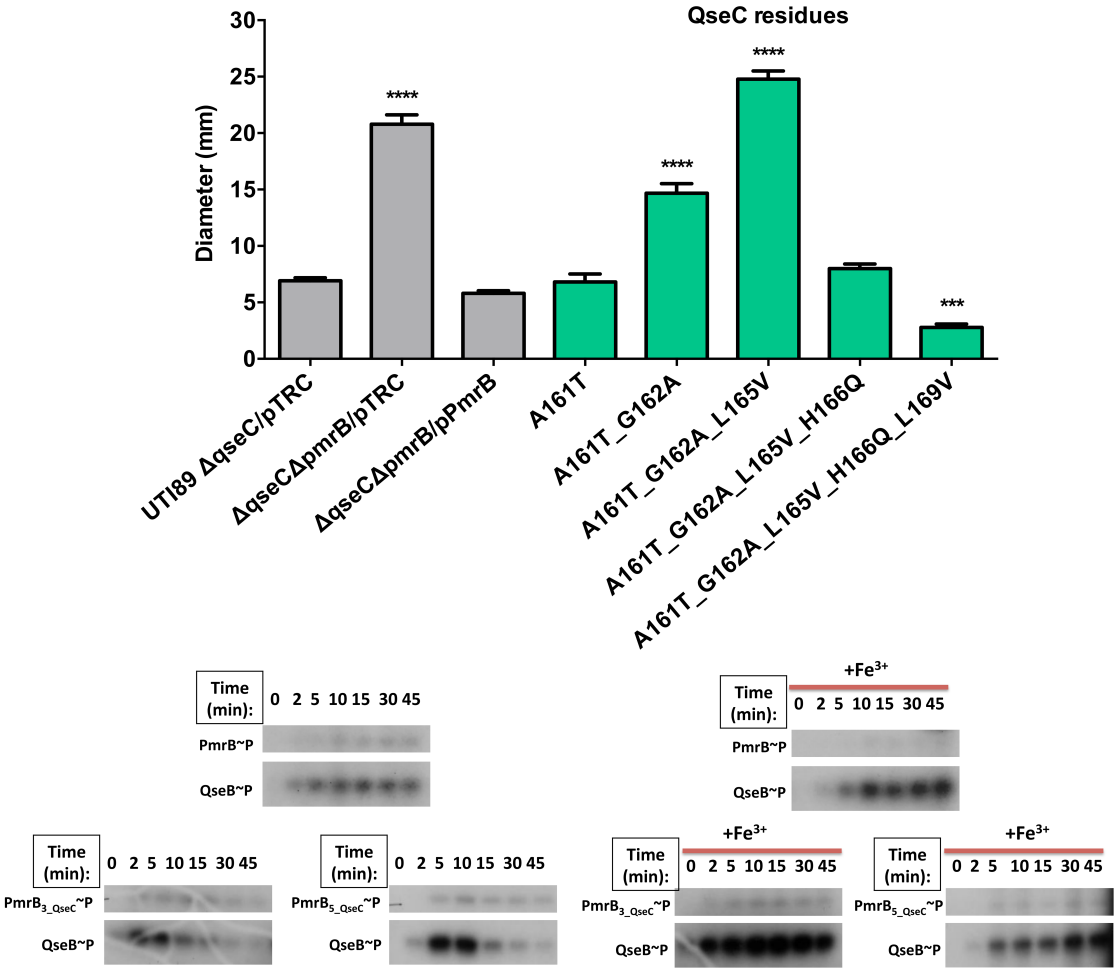


**Figure 26**: **Motility and phosphotransfer phenotypes of PmrB with QseC-like coevolving residues**. The motility for PmrB variants harboring QseC residues: 1 (A161T), 2 (A161T_G162A), 3 (A161T_G162A_L165V), 4 (A161T_G162A_L165V_ H166Q), and 5 (A161T_G162A_L165V_ H166Q_L168V) is shown in the bar graph. The phosphotransfer profiles of $PmrB_{\_WT}$, $PmrB_{3\_QseC}$, and $PmrB_{5\_QseC}$ to QseB in the absence and presence of ferric iron ($Fe^{3+}$) is shown below.

These results indicate that altering these residues does alter the interaction between PmrB and QseB to resemble a QseC-like phenotype in the absence of signal, but retains responsiveness to $Fe^{3+}$. The *in vitro* data does not account for the gain in motility however, indicating additional *in vivo* factors may regulate these non-cognate interactions.

*Ablating the PmrB residues does not interfere with in vitro phosphorylation*

To identify if these results are specific to QseC residues, we sequentially altering the PmrB co-evolving residues to alanine resulting in (253-$AA_{VR}AA_{L}$EA-261) as the final PmrB sequence (**Fig. 27**). Altering the residues to alanines resulted in constructs that no longer repressed motility in UTI89*ΔpmrBΔqseC* (**Fig. 27**), indicative of a loss of PmrB-QseB protein-protein interactions. These results suggested that the co-evolving residues of PmrB and QseC are similar enough to facilitate interaction of each of these kinases with QseB. However, when tested for their *in vitro* phosphorylation, we see that PmrB harboring alanines is a better kinase toward its cognate partner PmrA and displays QseC-like phenotype toward QseB in the absence of signal yet, phosphotransfers similarly to both RRs in the presence of $Fe^{3+}$ (**Fig. 27**). The contradiction in the motility and *in vitro* assays may be explained by the over activation of PmrA which may repress QseB activity.

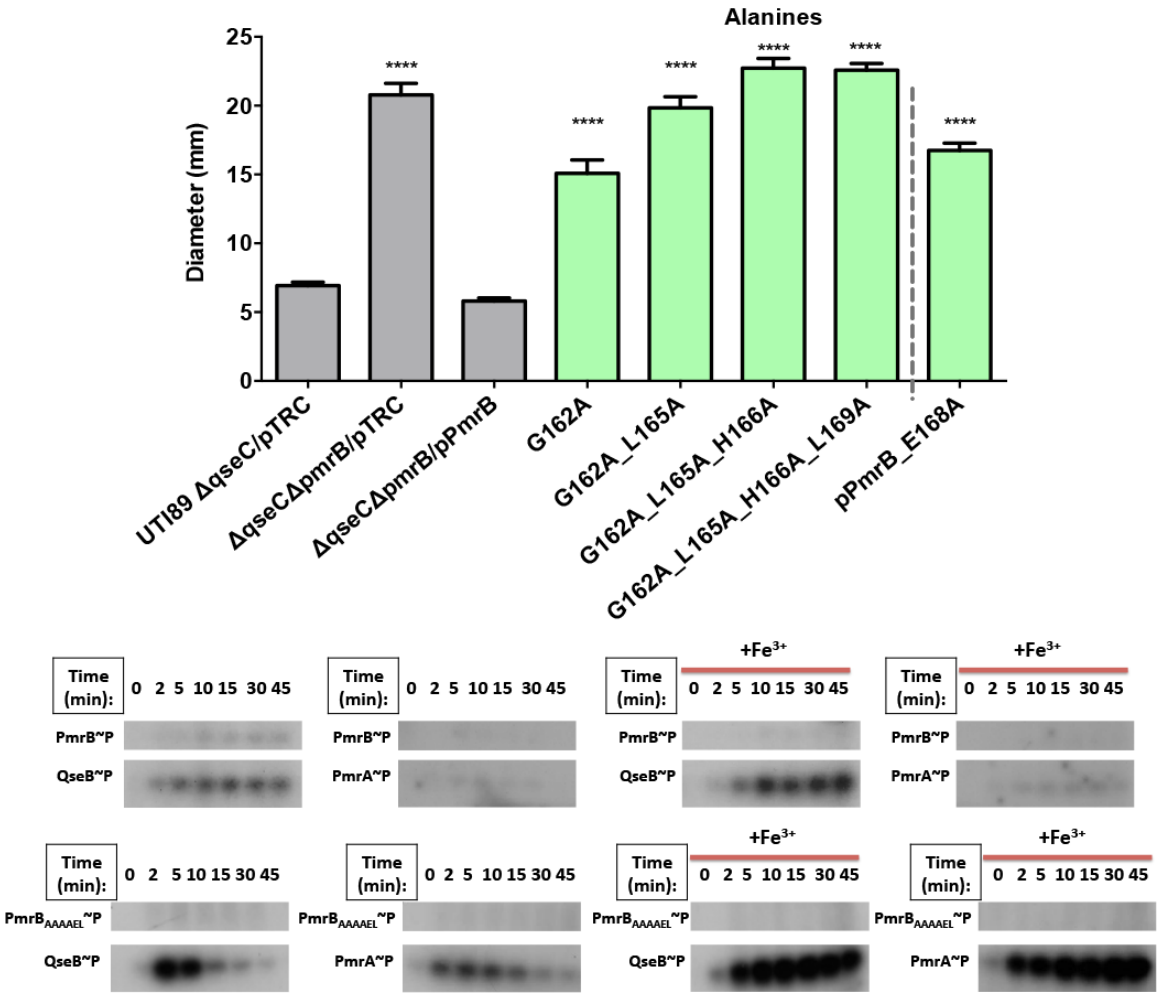


**Figure 27: Motility and phosphotransfer phenotypes of PmrB with alanine coevolving residues**. The motility for PmrB variants harboring additional alanines: 1 (G162A), 2 (G162A_L165A), 3 (G162A_L165A_ H166A), and 4 (G162A_L165A_ H166A_L168A) is shown in the bar graph. Additionally the conserved glutamic acid (E) was altered to an alanine alone to determine the role of the single conserved residue. The phosphotransfer profiles of $PmrB\_{WT}$ and $PmrB\_{AAAAEL}$ to PmrA and QseB in the absence and presence of ferric iron ($Fe^{3+}$) is shown below.

## 5.2. Future Studies

The signal for QseC in the UPEC strain UTI89 is yet unknown (Chapter III, (230)) however, in the absence of QseC there is misregulation of roughly 8% of the UTI89 genome stemming from activation of QseB by PmrB (101, 230). In the UPEC strain UTI89 PmrAB and QseBC overlap in signaling network; and share partial sequence homology. The coevolving residues found on the interacting surface were conserved entirely across all 49 strains of *E. coli* tested. This indicates that these residues alone do not dictate differential regulation among strains, however, the clade specific differences in sequences may be more indicative of differential signal regulation.

During evolution or adaptation, initial changes to the genome typically result in loss of fitness yet; there may be positive selection to keep the duplication. Gene duplication or amplification plays a major role in antibacterial resistance (252). This may explain the changes seen in ExPEC due to the changes in location and exposure to antibacterials in the gut, concentrated antibacterials in the urine/bladder, and those used in farming practices. We will continue to test the antibiotic resistance of the clinical isolates and different strains of *E. coli* among the different clades, to see if the interactions between PmrAB and QseBC uniformly predispose these strains to antibacterial resistance. Based on the research presented in this dissertation, there are many unanswered questions and avenues of future study. Future directions pertaining directly to my aims include identifying signals for QseC, further testing the coevolution of PmrB and QseB, testing the role of QseBC and PmrAB in colony-biofilm development, and delineating the integrative response of the four-component system with respect to additional inputs and outputs. Additional routes of testing include dissecting the role of the four-component system in antimicrobial resistance, delineating strain specific interactions, and identifying how differential PmrAB-QseBC signaling affects the outer membrane structure.

*Further examining the four-component interactions*

We have shown that all four components PmrAB and QseBC are required for proper signaling in response to $Fe^{3+}$ (Chapter III, (230)) however the molecular interactions between and within all the components are still unknown. Testing the i*n vivo* interactions via co-immunoprecipitation and mass spectrometry will add further insight into the molecular interactions. We are especially interested in the interactions between QseC and PmrA. Seeing that altering the co-evolving residues to mirror those of QseC changes the *in vitro* transfer kinetics, we want to see what non-cognate residues grafted onto PmrB would do. This will provide insight into cognate specificity, default sensor interactions, and role of co-evolving residues in maintaining signal specificity in this four-component system.

Based on our current findings in collaboration with the Broad Institute (Chapter V), we are going to compare the differentially conserved residues and protein specific residues between EHEC and UPEC QseBC-PmrAB interactions. This will help us to identify if there are clade specific interactions or co-evolution within this four-component system.

Simultaneously, we will start analyzing our urinary *E. coli* isolates for differences in QseBC-PmrAB sequences to see if any of the isolates we have recovered have altered signaling within the four-component signaling network. Concurrently, we will swap regions of QseC between different clades to identify any differences between pathotype signaling. We also want to identify the role of the coevolving nucleotides within the promoter regions of the *qseBC* promoter. We will use SDM to determine if the difference in nucleotide affects *qseBC* signaling as described in Chapter V.

For example, during acute urinary tract infection, bacteria are starved for iron (98, 101, 253), yet, at the same time, they must be able to distinguish between the metals that are required for cellular metabolism and detrimental cations and cationic polypeptides that are deployed by the

innate immune response because they are catastrophic to bacterial membrane integrity. Increased tolerance to PMB was not specific to strain UTI89 because other ExPEC strains, especially VUTI77 and CFT073 (Chapter III, **Fig. 15**), exhibited increased PMB tolerance after $Fe^{3+}$ preconditioning. Although the increase in survival was not as robust as that observed in UTI89, there could be differences in the extent of cross-interactions between the QseBC and PmrAB TCSs or the amino acid sequence differences in PmrAB and QseBC that may exist between these strains. For example, the enterohemorrhagic *E. coli* strain Sakai harbors a truncated QseC. Ongoing deep sequencing experiments probe the PmrAB-QseBC regulon in response to $Fe^{3+}$, aiming to further elucidate the cationic response driven by cross-interactions between PmrAB and QseBC in UPEC.

*Identifying the functional role of QseC*

Chapter IV introduces the functional role of the conserved histidine in regulating QseB via reverse phosphotransfer. We have accumulated data through random and site-directed mutagenesis that indicates there are additional specific residues required for *in vitro* and *in vivo* QseC function (**Figs. 28 and 29**)**.** Despite near complete coverage of the sensing domain region of QseC, none of the resulting single point mutations tested in our studies impaired QseC function, as evidenced by the ability of each construct to rescue motility in UTI89Δ*qseC* (**Fig. 30**).

ATP binding and hydrolysis is integral to histidine kinase function. The predicted ATP binding domain of QseC lies within residues 363-442 (**Figs. 28 and 29**). Of the seven identified critical residues, three (L417, V422, and H429) were found in or near the predicted G2 and G3

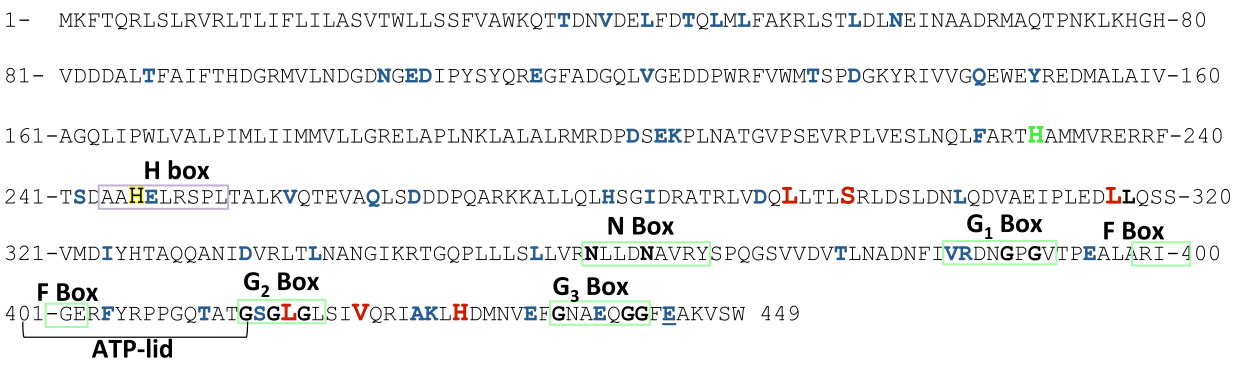


**Figure 28: QseC amino acid sequence, indicating important predicted domains and residues covered by mutagenesis**. Annotated QseC (UTI89_C3451) amino acid sequence from UPEC strain UTI89. In boxes are well-defined domains, common to many sensor histidine kinases: in purple is the H box harboring the conserved phosphorylated histidine residue (yellow). In light green are the conserved N, F, and G1-3 boxes within the ATP binding domain. In different colors are residues tested by mutagenesis. Highlighted in purple is the co-evolving residue sequence. Blue residues, when mutated confer no change to QseC function. The histidine shown in green (H231) was tested for its ability to potentially act as the phospho-accepting histidine in the absence of H246. Finally, residues in red, when mutated, alter the function of QseC.

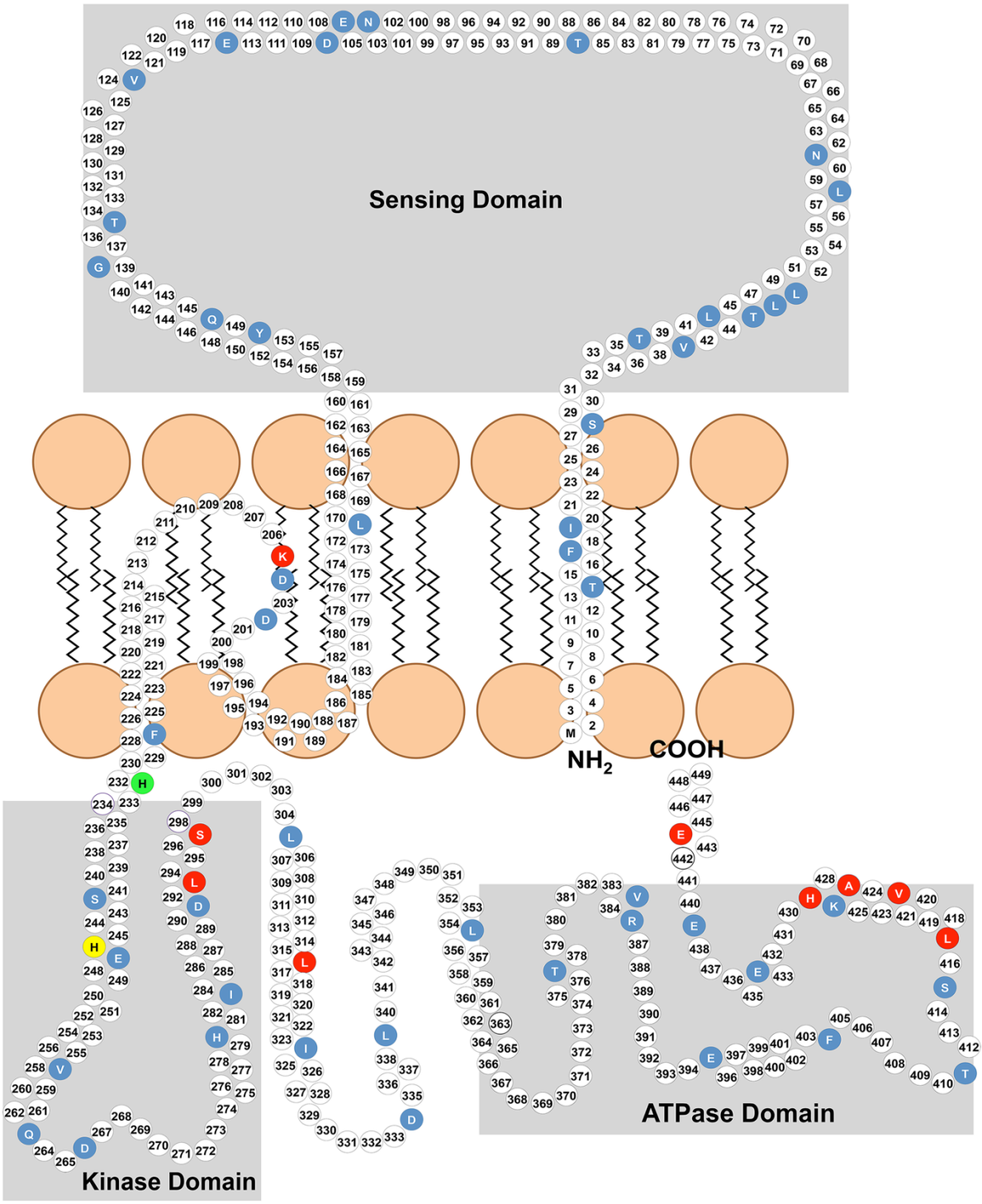


**Figure 29**: **Schematic representing single amino acid changes tested for function in QseC.** Representative schematic of QseC shown embedded in the inner membrane (lipid bilayer). Numbered circles represent individual amino acids; colored circles indicate residues hits that were altered during random mutagenesis. Color code: Blue and green depict altered residues with no change during functional assessment; red depicts residues were altered and did not complement wild-type (WT) phenotype during functional assays. Yellow depicts the conserved phospho-accepting histidine. The sensing domain lies between the residues 32 and 158, the kinase domain between residues 234 and 298, finally, the ATPase domain lies between residues 363 and 442.

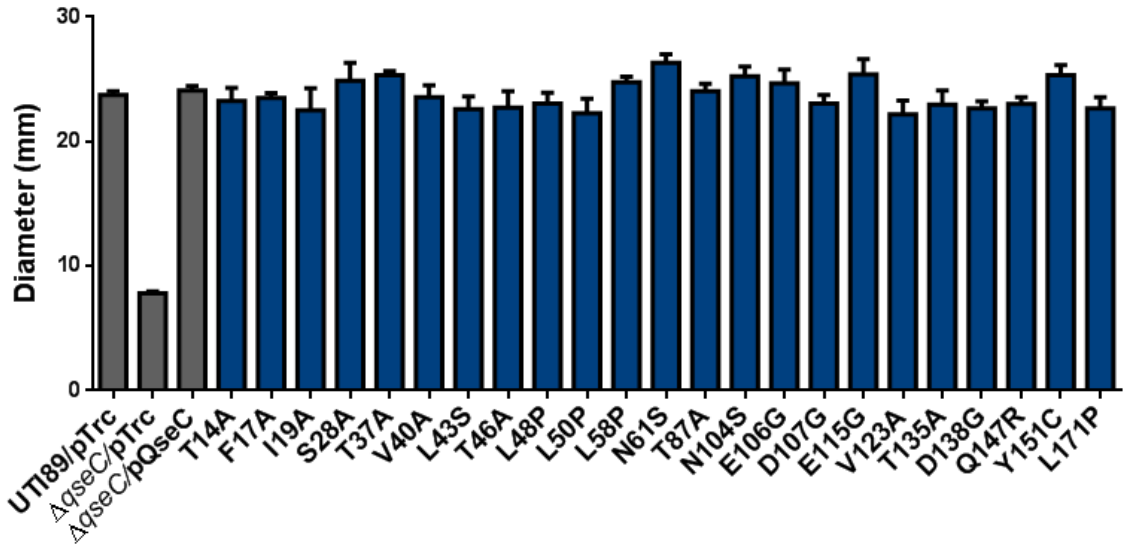


**Figure 30: Sensing domain variants complement *qseC* deletion phenotype.** Graph depicts average motility for sensing domain variants using motility as a proxy for function, the diameter of movement through soft agar is shown for 61 QseC variants. Color scheme the same as above. No alteration in motility (blue and green bars), significant alteration to motility (red bars), and the conserved histidine residue (yellow bar). Graphs depict averages of 5 biological experiments with 3 technical replicates per each experiment. Statistical analysis was performed using one-way ANOVA and a Dunnett's multiple comparison correction, with **** $p \leq 0.0001$, *** $p \leq 0.001$, ** $p \leq 0.01$, and * $p \leq 0.05$.

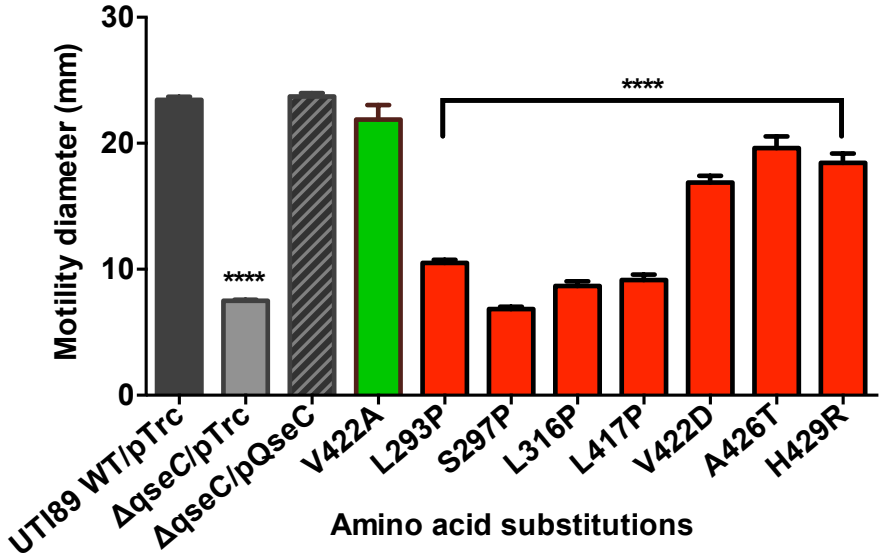


**Figure 31**: **Motility phenotype of partially and non-functional QseC variants.** Graph shows the average motility of QseC variants in soft agar for non-altering residue (green) and residues that alter QseC function *in vivo*.

boxes that follow the ATP lid of the QseC ATP binding domain (**Figs. 28, 29, and 31**). As expected, mutations in each of these residues interfered with QseC ATP binding and/or hydrolysis, as evidenced by the inability of QseC_L417P, QseC_V422D, and QseC_H429R to auto-phosphorylate, phosphotransfer to QseB (**Fig. 32**) or de-phosphorylate QseB *in vitro* (**Fig. 33)**. Interestingly, a separate mutation of V422 to alanine (V422A) did not affect QseC function (**Fig. 31**) This difference indicates that altering residue size or charge can modify local and/or global interactions thus resulting in the differential effect of altering residues in a critical site, or domain.

QseC_L293P and QseC_S297P were unable to rescue the motility defects of UTI89Δ*qseC* (**Fig. 31**). QseC_L293P and QseC_S297P exhibited drastically diminished phosphotransfer abilities (**Fig. 34**). Specifically, QseC_L293P-mediated phosphorylation of purified QseB was only observed during extended incubation (45-65 minutes, **Fig. 35**), while QseC_S297P was able to phosphorylate QseB by 30-45 minutes of incubation and reproducibly migrated as a dimer during the phosphotransfer assays (**Figs. 34 and 35**). Both of these variants also exhibited slower de-phosphorylation kinetics towards *in vitro* phosphorylated QseB (QseB~P) (**Fig. 33**) that resembled the de-phosphorylation properties exhibited by PmrB in our previous studies (186). Another mutation, at residue L316, found in the linker domain between the kinase and the ATP binding regions of QseC, also abolished the autophosphorylation properties of QseC (**Fig. 32**)

Further studies to identify how these residues impact QseC function include incorporating of loss of function residues (L293, S297, L316, L417, V422, A426, and H429) within the genomic locus of *qseC*. This will provide physiologic relevance with proper stoichiometric ratios. Then we will perform random mutagenesis on PmrB and QseB to identify

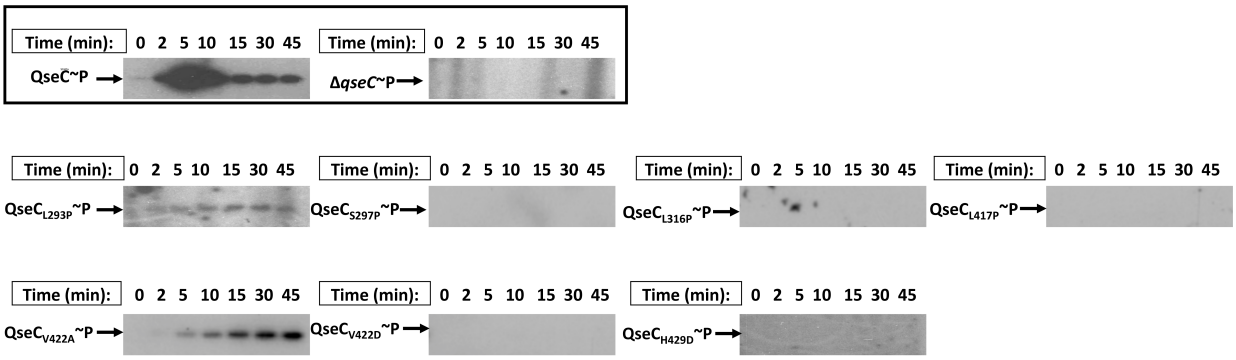


**Figure 32:** ***In vitro*** **auto-phosphorylation properties of partially functional and non-functional QseC variants.** Panels depict radiographs that track auto-phosphorylation of $^{32}$P-γATP by QseC enriched membrane vesicles. Boxed are the positive wild-type (WT) and negative Δ*qseC* enriched membranes followed by QseC partially and non-functional variants. Images are representative of 3 biological replicates.

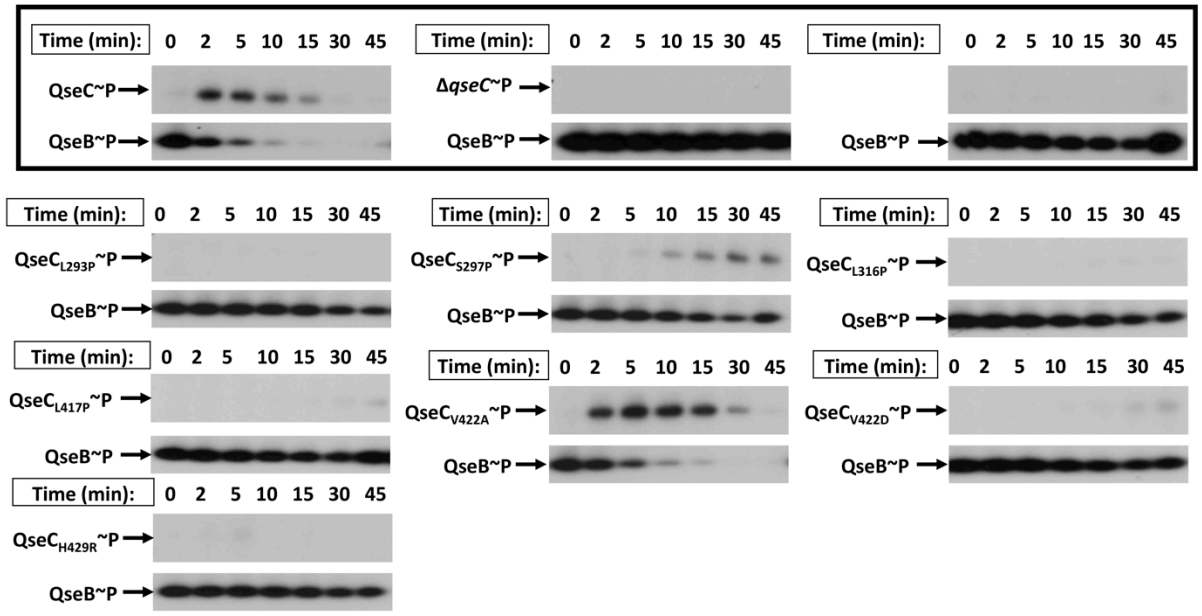


**Figure 33:** **De-phosphorylation properties of partially functional and non-functional QseC variants.** Panels depict radiographs that track de-phosphorylation of *in vitro*-phosphorylated QseB to further assess the properties of partially functional and non-functional QseC variants. In the box shows controls where de-phosphorylation of QseB is measured overtime. Controls include membrane vesicles enriched for QseC, membranes lacking QseC as a negative control, and QseB alone. Panels of QseC variants follow these controls. Images are representative of 3 biological replicates.

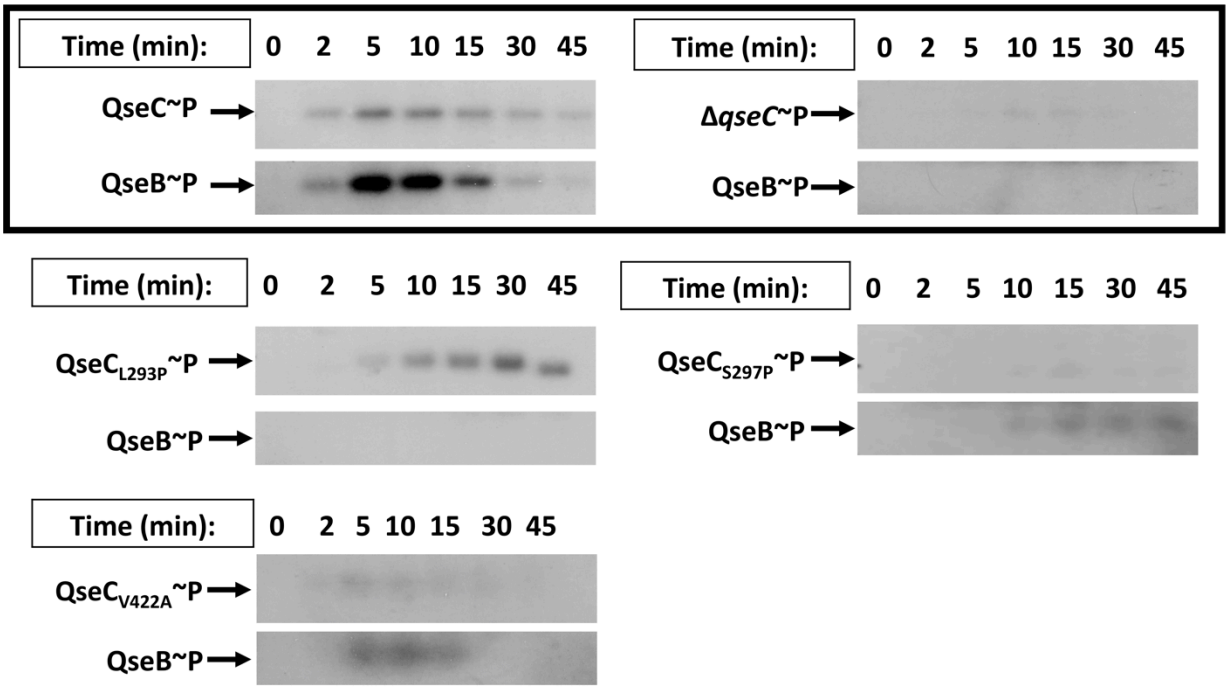


**Figure 34: Phosphotransfer activity of partially functional QseC variants.** Panels depict radiographs that track auto-phosphorylation and subsequent phospho-transfer of $^{32}$P-γATP to QseB by QseC variants with single point mutations L293P, S297P, and V422A. Controls with wild-type QseC or with membranes lacking QseC are shown in the box first followed by the QseC variants. Images are representative of 3 biological replicates.

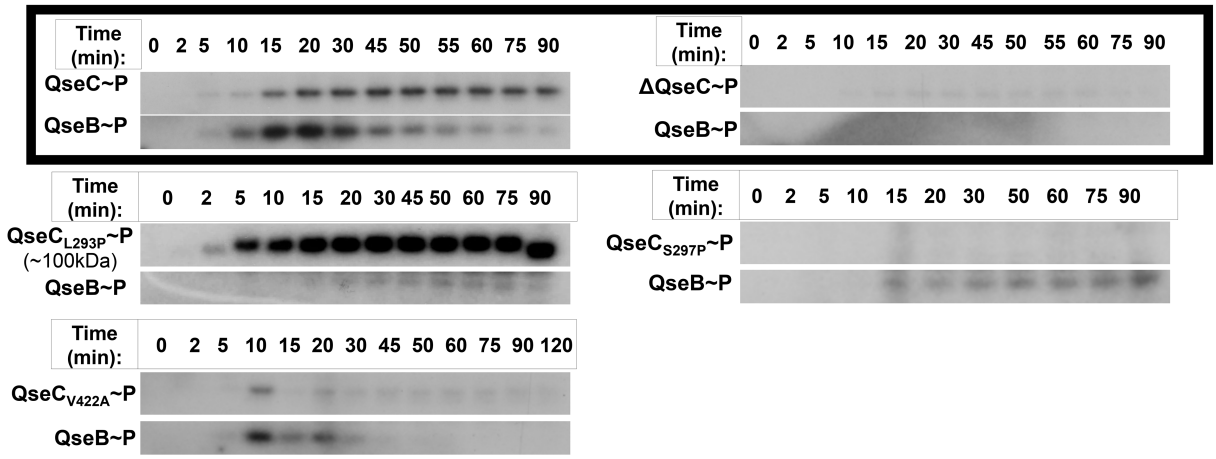


**Figure 35: Extended phosphotransfer activity of partially functional QseC variants.** Panels depict radiographs that track auto-phosphorylation and subsequent phospho-transfer of $^{32}$P-γATP to QseB by QseC variants with single point mutations L293P, S297P, and V422A. Controls with wild-type QseC or with membranes lacking QseC are shown in the box first followed by the QseC variants. Images are representative of 3 biological replicates.

suppressor mutations within the specific sequences that may restore wild-type signaling. These suppressor mutations will hint at variants that compensate for the loss of functional QseC and will provide insight into the interactions between the four components in the system.

*Identifying signals that activate QseC*

Despite only eight different residues in QseC between EHEC strain 86-24 and UPEC strain UTI89, the response to signal is not conserved. Activation of QseC in response to the catecholamines epinephrine and norepinephrine, as well as the bacterial autoinducer-3 have been previously reported for the QseC protein in enterohemorrhagic *E. coli* (EHEC) (179), yet in UPEC, we have not seen activation by these molecules ((230), unpublished). We have previously shown that loss of *qseC* leads to QseB-mediated de-regulation of gene expression in EHEC, in a similar fashion as we have reported for UPEC (177, 180). However, unlike EHEC QseC, the UPEC QseC protein appears to be unaffected by the LED209 pro-drug (221) reported to inhibit QseC function in EHEC (254, 255). Moreover, we previously reported that *qseBC* induction occurs in WT UPEC in response to $Fe^{3+}$, in a manner that involves PmrB, QseB, and PmrA (186). It is possible that UPEC QseC does not respond to the same extra-cytoplasmic cues as EHEC QseC (179). This may be a result of the three residues that differ specifically within the sensing domain.

To identify residues that activate UPEC-specific QseC, we used the previously described promoter fusion P*qse*:*gfp* construct (177) to screen the Spectrum Collection from the Vanderbilt High-Throughput Core screening core, a 2,000 compound library. Of the 2,000 compounds there were a handful that had increased GFP fluorescence above WT following addition of the compound. Of these, only two increased over time following the addition of the compound. Only

one compound recapitulated Δ*qseC* levels of fluorescence (**Fig. 36**). This compound was identified as dequalinium chloride (DQC), which is an anti-microbial antiseptic agent with a broad bactericidal and fungicidal activity. It has been reported several times for use in vaginal infections.

While UTI89 shows a dose response to DQC (**Fig. 37**), unfortunately, this compound is not specific QseC alone. We did show that in order to get maximum fluorescence the PmrAB-QseBC four-component system is required (**Fig. 38**). While not a direct therapeutic against QseC, DQC has the potential as a UTI therapeutic and may have additional effects on UPEC infections. Future studies identifying the mechanism by which *qseBC* are activated in response to DQC will provide further insight into the signaling network and regulatory effects of QseBC.

Previous publications showed that motility in UPEC was decreased in the presence of indole potentially indicating involvement of QseBC (256). Traditionally, indole is sensed by the BaeSR and CpxAR TCS (256) however, UPEC was able to respond to indole in the absence of both TCSs. To test if the PmrAB or QseBC systems were involved, we used deletion constructs and tested motility in the presence and absence of 2mM indole (**Fig. 39**). Our results indicated that indole does result in a non-motile phenotype, but this is not dependent on QseB or QseC alone. Future work will look at combinations of TCS knockouts to identify if these systems interact in response to indole.

Using our current and future studies, we will continue to dissect the molecular interactions of this four-component system, identify specific signals, and determine the range of outputs mediated by the PmrAB-QseBC system. Furthering our understanding of these non-partner interactions will increase our ability to prevent and resolve UTIs caused by UPEC.

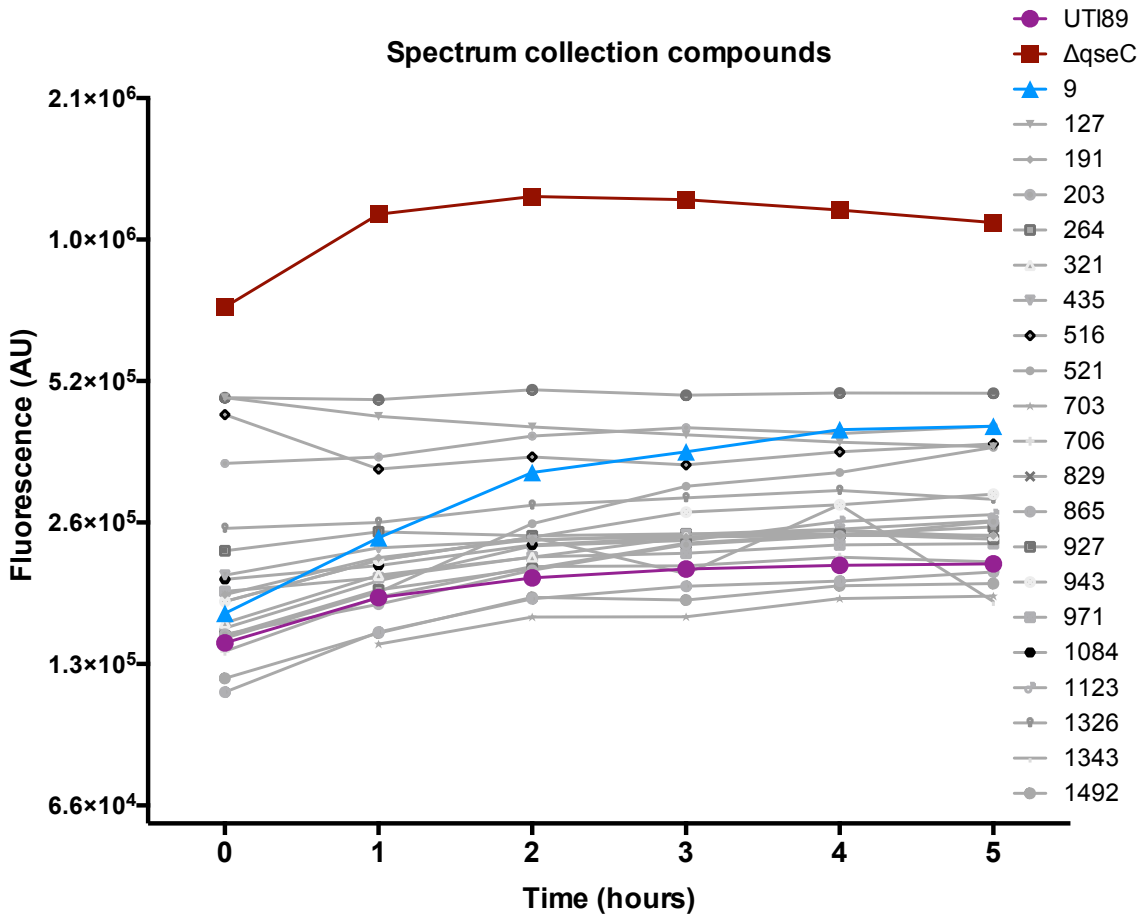


**Figure 36: GFP fluorescence driven by the *qse* promoter.** Tracking relative GFP fluorescence on the SpectraMax I3 plate reader over time in UTI89 in the presence of different compounds from the Vanderbilt Spectrum Collection. Fluorescence is compared to constitutively high fluorescence in UTI89Δ*qseC* and basal level of UTI89 in the absence of compounds. Compound 9 (blue triangles) is the only compound to cause a drastic increase in fluorescence overtime.

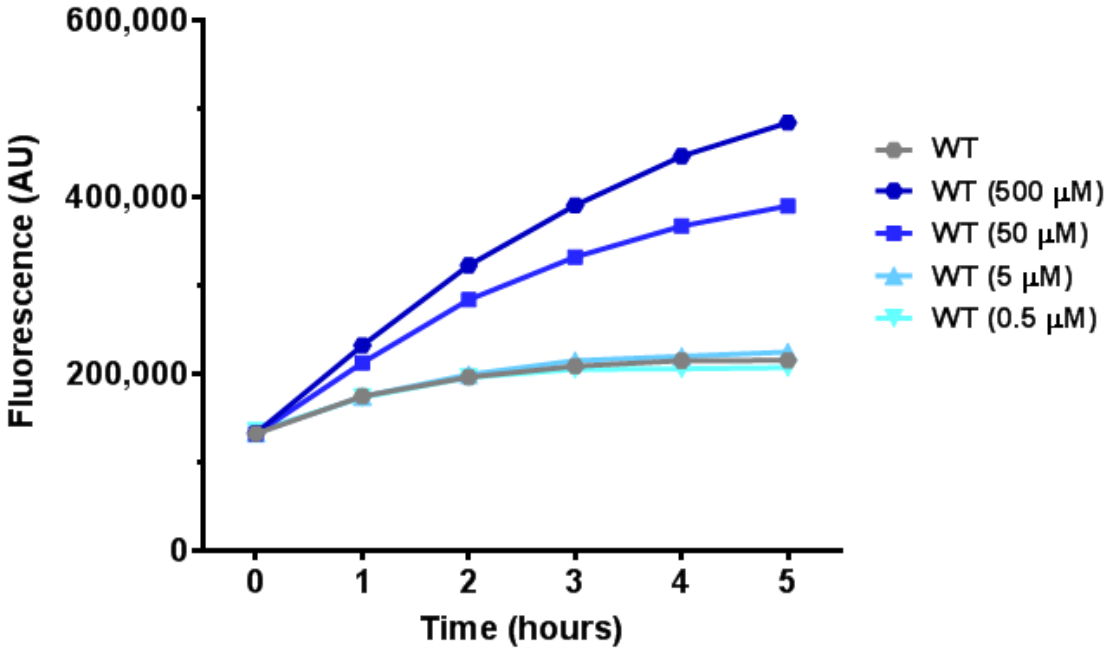


**Figure 37: DQC dilution shows dose response in UTI89.** There is a dose dependent response in UTI89 to Compound 9 (DQC). Concentrations between 0.5 and 500 μM were used to track P*qse* promoter activity on the SpectraMax I3 plate reader after the addition of compound.

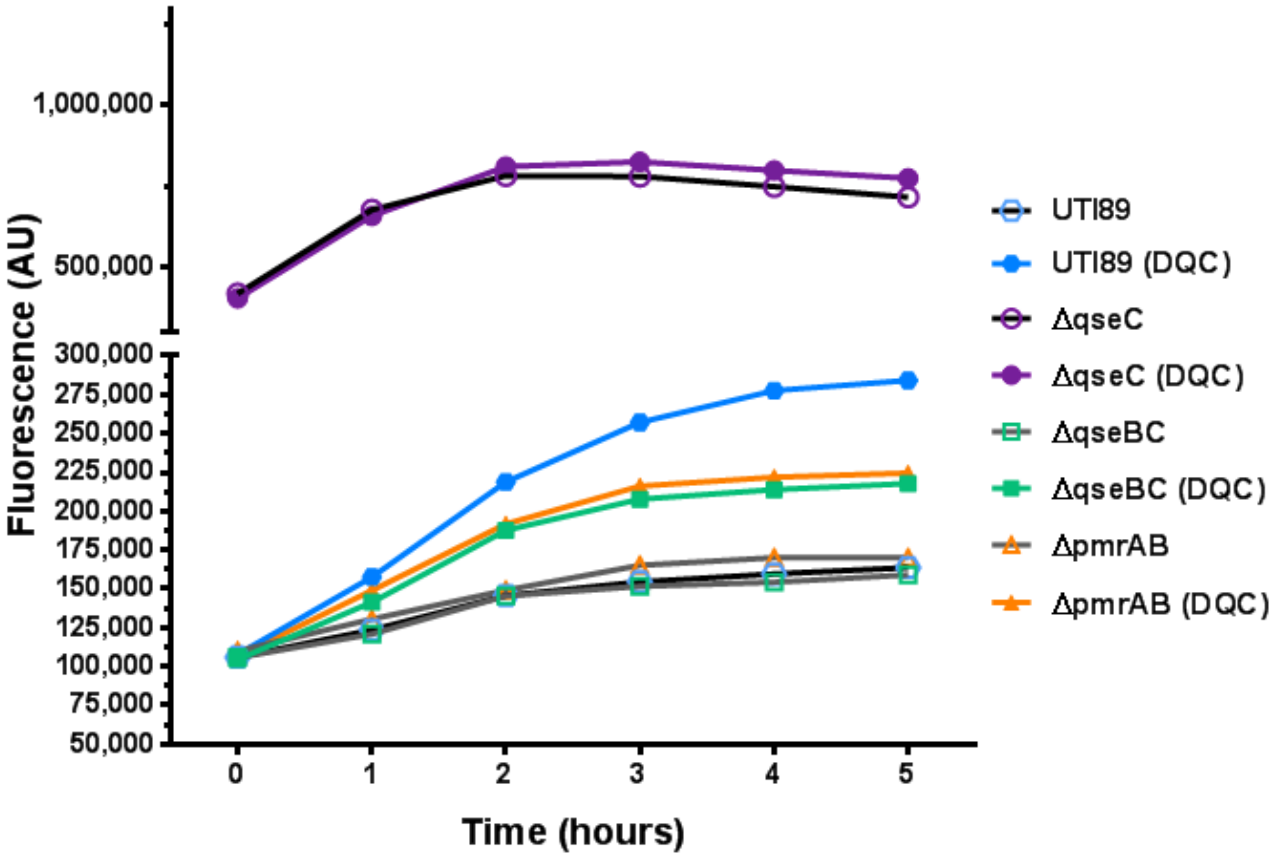


**Figure 38: DQC induced fluorescence requires at least one component from the PmrAB and QseBC system to achieve maximum activity.** Fluorescence in the presence of compound 9 (DQC) is tracked over time in N-minimal media for the WT, *ΔqseC, ΔqseBC,* and *ΔpmrAB* strains.

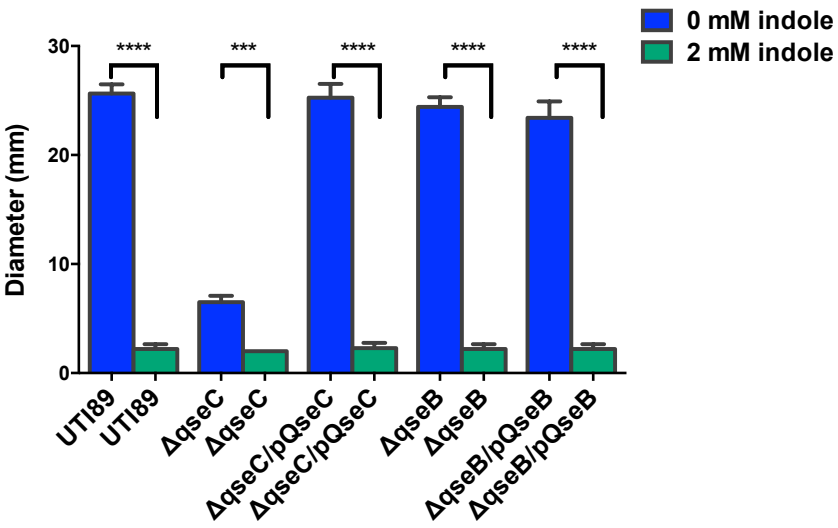


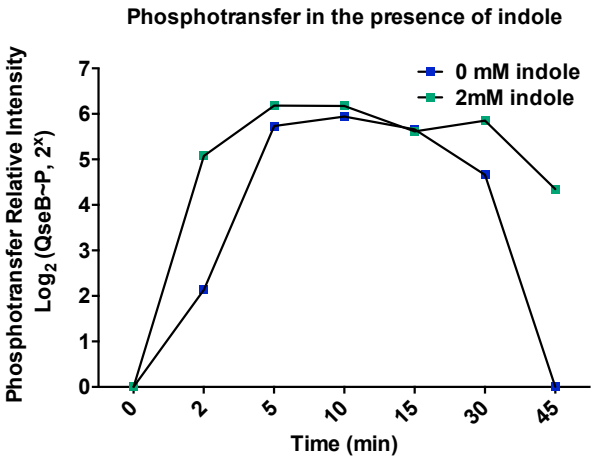


**Figure 39: Affect of indole on UPEC motility and *in vitro* phosphotrasnfer kinetics**. Indole decreases the motility of UPEC. When indole is present in soft agar, UTI89 is non-motile. This is true for WT and strains lacking *qseB, qseC* and those complemented by *PqseB and PqseC*. This is not a direct effect of QseC increasing phosphotrasnfer to QseB, as the presence of indole does not alter *in vitro* phospho-kinetics.

APPENDIX

**Table A1: Primers and probes used in this work**

| Primer/Probe | Nucleotide sequence 5'→3' | Purpose |
|---|---|---|
| | **Chapter 3** | |
| rrsH483_Fwd | CGTTACCCGCAGAAGAAGCAC | qRT-PCR |
| rrsH637_Rev | GATGCAGTTCCCAGGTTGAGC | qRT-PCR |
| rrsH probe | VIC-CGTTAATCGGAATTACTG | qRT-PCR |
| gfp_qrt_Fwd | GTGCCATGCCCGAAGGTTATGTAC | qRT-PCR |
| gfp_qrt_Rev | GTTGTATTCCAATTTGTGTCCAAGAAT | qRT-PCR |
| gfp probe | FAM-ACGTGCTGAAGTCAAG | qRT-PCR |
| gyrB_qrt_Fwd | GATGCGCGTGAAGGCCTGATTG | qRT-PCR |
| gyrB_qrt_Rev | CACGGGCACGGGCAGCATC | qRT-PCR |
| gyrB probe | VIC-ACGAACTGCTGGCGGA | qRT-PCR |
| yibD_qrt_Fwd | GGTTCAACGGATAATTCTGTT | qRT-PCR |
| yibD_qrt_Rev | ACTTCAATCCCACGATTACG | qRT-PCR |
| yibD probe | NED-CACGTTCGTTTGTTGCATC | qRT-PCR |
| | **Chapter 4** | |
| rrsH483_Fwd | CGTTACCCGCAGAAGAAGCAC | qRT-PCR |
| rrsH637_Rev | GATGCAGTTCCCAGGTTGAGC | qRT-PCR |
| *rrSH* probe | VIC-CGTTAATCGGAATTACTG | qRT-PCR |
| QseB_130 Fwd | CCT TAT GAT GCG GTG ATC CTG G | qRT-PCR |
| QseB_283 Rev | TCC CAG ACG CAG CCC TTC TA | qRT-PCR |
| *qseB* probe | FAM-TGCGCGAATGGCGA | qRT-PCR |
| | **Site-directed mutagenesis** | |
| QseC_H246A_forw | CGCTTTACCTCCGACGCAGCT**GCC**GAACTTCGTA GCCCGTTAAC | C**A**C → GCC to make QseC_H246A |
| QseC_H246A_rev | GTTAACGGGCTACGAAGTTC**GGC**AGCTGCGTCGG AGGTAAAGCG | C**A**C → GCC to make QseC_H246A |
| QseC_H246D_forw | CGCTTTACCTCCGACGCAGCT**GAC**GAACTTCGTA GCCCGTTAAC | C**A**C → GAC to make QseC_H246D |
| QseC_H246D_rev | GTTAACGGGCTACGAAGTTC**GTC**AGCTGCGTCGG AGGTAAAGCG | C**A**C → GAC to make QseC_H246D |
| QseC_ H246L_forw | CCTCCGACGCAGCT**CTC**GAACTTCGTAGCCCG | C**A**C → C**U**C to make H246L in QseC |
| QseC_ H246L_rev | CGG GCT ACG AAG TTC **GAG** AGC TGC GTC GGA GG | C**A**C → C**U**C to make H246L in QseC |
| | **Co-evolving residues (PmrB → QseC)** | |
| PmrB_A161T_forw | GAACGCCACTG**ACG**GGGGTGCGTTTGC | To make the point mutation A161T in PmrB |
| PmrB_A161T_rev | GCAAACGCACCCC**CGT**CAGTGGCGTTC | Reverse primer to make the point mutation A161T in PmrB |
| PmrB_A161T;G162A_forw | CGCCACTGACG**GCG**GTGCGTTTGC | To make the point mutation |

| | | |
|---|---|---|
| | | G162A in PmrB harboring A161T |
| PmrB_A161T;G162A_rev | GCAAACGCACCGCCGTCAGTGGCG | Reverse primer to make the point mutation G162A in PmrB harboring A161T |
| PmrB_A161T;G162A; L165V_forw | CGGCGGTGCGTGTGCATCTGGAACTGC | To make the point mutation L165V in PmrB harboring A161T and G162A |
| PmrB_A161T;G162A; L165V_rev | GCAGTTCCAGATGCACACGCACCGCCG | Reverse primer to make the point mutation L165V in PmrB harboring A161T and G162A |
| PmrB_A161T;G162A; L165V;H166Q_forw | GGCGGTGCGTGTGCAGCTGGAACTGCTGGC | To make the point mutation H166Q in PmrB harboring A161T, G162A, and L165V |
| PmrB_A161T;G162A; L165V;H166Q_rev | GCCAGCAGTTCCAGCTGCACACGCACCGCC | Reverse primer make the point mutation H166Q in PmrB harboring A161T, G162A, and L165V |
| PmrB_A161T;G162A;L165 V;H166Q;L169V_forw | CGTGTGCAGCTGGAAGTGCTGGCGAAAACGC | To make the point mutation L169V in PmrB harboring A161T, G162A, L165V, and H166Q |
| | **Co-evolving residues (PmrB → alanines)** | |
| PmrB_G162A_forw | CGCCACTGGCGGCGGTGCGTTTGC | To make the point mutation G162A in PmrB |
| PmrB_G162A_rev | GCAAACGCACCGCCGCCAGTGGCG | Reverse primer to make the point mutation G162A in PmrB |
| PmrB_G162A;L165A_forw | CGGCGGTGCGTGCGCATCTGGAACTGC | To make the point mutation L165A in PmrB harboring G162A |
| PmrB_G162A;L165A_rev | GCAGTTCCAGATGCGCACGCACCGCCG | Reverse primer to make the point mutation L165A in PmrB harboring G162A |
| PmrB_G162A;L165A; H166A_forw | GCGGTGCGTGCGGCGCTGGAACTGCTGGC | To make the point mutation H166A in PmrB harboring G162A and L165A |
| PmrB_G162A;L165A; H166A_rev | GCCAGCAGTTCCAGCGCCGCACGCACCGC | Reverse primer to make the point mutation H166A in PmrB harboring G162A and L165A |
| PmrB_G162A;L165A; H166A;L169A_forw | CGTGCGGCGCTGGAAGCGCTGGCGAAAACGC | To make the point mutation L169A in PmrB harboring G162A, L165A, and H166A |
| PmrB_G162A;L165A; H166A;L169A_rev | GCGTTTTCGCCAGCGCTTCCAGCGCCGCACG | Reverse primer to make the point mutation L169A in PmrB harboring G162A, L165A, and H166A |

**Sequence alignments**

The following pages contain the sequence alignments for the *qseBC* and *pmrAB* promoter regions as well as the protein alignments for QseC, QseB, PmrB, and PmrA. Highlighted residues depict changes from the 49-strain consensus. The colored bars to the left of the strains designate clade, which corresponds to the clade color designations listed below. For the promoter alignments, the genes flanking the promoter are underlined in the first strain.

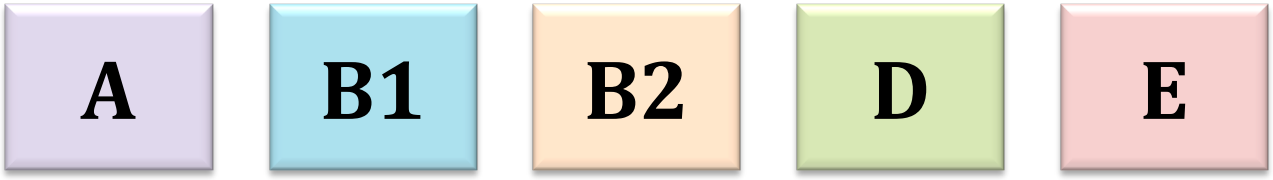

# *qseBC* promoter nucleic acid alignment

# *pmrAB* promoter nucleic acid alignment

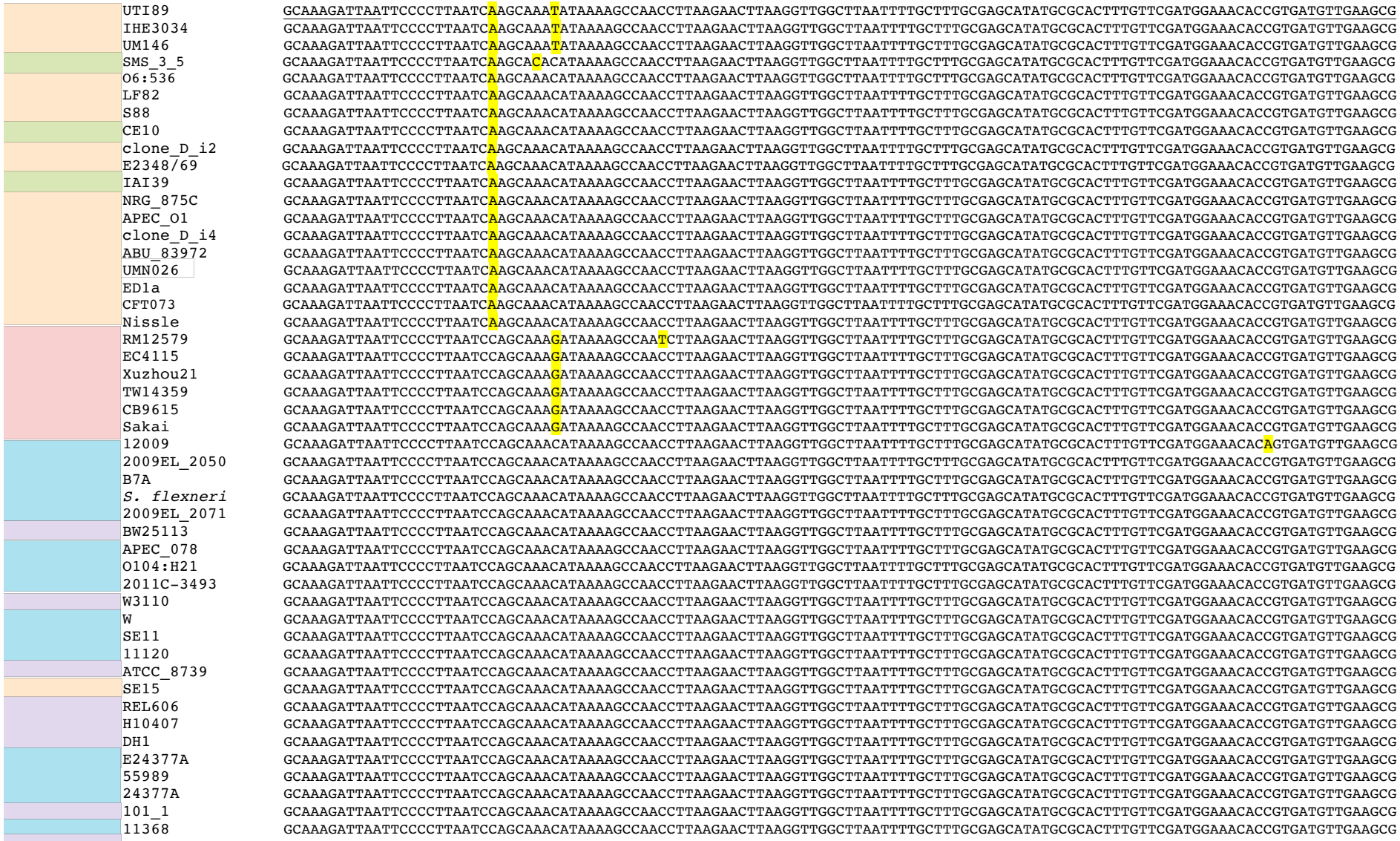

# QseC protein sequence alignment

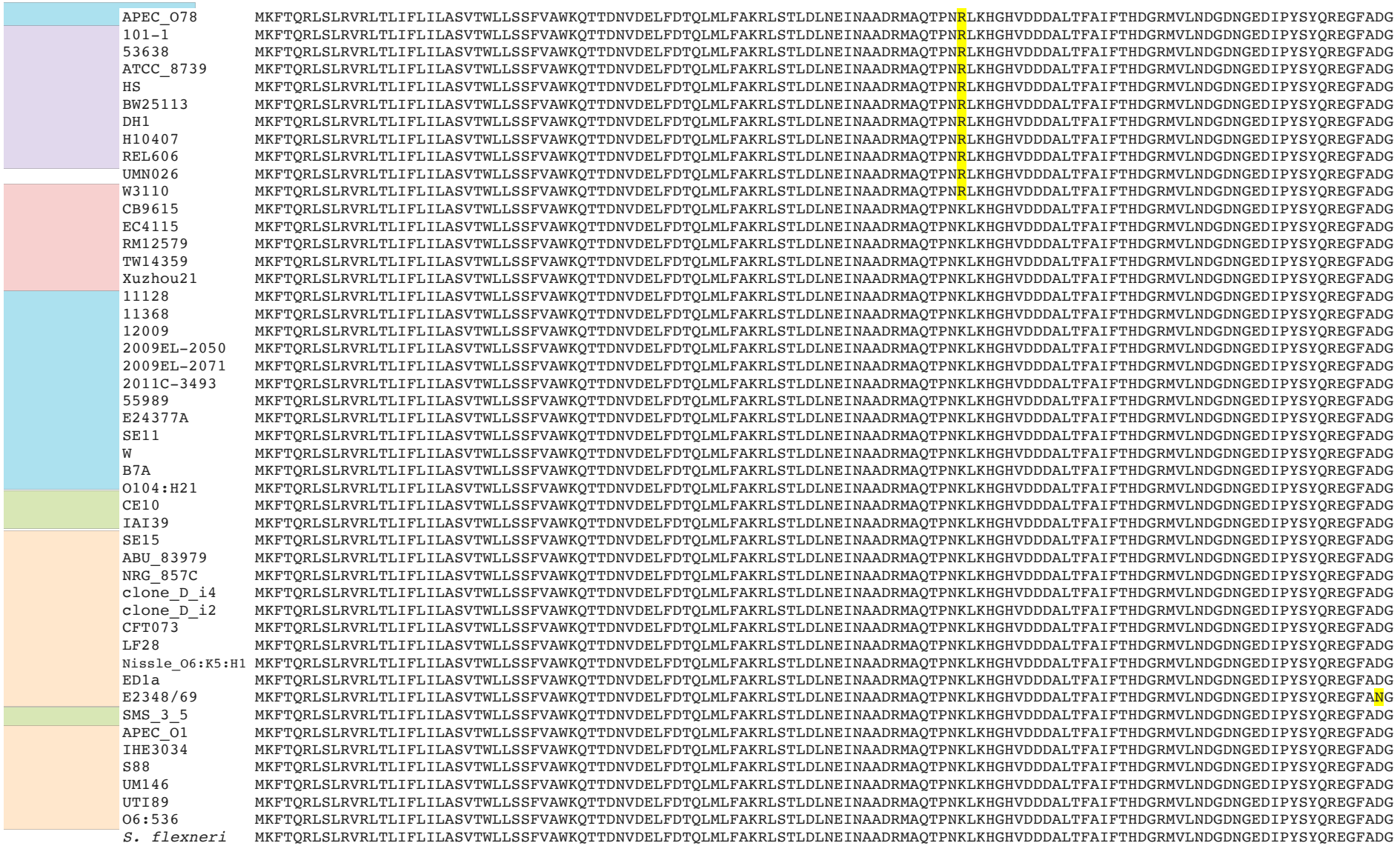

## QseC protein sequence alignment continued

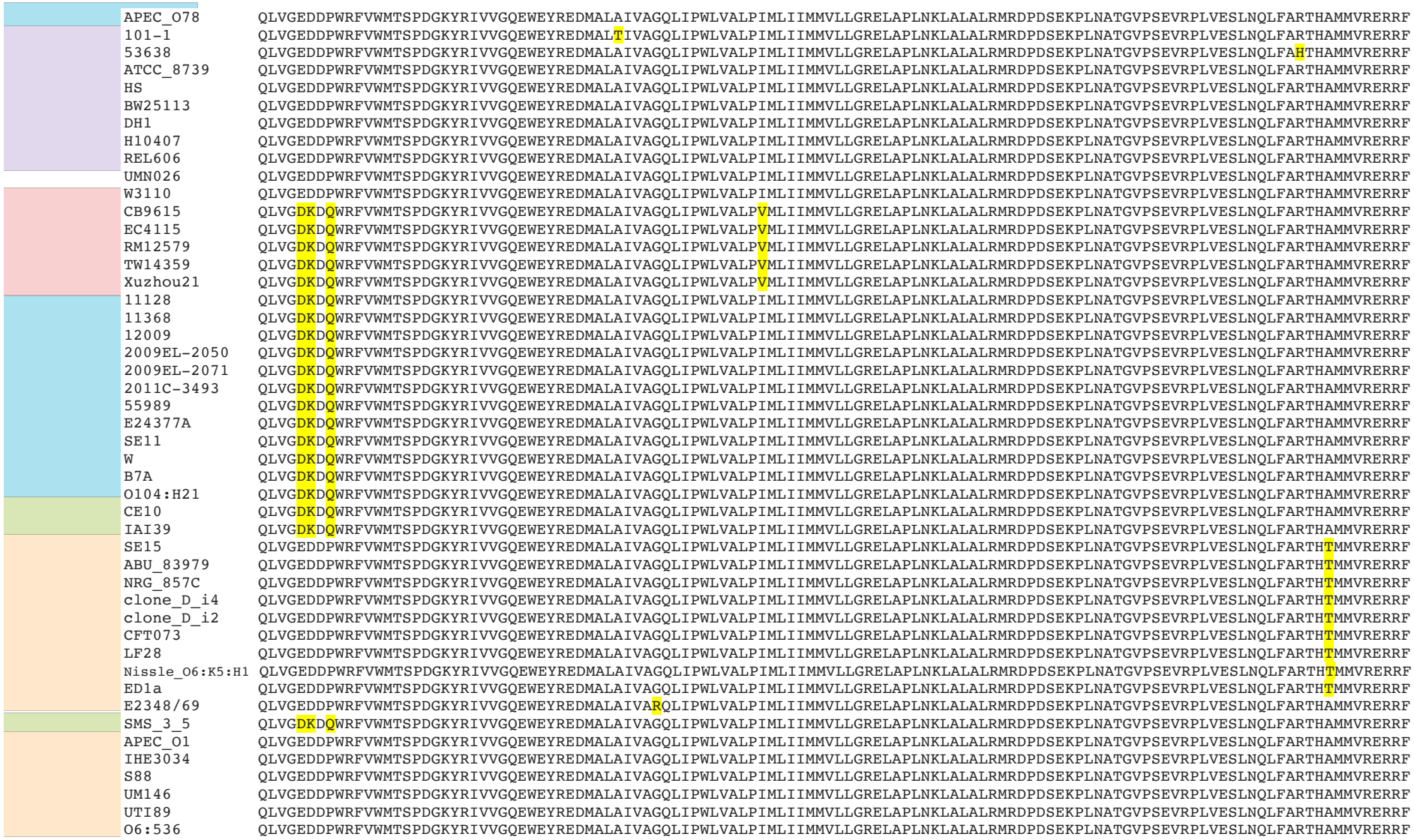

# QseC protein sequence alignment continued

# QseC protein sequence alignment continued

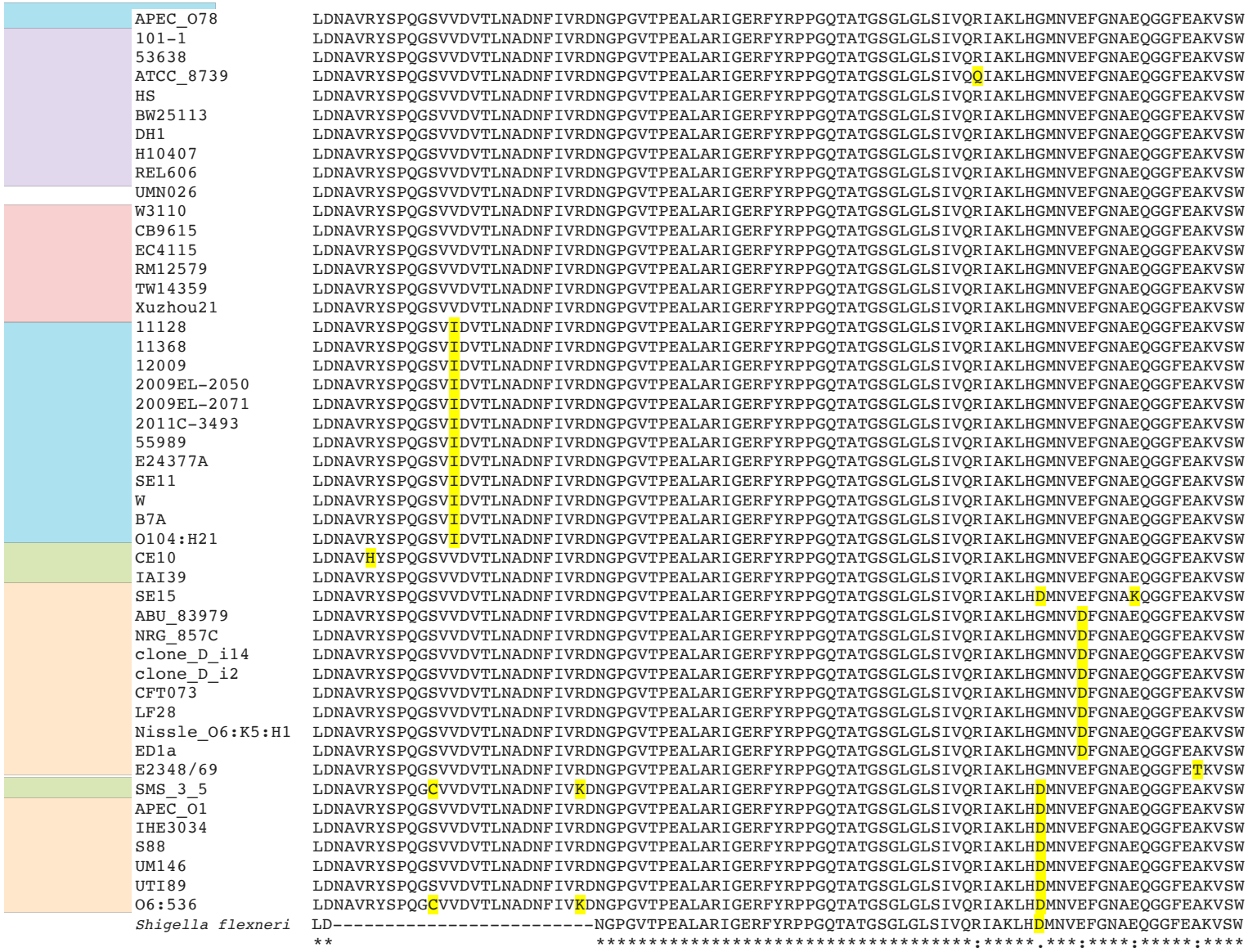

# QseB protein sequence alignment

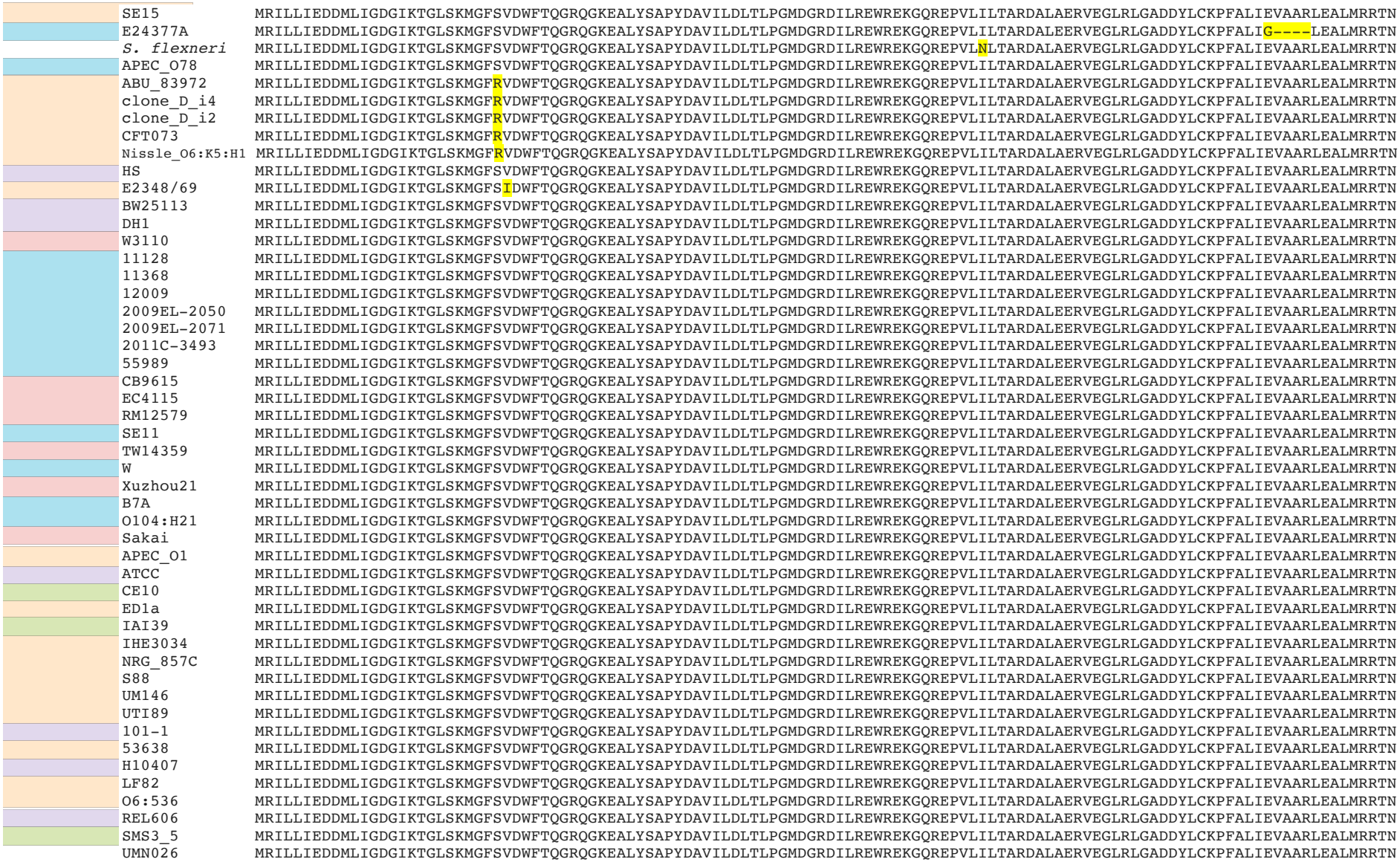

# QseB protein sequence alignment continued

```
SE15                GQASNELLRGNVMLDPGKRIATLAGEPLTLKPKEFALLELLMRNAGRVLPRKLIEEKLYTWDEEVTSNAVEVHVHHLRRKLGSDFIRTVHGIGYTLGEK
E24377A             GQASNELRHGNVMLDPGKRIATLAGEPLTLKPKEFALLELLMRNAGRVLPRKLIEEKLYTWDEEVTSNAVEVHVHHLRRKLGSDFIRTVHGIGYTLGEK
Shigella flexneri   GQASNELRHGNVMLDPGKRIATLAGEPLTLKPKEFALLELLMRNAGRVLPRKLIEEKLYTWDEEVTSNAVEVHVHHLRRKLGSDFIRTVHGIGYTLGEK
APEC_O78            GQASNELRHGNVMLDPDKRIATLAGEPLTLKPKEFALLELLMRNAGRVLPRKLIEEKLYTWDEEVTSNAVEVHVHHLRRKLGSDFIRTVHGIGYTLGEK
ABU_83972           GQASNELRHGNVMLDPGKRIATLAGEPLTLKPKEFALLELLMRNAGRVLPRKLIEEKLYTWDEEVTSNAVEVHVHHLRRKLGSDFIRTVHGIGYTLGEK
clone_D_i14         GQASNELRHGNVMLDPGKRIATLAGEPLTLKPKEFALLELLMRNAGRVLPRKLIEEKLYTWDEEVTSNAVEVHVHHLRRKLGSDFIRTVHGIGYTLGEK
clone_D_i2          GQASNELRHGNVMLDPGKRIATLAGEPLTLKPKEFALLELLMRNAGRVLPRKLIEEKLYTWDEEVTSNAVEVHVHHLRRKLGSDFIRTVHGIGYTLGEK
CFT073              GQASNELRHGNVMLDPGKRIATLAGEPLTLKPKEFALLELLMRNAGRVLPRKLIEEKLYTWDEEVTSNAVEVHVHHLRRKLGSDFIRTVHGIGYTLGEK
Nissle_O6:K5:H1     GQASNELRHGNVMLDPGKRIATLAGEPLTLKPKEFALLELLMRNAGRVLPRKLIEEKLYTWDEEVTSNAVEVHVHHLRRKLGSDFIRTVHGIGYTLGEK
HS                  GQASNELRHGNVMLDPGKRIATLAGDPLTLKPKEFALLELLMRNAGRVLPRKLIEEKLYTWDEEVTSNAVEVHVHHLRRKLGSDFIRTVHGIGYTLGEK
E2348/69            GQASNELRHGNVMLDPGKRIATLAGEPLTLKPKEFALLELLMRNAGRVLPRKLIEEKLYTWDEEVTSNAVEVHVHHLRRKLGSDFIRTVHGIGYTLGEK
BW25113             GQASNELRHGNVMLDPGKRIATLAGEPLTLKPKEFALLELLMRNAGRVLSRKLIEEKLYTWDEEVTSNAVEVHVHHLRRKLGSDFIRTVHGIGYTLGEK
DH1                 GQASNELRHGNVMLDPGKRIATLAGEPLTLKPKEFALLELLMRNAGRVLSRKLIEEKLYTWDEEVTSNAVEVHVHHLRRKLGSDFIRTVHGIGYTLGEK
W3110               GQASNELRHGNVMLDPGKRIATLAGEPLTLKPKEFALLELLMRNAGRVLSRKLIEEKLYTWDEEVTSNAVEVHVHHLRRKLGSDFIRTVHGIGYTLGEK
11128               GQASNELRHGNVMLDPGKRIATLAGEPLTLKPKEFALLELLMRNAGRVLPRKLIEEKLYTWDEEVTSNAVEVHVHHLRRKLGSDFIRTVHGIGYTLGEK
11368               GQASNELRHGNVMLDPGKRIATLAGEPLTLKPKEFALLELLMRNAGRVLPRKLIEEKLYTWDEEVTSNAVEVHVHHLRRKLGSDFIRTVHGIGYTLGEK
12009               GQASNELRHGNVMLDPGKRIATLAGEPLTLKPKEFALLELLMRNAGRVLPRKLIEEKLYTWDEEVTSNAVEVHVHHLRRKLGSDFIRTVHGIGYTLGEK
2009EL-2050         GQASNELRHGNVMLDPGKRIATLAGEPLTLKPKEFALLELLMRNAGRVLPRKLIEEKLYTWDEEVTSNAVEVHVHHLRRKLGSDFIRTVHGIGYTLGEK
2009EL-2071         GQASNELRHGNVMLDPGKRIATLAGEPLTLKPKEFALLELLMRNAGRVLPRKLIEEKLYTWDEEVTSNAVEVHVHHLRRKLGSDFIRTVHGIGYTLGEK
2011C-3493          GQASNELRHGNVMLDPGKRIATLAGEPLTLKPKEFALLELLMRNAGRVLPRKLIEEKLYTWDEEVTSNAVEVHVHHLRRKLGSDFIRTVHGIGYTLGEK
55989               GQASNELRHGNVMLDPGKRIATLAGEPLTLKPKEFALLELLMRNAGRVLPRKLIEEKLYTWDEEVTSNAVEVHVHHLRRKLGSDFIRTVHGIGYTLGEK
CB9615              GQASNELRHGNVMLDPGKRIATLAGEPLTLKPKEFALLELLMRNAGRVLPRKLIEEKLYTWDEEVTSNAVEVHVHHLRRKLGSDFIRTVHGIGYTLGEK
EC4115              GQASNELRHGNVMLDPGKRIATLAGEPLTLKPKEFALLELLMRNAGRVLPRKLIEEKLYTWDEEVTSNAVEVHVHHLRRKLGSDFIRTVHGIGYTLGEK
RM12579             GQASNELRHGNVMLDPGKRIATLAGEPLTLKPKEFALLELLMRNAGRVLPRKLIEEKLYTWDEEVTSNAVEVHVHHLRRKLGSDFIRTVHGIGYTLGEK
SE11                GQASNELRHGNVMLDPGKRIATLAGEPLTLKPKEFALLELLMRNAGRVLPRKLIEEKLYTWDEEVTSNAVEVHVHHLRRKLGSDFIRTVHGIGYTLGEK
TW14359             GQASNELRHGNVMLDPGKRIATLAGEPLTLKPKEFALLELLMRNAGRVLPRKLIEEKLYTWDEEVTSNAVEVHVHHLRRKLGSDFIRTVHGIGYTLGEK
W                   GQASNELRHGNVMLDPGKRIATLAGEPLTLKPKEFALLELLMRNAGRVLPRKLIEEKLYTWDEEVTSNAVEVHVHHLRRKLGSDFIRTVHGIGYTLGEK
Xuzhou21            GQASNELRHGNVMLDPGKRIATLAGEPLTLKPKEFALLELLMRNAGRVLPRKLIEEKLYTWDEEVTSNAVEVHVHHLRRKLGSDFIRTVHGIGYTLGEK
B7A                 GQASNELRHGNVMLDPGKRIATLAGEPLTLKPKEFALLELLMRNAGRVLPRKLIEEKLYTWDEEVTSNAVEVHVHHLRRKLGSDFIRTVHGIGYTLGEK
O104:H21            GQASNELRHGNVMLDPGKRIATLAGEPLTLKPKEFALLELLMRNAGRVLPRKLIEEKLYTWDEEVTSNAVEVHVHHLRRKLGSDFIRTVHGIGYTLGEK
Sakai               GQASNELRHGNVMLDPGKRIATLAGEPLTLKPKEFALLELLMRNAGRVLPRKLIEEKLYTWDEEVTSNAVEVHVHHLRRKLGSDFIRTVHGIGYTLGEK
APEC_O1             GQASNELRHGNVMLDPGKRIATLAGEPLTLKPKEFALLELLMRNAGRVLPRKLIEEKLYTWDEEVTSNAVEVHVHHLRRKLGSDFIRTVHGIGYTLGEK
ATCC                GQASNELRHGNVMLDPGKRIATLAGEPLTLKPKEFALLELLMRNAGRVLPRKLIEEKLYTWDEEVTSNAVEVHVHHLRRKLGSDFIRTVHGIGYTLGEK
CE10                GQASNELRHGNVMLDPGKRIATLAGEPLTLKPKEFALLELLMRNAGRVLPRKLIEEKLYTWDEEVTSNAVEVHVHHLRRKLGSDFIRTVHGIGYTLGEK
ED1a                GQASNELRHGNVMLDPGKRIATLAGEPLTLKPKEFALLELLMRNAGRVLPRKLIEEKLYTWDEEVTSNAVEVHVHHLRRKLGSDFIRTVHGIGYTLGEK
IAI39               GQASNELRHGNVMLDPGKRIATLAGEPLTLKPKEFALLELLMRNAGRVLPRKLIEEKLYTWDEEVTSNAVEVHVHHLRRKLGSDFIRTVHGIGYTLGEK
IHE3034             GQASNELRHGNVMLDPGKRIATLAGEPLTLKPKEFALLELLMRNAGRVLPRKLIEEKLYTWDEEVTSNAVEVHVHHLRRKLGSDFIRTVHGIGYTLGEK
NRG                 GQASNELRHGNVMLDPGKRIATLAGEPLTLKPKEFALLELLMRNAGRVLPRKLIEEKLYTWDEEVTSNAVEVHVHHLRRKLGSDFIRTVHGIGYTLGEK
S88                 GQASNELRHGNVMLDPGKRIATLAGEPLTLKPKEFALLELLMRNAGRVLPRKLIEEKLYTWDEEVTSNAVEVHVHHLRRKLGSDFIRTVHGIGYTLGEK
UM146               GQASNELRHGNVMLDPGKRIATLAGEPLTLKPKEFALLELLMRNAGRVLPRKLIEEKLYTWDEEVTSNAVEVHVHHLRRKLGSDFIRTVHGIGYTLGEK
UTI89               GQASNELRHGNVMLDPGKRIATLAGEPLTLKPKEFALLELLMRNAGRVLPRKLIEEKLYTWDEEVTSNAVEVHVHHLRRKLGSDFIRTVHGIGYTLGEK
101-1               GQASNELRHGNVMLDPGKRIATLAGEPLTLKPKEFALLELLMRNAGRVLPRKLIEEKLYTWDEEVTSNAVEVHVHHLRRKLGSDFIRTVHGIGYTLGEK
53638               GQASNELRHGNVMLDPGKRIATLAGEPLTLKPKEFALLELLMRNAGRVLPRKLIEEKLYTWDEEVTSNAVEVHVHHLRRKLGSDFIRTVHGIGYTLGEK
H10407              GQASNELRHGNVMLDPGKRIATLAGEPLTLKPKEFALLELLMRNAGRVLPRKLIEEKLYTWDEEVTSNAVEVHVHHLRRKLGSDFIRTVHGIGYTLGEK
LF82                GQASNELRHGNVMLDPGKRIATLAGEPLTLKPKEFALLELLMRNAGRVLPRKLIEEKLYTWDEEVTSNAVEVHVHHLRRKLGSDFIRTVHGIGYTLGEK
O6:536              GQASNELRHGNVMLDPGKRIATLAGEPLTLKPKEFALLELLMRNAGRVLPRKLIEEKLYTWDEEVTSNAVEVHVHHLRRKLGSDFIRTVHGIGYTLGEK
REL606              GQASNELRHGNVMLDPGKRIATLAGEPLTLKPKEFALLELLMRNAGRVLPRKLIEEKLYTWDEEVTSNAVEVHVHHLRRKLGSDFIRTVHGIGYTLGEK
SMS3_5              GQASNELRHGNVMLDPGKRIATLAGEPLTLKPKEFALLELLMRNAGRVLPRKLIEEKLYTWDEEVTSNAVEVHVHHLRRKLGSDFIRTVHGIGYTLGEK
UMN026              GQASNELRHGNVMLDPGKRIATLAGEPLTLKPKEFALLELLMRNAGRVLPRKLIEEKLYTWDEEVTSNAVEVHVHHLRRKLGSDFIRTVHGIGYTLGEK
                    ******* :*******.********:********************** **************************************************
```

# PmrB protein sequence alignment

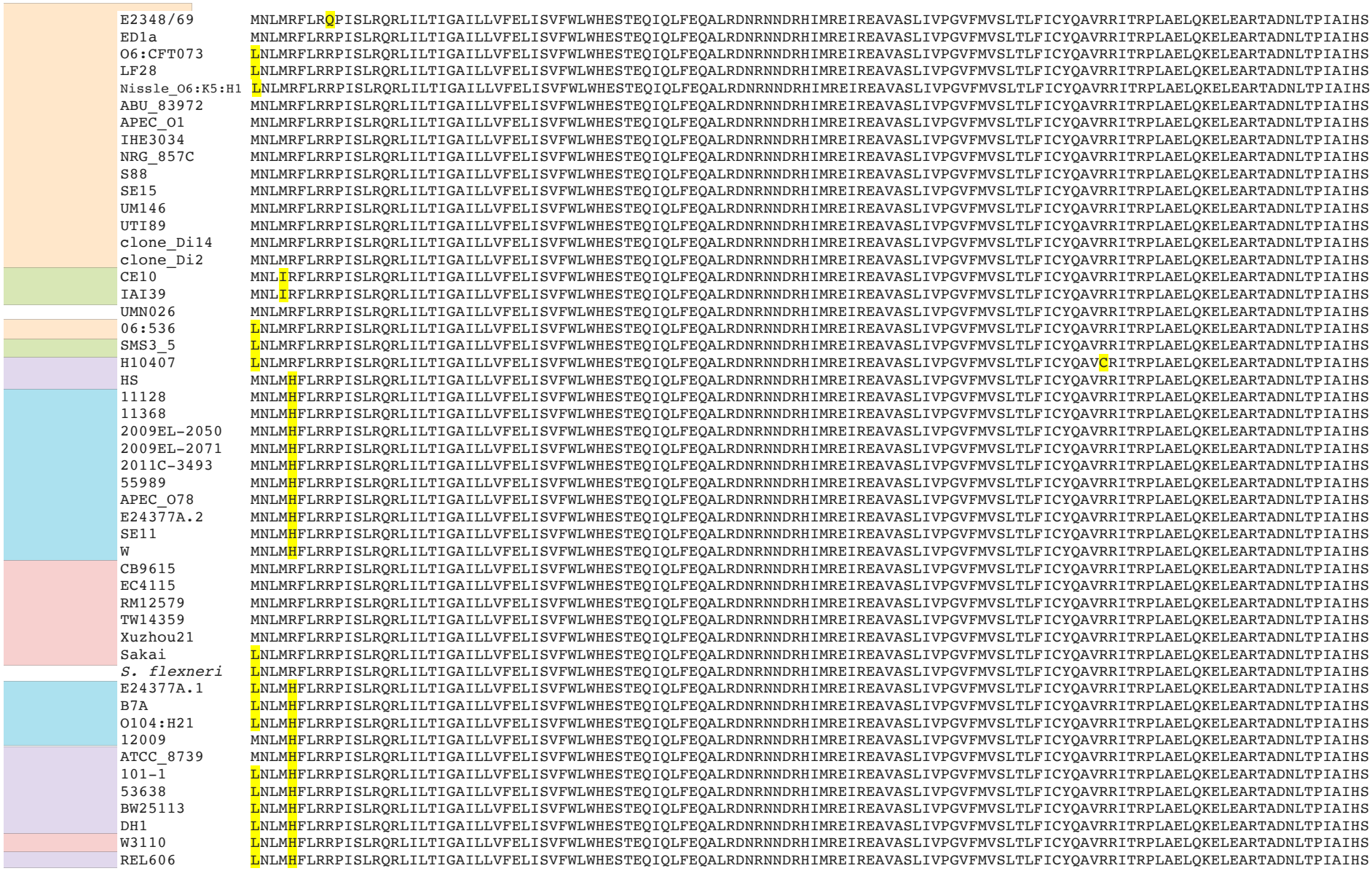

# PmrB protein sequence alignment continued

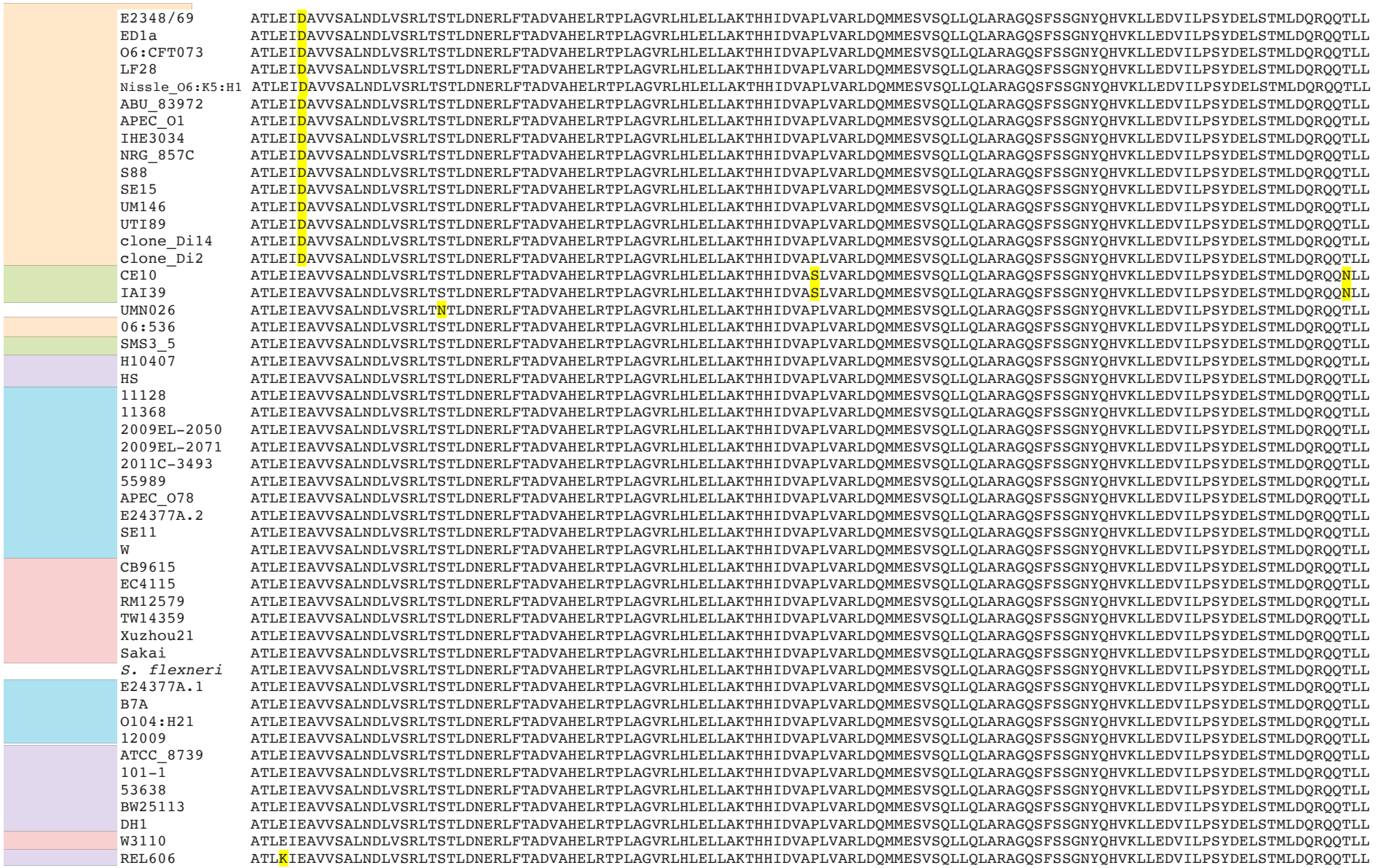

## PmrB protein sequence alignment continued

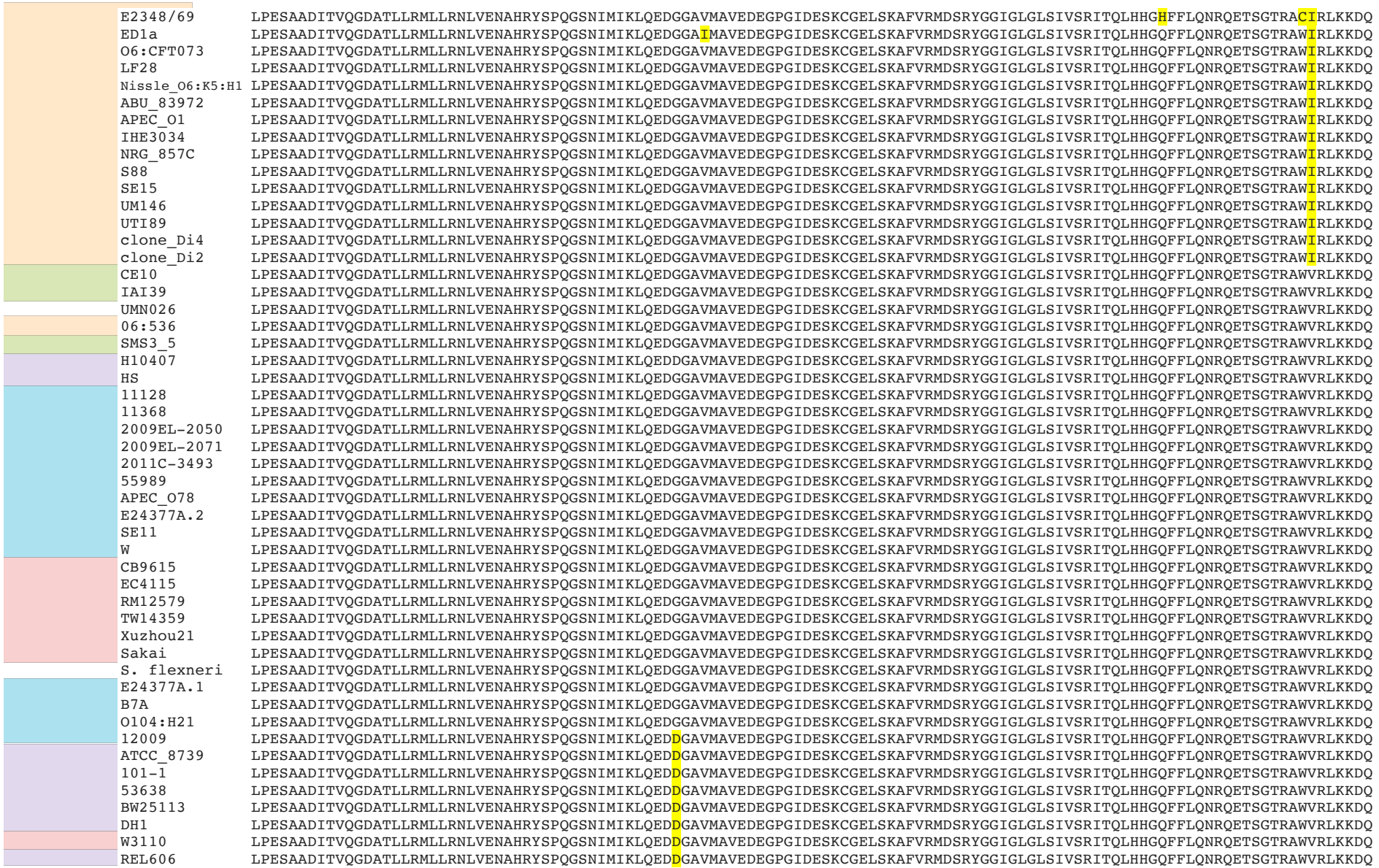

## PmrB protein sequence alignment continued

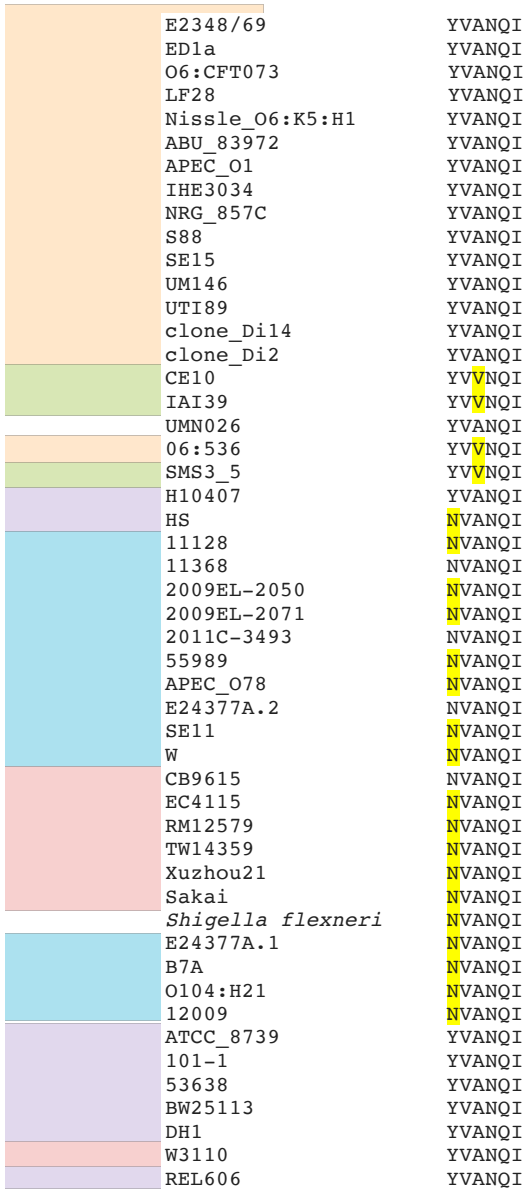

```
E2348/69                YVANQI
ED1a                    YVANQI
O6:CFT073               YVANQI
LF28                    YVANQI
Nissle_O6:K5:H1         YVANQI
ABU_83972               YVANQI
APEC_O1                 YVANQI
IHE3034                 YVANQI
NRG_857C                YVANQI
S88                     YVANQI
SE15                    YVANQI
UM146                   YVANQI
UTI89                   YVANQI
clone_Di14              YVANQI
clone_Di2               YVANQI
CE10                    YVVNQI
IAI39                   YVVNQI
UMN026                  YVANQI
06:536                  YVVNQI
SMS3_5                  YVVNQI
H10407                  YVANQI
HS                      NVANQI
11128                   NVANQI
11368                   NVANQI
2009EL-2050             NVANQI
2009EL-2071             NVANQI
2011C-3493              NVANQI
55989                   NVANQI
APEC_O78                NVANQI
E24377A.2               NVANQI
SE11                    NVANQI
W                       NVANQI
CB9615                  NVANQI
EC4115                  NVANQI
RM12579                 NVANQI
TW14359                 NVANQI
Xuzhou21                NVANQI
Sakai                   NVANQI
Shigella flexneri       NVANQI
E24377A.1               NVANQI
B7A                     NVANQI
O104:H21                NVANQI
12009                   NVANQI
ATCC_8739               YVANQI
101-1                   YVANQI
53638                   YVANQI
BW25113                 YVANQI
DH1                     YVANQI
W3110                   YVANQI
REL606                  YVANQI
                         *.***
```

# PmrA protein sequence alignment

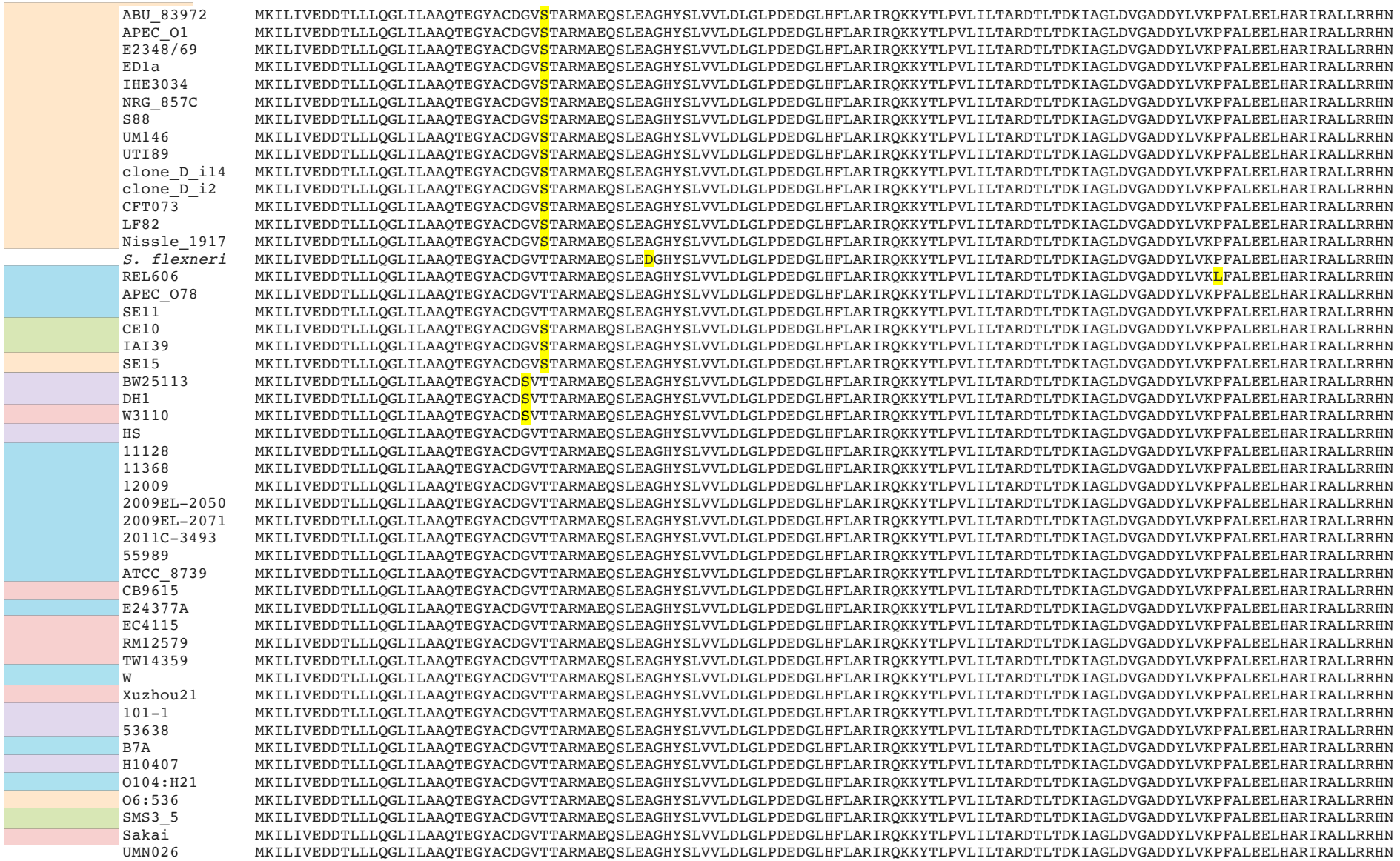

# PmrA protein sequence alignment continued

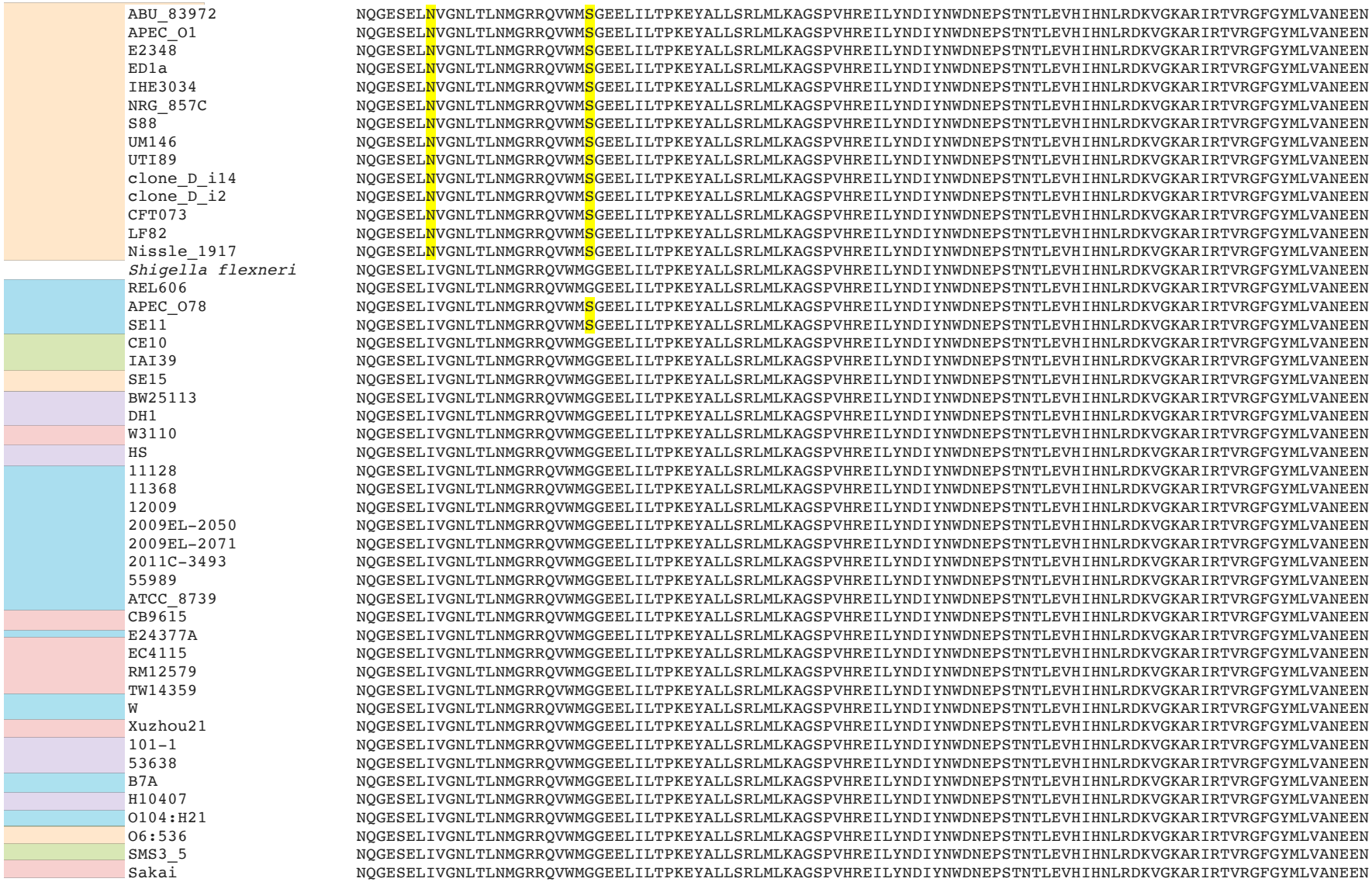

## Permissions

LAST UPDATED: January 2017

# ASM Journals Statement of Authors' Rights

### Authors may post their articles to their institutional repositories

ASM grants authors the right to post their accepted manuscripts in publicly accessible electronic repositories maintained by funding agencies, as well as appropriate institutional or subject-based open repositories established by a government or non-commercial entity. Since ASM makes the final, typeset articles from its primary-research journals available free of charge on the ASM Journals and PMC websites 6 months after final publication, ASM recommends that when submitting the accepted manuscript to PMC or institutional repositories, the author specify that the posting release date for the manuscript be no earlier than 6 months after the final publication of the typeset article by ASM. Please note that the information outlined above, in addition to the **new author fee structure**, allows authors to comply with the **Policy for open access in the post-2014 Research Excellence Framework**.

### Authors may post their articles in full on personal or employer websites

ASM grants the author the right to post his/her article (after publication by ASM) on the author's personal or university-hosted website, but not on any corporate, government, or similar website, without ASM's prior permission, provided that proper credit is given to the original ASM publication.

### Authors may make copies of their articles in full

Corresponding authors are entitled to 10 free downloads of their papers. Additionally, all authors may make up to 99 copies of his/her own work for personal or professional use (including teaching packs that are distributed free of charge within your own institution). For orders of 100 or more copies, you should seek ASM's permission or purchase access through Highwire's Pay-Per-View option, available on the ASM online journal sites.

### Authors may republish/adapt portions of their articles

ASM also grants the authors the right to republish discrete portions of his/her article in any other publication (including print, CD-ROM, and other electronic formats) of which he or she is author or editor, provided that proper credit is given to the original ASM publication. ASM authors also retain the right to reuse the full article in his/her dissertation or thesis. "Proper credit" means either the copyright lines shown on the top of the first page of the PDF version, or "Copyright © American Society for Microbiology, [insert journal name, volume number, year, page numbers and DOI]" of the HTML version. For technical questions about using Rightslink, please contact Customer Support via phone at (877) 622-5543 (toll free) or (978) 777-9929, or e-mail Rightslink customer care at **customercare@copyright.com.**

Please note that the ASM is in full **compliance with NIH Policy.**

Back to **Top^**

PubMed Abstract | CrossRef Full Text | Google Scholar

**Keywords:** APEC, ExPEC, MAEC/NMEC, UPEC, two-component systems, signal transduction, virulence factors

**Citation:** Breland EJ, Eberly AR and Hadjifrangiskou M (2017) An Overview of Two-Component Signal Transduction Systems Implicated in Extra-Intestinal Pathogenic *E. coli* Infections. *Front. Cell. Infect. Microbiol.* 7:162. doi: 10.3389/fcimb.2017.00162

**Received:** 01 March 2017; **Accepted:** 18 April 2017;
**Published:** 09 May 2017.

Edited by:
**Alfredo G. Torres**, University of Texas Medical Branch, USA

Reviewed by:
**Chitrita Debroy**, Pennsylvania State University, USA
**Catherine M. Logue**, Iowa State University, USA
**Sheryl S. Justice**, Ohio State University at Columbus, USA



***Correspondence:** Maria Hadjifrangiskou, **maria.hadjifrangiskou@vanderbilt.edu**

## THE AMERICAN ASSOCIATION FOR THE ADVANCEMENT OF SCIENCE ORDER DETAILS

Jun 14, 2017

| | |
|---|---|
| Order Number | 501279671 |
| Order date | Jun 14, 2017 |
| Licensed Content Publisher | The American Association for the Advancement of Science |
| Licensed Content Publication | Science Signaling |
| Licensed Content Title | Signaling by two-component system noncognate partners promotes intrinsic tolerance to polymyxin B in uropathogenic *Escherichia coli* |
| Licensed Content Author | Kirsten R. Guckes,Erin J. Breland,Ellisa W. Zhang,Sarah C. Hanks,Navleen K. Gill,Holly M. S. Algood,Jonathan E. Schmitz,Charles W. Stratton,Maria Hadjifrangiskou |
| Licensed Content Date | Jan 10, 2017 |
| Licensed Content Volume | 10 |
| Licensed Content Issue | 461 |
| Volume number | 10 |
| Issue number | 461 |
| Type of Use | Thesis / Dissertation |
| Requestor type | Author of the AAAS published paper |
| Format | Print and electronic |
| Portion | Full Text |
| Order reference number | |
| Title of your thesis / dissertation | DISSECTING THE ROLE OF QSEC IN MEDIATING QSEBC-PMRAB SIGNALING IN UROPATHOGENIC ESCHERICHIA COLI |
| Expected completion date | Aug 2017 |
| Estimated size(pages) | 150 |
| Requestor Location | Erin Breland<br>2045 Traemoor Village Dr.<br><br>NASHVILLE, TN 37209<br>United States<br>Attn: Erin Breland |
| Total | Not Available |

## PERMISSION REQUEST - Science Signaling in a thesis

**Elizabeth Sandler** <esandler@aaas.org> Fri, Jun 23, 2017 at 2:35 PM
To: "ejbreland22@gmail.com" <ejbreland22@gmail.com>

**AAAS Material:**

"Signaling by two-component system noncognate partners promotes intrinsic tolerance to polymyxin B in uropathogenic Escherichia coli" http://stke.sciencemag.org/content/10/461/eaag1775

**Reuse in your thesis**

"DISSECTING THE ROLE OF QSEC IN MEDIATING QSEBC-PMRAB SIGNALING IN UROPATHOGENIC ESCHERICHIA COLI" (August 2017)

Dear Erin:

I am following up on your request to reuse your Science Signaling article in your thesis - submitted via CCC/RightsLink job ticket # 501279671.

Thank you very much for getting in touch. This letter is to inform you of AAAS's policy on author use of his/her AAAS journal article(s) in a thesis or dissertation that he/she is writing. Because I'm sending you the guidelines directly, I'll be canceling the CCC/RightsLink job ticket, you'll receive an email from CCC confirming this.

1. After publication of a manuscript in an AAAS journal, the author may reprint his/her manuscript, in print format, in a thesis or dissertation written by the author as part of a course of study at an educational institution. Credit must be given to the first appearance of the material in the appropriate issue of the AAAS journal.

2. If the thesis or dissertation is to be published in electronic format, the accepted version of the work (the accepted version of the paper before Science's copy-editing and production) should be used and a link to the work on the AAAS journal website included.

3. Permission covers future revisions and editions of the thesis or dissertation by the author and author institution, provided the AAAS material covered by this permission remains in situ and is not distributed outside of the context of your thesis or dissertation.

4. Permission covers the distribution of your thesis or dissertation on demand by a third party distributor (e.g. ProQuest / UMI), provided the AAAS material covered by this permission remains in situ and is not distributed by that third party outside of the context of your thesis or dissertation.

5. The author may not permit others to reproduce the AAAS journal manuscript in a thesis or dissertation. In these cases, requesting parties should be instructed to contact AAAS directly for permission.

If you have any questions regarding this policy, please just let me know.

PNAS

**About PNAS (/site/aboutpnas/index.xhtml#PNAS_Online)**

Free Content (/site/aboutpnas/index.xhtml#free)

Special Features (/site/aboutpnas/special.xhtml)

Colloquium Papers (/site/aboutpnas/colloquia.xhtml)

Article and Journal Metrics (/site/aboutpnas/metrics.xhtml)

Developing Countries With Free Access to PNAS Online (/site/aboutpnas/developingcountries.xhtml)

Marketing Brochure (/site/misc/pnasmarketingbrochure.pdf)

RSS Feeds (/site/aboutpnas/rss.xhtml)

About Direct Submission (/site/aboutpnas/submiss.xhtml)

Reprints (/site/aboutpnas/reprints.xhtml)

**Rights and Permissions** (/site/aboutpnas/rightperm.xhtml)

Author Rights and Permissions Frequently Asked Questions (/site/aboutpnas/rightpermfaq.xhtml)

Frequently Asked Questions (/site/aboutpnas/faq.xhtml)

PNAS Portals (/site/misc/pnas_portals.xhtml)

PNAS Full-Text App (/site/misc/pnas_mobile.xhtml)

Android App Permissions (/site/misc/androidfaq.xhtml)

PNAS Alerts (/site/misc/PNASalerts.xhtml)

Editorial Board (/site/misc/masthead.xhtml)

News & Multimedia (/multimedia)

Subscriptions (/site/subscriptions/index.xhtml)

Contact (/site/misc/contact.xhtml)

# Rights and Permissions



The PNAS listing on the Sherpa RoMEO publisher copyright policies and self-archiving detail pages can be found here (http://www.sherpa.ac.uk/romeo/search.php?id=94&la=en&fIDnum=|).

**Requests for Permission to Reprint Material Published in PNAS**

Anyone may, without requesting permission, use original figures or tables published in PNAS for noncommercial and educational use (i.e., in a review article, in a book that is not for sale), provided that the full journal reference is cited and, for articles published in volumes 90–105 (1993–2008), "Copyright (copyright year) National Academy of Sciences." Commercial reuse of figures and tables (i.e., in promotional materials, in a textbook for sale) requires permission from PNAS.

PNAS authors need not obtain permission for the following cases: 1) to use their original figures or tables in their future works; 2) to make copies of their papers for their own personal use, including classroom use, or for the personal use of colleagues, provided those copies are not for sale and are not distributed in a systematic way; 3) to include their papers as part of their dissertations; or 4) to use all or part of their articles in printed compilations of their own works. The full journal reference must be cited and, for articles published in volumes 90–105 (1993–2008), "Copyright (copyright year) National Academy of Sciences."

For permission to reprint material in volumes 1–89 (1915–1992), requests should be sent to the original authors, who hold the copyright. The full journal reference must be cited.

For permission to reprint material in volumes 90–present (1993–present), requests should be sent via email to PNASPermissions@nas.edu (mailto:PNASPermissions@nas.edu) and must include the following information:

1. Your full name, affiliation, and title
2. Your complete mailing address, phone number, and email
3. PNAS volume number, issue number, and issue date
4. PNAS article title
5. PNAS authors' names
6. Page numbers of items to be reprinted
7. Figure/table number or portion of text to be reprinted

Requests must also include the following information about the intended use of the material:

1. Title of work in which PNAS material will appear
2. Authors/editors of work
3. Publisher of work
4. Retail price of work
5. Number of copies of work to be produced
6. Intended audience
7. Whether work is for nonprofit or commercial use

(/content/current)

Current Issue (/content/current)

Email Alerts (/site/misc/PNASalerts.xhtml)

Subscribe (/site/subscriptions/index.xhtml)

RSS (/site/aboutpnas/rss.xhtml)

Don't Miss

(https://itunes.apple.com/us/app/pnas/id399312700?mt=8)

PNAS Full-Text iOS App (https://itunes.apple.com/us/app/pnas mt=8) Download the app for free from iTunes today!

Other PNAS Media

Image Gallery (/site/media/imagegallery.xhtml)

Video Library (/site/media/videolibrary.xhtml)

Follow Us on Twitter (https://twitter.com/PNASNews)

Find Us on Facebook (http://www.facebook.com/pages/PNAS/18262365(

**MOST READ** **MOST CITED**

1. Investigation of hindwing folding in ladybird beetles by artificial elytron transplantation and microcomputed tomography (/cgi/content/short/pnas;114/22/5624?rss=1&ssource=mfr)
2. Exceptional and rapid accumulation of anthropogenic debris on one of the worlds most remote and pristine islands (/cgi/content/short/pnas;1619818114v1?rss=1&ssource=mfr)
3. Opinion: On being an advisor to todays junior scientists (/cgi/content/short/pnas;114/21/5321?rss=1&ssource=mfr)
4. Facial appearance affects science communication (/cgi/content/short/pnas;1620542114v1?rss=1&ssource=mfr)

Authors whose work will be reused should be notified. PNAS cannot supply original artwork. Use of PNAS material must not imply any endorsement by PNAS or the National Academy of Sciences. The full journal reference must be cited and, for articles published in volumes 90–105 (1993–2008), "Copyright (copyright year) National Academy of Sciences."

**Requests for Permission to Photocopy Material Published in PNAS**

For permission to photocopy beyond that permitted by Section 107 or 108 of the US Copyright Law (http://www.copyright.gov/title17/92chap1.html#107), contact:

Copyright Clearance Center (http://www.copyright.com)
222 Rosewood Drive
Danvers, MA 01923
Phone: 978-750-8400
Fax: 978-750-4770
Email: info@copyright.com (mailto:info@copyright.com)

Authorization to photocopy items for the internal or personal use of specific clients is granted by the National Academy of Sciences provided that the proper fee is paid directly to CCC.

[08/16]

5. Regulation of the sperm calcium channel CatSper by endogenous steroids and plant triterpenoids (/cgi/content/short/pnas;114/22/5743?rss=1&ssource=mfr)

**50 Most-Read Articles »**
(/reports/most-read)

REFERENCES


1. Mulvey MA, Schilling JD, Hultgren SJ. 2001. Establishment of a persistent Escherichia coli reservoir during the acute phase of a bladder infection. Infect Immun 69:4572-9.

2. DUBOS R, SCHAEDLE RW. 1964. THE DIGESTIVE TRACT AS AN ECOSYSTEM. Am J Med Sci 248:267-72.

3. Jones DM, Nisbet DJ. 1980. The gram negative bacterial flora of the avian gut. Avian Pathol 9:33-8.

4. Herzer PJ, Inouye S, Inouye M, Whittam TS. 1990. Phylogenetic distribution of branched RNA-linked multicopy single-stranded DNA among natural isolates of Escherichia coli. J Bacteriol 172:6175-81.

5. Clermont O, Christenson JK, Denamur E, Gordon DM. 2013. The Clermont Escherichia coli phylo-typing method revisited: improvement of specificity and detection of new phylo-groups. Environ Microbiol Rep 5:58-65.

6. Reid SD, Herbelin CJ, Bumbaugh AC, Selander RK, Whittam TS. 2000. Parallel evolution of virulence in pathogenic Escherichia coli. Nature 406:64-7.

7. Russo TA, Johnson JR. 2000. Proposal for a new inclusive designation for extraintestinal pathogenic isolates of Escherichia coli: ExPEC. J Infect Dis 181:1753-4.

8. Lo Y, Zhang L, Foxman B, Zöllner S. 2015. Whole-genome sequencing of uropathogenic Escherichia coli reveals long evolutionary history of diversity and virulence. Infect Genet Evol 34:244-50.

9. Johnson JR, Delavari P, Kuskowski M, Stell AL. 2001. Phylogenetic distribution of extraintestinal virulence-associated traits in Escherichia coli. J Infect Dis 183:78-88.

10. Sokurenko EV, Feldgarden M, Trintchina E, Weissman SJ, Avagyan S, Chattopadhyay S, Johnson JR, Dykhuizen DE. 2004. Selection footprint in the FimH adhesin shows pathoadaptive niche differentiation in Escherichia coli. Mol Biol Evol 21:1373-83.

11. Nicolas-Chanoine MH, Bertrand X, Madec JY. 2014. Escherichia coli ST131, an intriguing clonal group. Clin Microbiol Rev 27:543-74.

12. Totsika M, Beatson SA, Sarkar S, Phan MD, Petty NK, Bachmann N, Szubert M, Sidjabat HE, Paterson DL, Upton M, Schembri MA. 2011. Insights into a multidrug resistant Escherichia coli pathogen of the globally disseminated ST131 lineage: genome analysis and virulence mechanisms. PLoS One 6:e26578.

13. Moulin-Schouleur M, Répérant M, Laurent S, Brée A, Mignon-Grasteau S, Germon P, Rasschaert D, Schouler C. 2007. Extraintestinal pathogenic Escherichia coli strains of

avian and human origin: link between phylogenetic relationships and common virulence patterns. J Clin Microbiol 45:3366-76.

14. de Brito BG, Gaziri LC, Vidotto MC. 2003. Virulence factors and clonal relationships among Escherichia coli strains isolated from broiler chickens with cellulitis. Infect Immun 71:4175-7.

15. Mitchell NM, Johnson JR, Johnston B, Curtiss R, Mellata M. 2015. Zoonotic potential of Escherichia coli isolates from retail chicken meat products and eggs. Appl Environ Microbiol 81:1177-87.

16. Merck & Co. 1955. The Merck veterinary manual, p v. Merck and Co. Merck & Co, Rahway, N.J. Whitehouse Station, N.J.

17. Johnson JR, Delavari P, Stell AL, Whittam TS, Carlino U, Russo TA. 2001. Molecular comparison of extraintestinal Escherichia coli isolates of the same electrophoretic lineages from humans and domestic animals. J Infect Dis 183:154-9.

18. Hutchins RG, Vaden SL, Jacob ME, Harris TL, Bowles KD, Wood MW, Bailey CS. 2014. Vaginal microbiota of spayed dogs with or without recurrent urinary tract infections. J Vet Intern Med 28:300-4.

19. Oluoch AO, Kim CH, Weisiger RM, Koo HY, Siegel AM, Campbell KL, Burke TJ, McKiernan BC, Kakoma I. 2001. Nonenteric Escherichia coli isolates from dogs: 674 cases (1990-1998). J Am Vet Med Assoc 218:381-4.

20. Ewers C, Bethe A, Stamm I, Grobbel M, Kopp PA, Guerra B, Stubbe M, Doi Y, Zong Z, Kola A, Schaufler K, Semmler T, Fruth A, Wieler LH, Guenther S. 2014. CTX-M-15-D-ST648 Escherichia coli from companion animals and horses: another pandemic clone combining multiresistance and extraintestinal virulence? J Antimicrob Chemother 69:1224-30.

21. Bell ET, Lulich JP. 2015. Marked struvite crystalluria and its association with lower urinary tract signs in a cat with feline idiopathic cystitis. Aust Vet J 93:332-5.

22. Handt LK, Stoffregen DA, Prescott JS, Pouch WJ, Ngai DT, Anderson CA, Gatto NT, DebRoy C, Fairbrother JM, Motzel SL, Klein HJ. 2003. Clinical and microbiologic characterization of hemorrhagic pneumonia due to extraintestinal pathogenic Escherichia coli in four young dogs. Comp Med 53:663-70.

23. Sura R, Van Kruiningen HJ, DebRoy C, Hinckley LS, Greenberg KJ, Gordon Z, French RA. 2007. Extraintestinal pathogenic Escherichia coli-induced acute necrotizing pneumonia in cats. Zoonoses Public Health 54:307-13.

24. Carvalho VM, Osugui L, Setzer AP, Lopez RP, Pestana de Castro AF, Irino K, Catão-Dias JL. 2012. Characterization of extraintestinal pathogenic Escherichia coli isolated from captive wild felids with bacteremia. J Vet Diagn Invest 24:1014-6.

25. Yeruham I, Elad D, Avidar Y, Goshen T. 2006. A herd level analysis of urinary tract infection in dairy cattle. Vet J 171:172-6.

26. Tamura T, Nakamura H, Sato S, Seki M, Nishiki H. 2014. A modified catheterization procedure to reduce bladder damage when collecting urine samples from Holstein cows. J Vet Med Sci 76:819-26.

27. Rollin E, Dhuyvetter KC, Overton MW. 2015. The cost of clinical mastitis in the first 30 days of lactation: An economic modeling tool. Prev Vet Med 122:257-64.

28. Thompson-Crispi K, Atalla H, Miglior F, Mallard BA. 2014. Bovine mastitis: frontiers in immunogenetics. Front Immunol 5:493.

29. Shpigel NY, Elazar S, Rosenshine I. 2008. Mammary pathogenic Escherichia coli. Curr Opin Microbiol 11:60-5.

30. DebRoy C, Roberts E, Jayarao BM, Brooks JW. 2008. Bronchopneumonia associated with extraintestinal pathogenic Escherichia coli in a horse. J Vet Diagn Invest 20:661-4.

31. Liu C, Zheng H, Yang M, Xu Z, Wang X, Wei L, Tang B, Liu F, Zhang Y, Ding Y, Tang X, Wu B, Johnson TJ, Chen H, Tan C. 2015. Genome analysis and in vivo virulence of porcine extraintestinal pathogenic Escherichia coli strain PCN033. BMC Genomics 16:717.

32. Tan C, Xu Z, Zheng H, Liu W, Tang X, Shou J, Wu B, Wang S, Zhao GP, Chen H. 2011. Genome sequence of a porcine extraintestinal pathogenic Escherichia coli strain. J Bacteriol 193:5038.

33. Marshall BM, Levy SB. 2011. Food animals and antimicrobials: impacts on human health. Clin Microbiol Rev 24:718-33.

34. Nordstrom L, Liu CM, Price LB. 2013. Foodborne urinary tract infections: a new paradigm for antimicrobial-resistant foodborne illness. Front Microbiol 4:29.

35. Liu YY, Wang Y, Walsh TR, Yi LX, Zhang R, Spencer J, Doi Y, Tian G, Dong B, Huang X, Yu LF, Gu D, Ren H, Chen X, Lv L, He D, Zhou H, Liang Z, Liu JH, Shen J. 2016. Emergence of plasmid-mediated colistin resistance mechanism MCR-1 in animals and human beings in China: a microbiological and molecular biological study. Lancet Infect Dis 16:161-8.

36. Manges AR, Smith SP, Lau BJ, Nuval CJ, Eisenberg JN, Dietrich PS, Riley LW. 2007. Retail meat consumption and the acquisition of antimicrobial resistant Escherichia coli causing urinary tract infections: a case-control study. Foodborne Pathog Dis 4:419-31.

37. Riley HD. 1972. Neonatal meningitis. J Infect Dis 125:420-5.

38. Russo TA, Johnson JR. 2003. Medical and economic impact of extraintestinal infections due to Escherichia coli: focus on an increasingly important endemic problem. Microbes Infect 5:449-56.

39. Kaper JB. 2005. Pathogenic Escherichia coli. Int J Med Microbiol 295:355-6.

40. Mellata M. 2013. Human and avian extraintestinal pathogenic Escherichia coli: infections, zoonotic risks, and antibiotic resistance trends. Foodborne Pathog Dis 10:916-32.

41. Kim KS. 2016. Human Meningitis-Associated Escherichia coli. EcoSal Plus 7.

42. Foxman B. 2014. Urinary tract infection syndromes: occurrence, recurrence, bacteriology, risk factors, and disease burden. Infect Dis Clin North Am 28:1-13.

43. Becknell B, Schober M, Korbel L, Spencer JD. 2015. The diagnosis, evaluation and treatment of acute and recurrent pediatric urinary tract infections. Expert Rev Anti Infect Ther 13:81-90.

44. Jackson LA, Benson P, Neuzil KM, Grandjean M, Marino JL. 2005. Burden of community-onset Escherichia coli bacteremia in seniors. J Infect Dis 191:1523-9.

45. Al-Hasan MN, Eckel-Passow JE, Baddour LM. 2010. Bacteremia complicating gram-negative urinary tract infections: a population-based study. J Infect 60:278-85.

46. Vincent CR, Thomas TL, Reyes L, White CL, Canales BK, Brown MB. 2013. Symptoms and risk factors associated with first urinary tract infection in college age women: a prospective cohort study. J Urol 189:904-10.

47. Foxman B, Gillespie B, Koopman J, Zhang L, Palin K, Tallman P, Marsh JV, Spear S, Sobel JD, Marty MJ, Marrs CF. 2000. Risk factors for second urinary tract infection among college women. Am J Epidemiol 151:1194-205.

48. Hannan TJ, Totsika M, Mansfield KJ, Moore KH, Schembri MA, Hultgren SJ. 2012. Host-pathogen checkpoints and population bottlenecks in persistent and intracellular uropathogenic Escherichia coli bladder infection. FEMS Microbiol Rev 36:616-48.

49. Chromek M, Slamová Z, Bergman P, Kovács L, Podracká L, Ehrén I, Hökfelt T, Gudmundsson GH, Gallo RL, Agerberth B, Brauner A. 2006. The antimicrobial peptide cathelicidin protects the urinary tract against invasive bacterial infection. Nat Med 12:636-41.

50. Schilling JD, Mulvey MA, Vincent CD, Lorenz RG, Hultgren SJ. 2001. Bacterial invasion augments epithelial cytokine responses to Escherichia coli through a lipopolysaccharide-dependent mechanism. J Immunol 166:1148-55.

51. Hedges S, Svanborg C. 1994. The mucosal cytokine response to urinary tract infections. Int J Antimicrob Agents 4:89-93.

52. Hung CS, Dodson KW, Hultgren SJ. 2009. A murine model of urinary tract infection. Nat Protoc 4:1230-43.

53. Yamamoto T, Fujita K, Yokota T. 1990. Adherence characteristics to human small intestinal mucosa of Escherichia coli isolated from patients with diarrhea or urinary tract infections. J Infect Dis 162:896-908.

54. Connell I, Agace W, Klemm P, Schembri M, Marild S, Svanborg C. 1996. Type 1 fimbrial expression enhances Escherichia coli virulence for the urinary tract. Proc Natl Acad Sci U S A 93:9827-32.

55. Mulvey MA, Lopez-Boado YS, Wilson CL, Roth R, Parks WC, Heuser J, Hultgren SJ. 1998. Induction and evasion of host defenses by type 1-piliated uropathogenic Escherichia coli. Science 282:1494-7.

56. Martinez JJ, Mulvey MA, Schilling JD, Pinkner JS, Hultgren SJ. 2000. Type 1 pilus-mediated bacterial invasion of bladder epithelial cells. EMBO J 19:2803-12.

57. Mellata M, Dho-Moulin M, Dozois CM, Curtiss R, Lehoux B, Fairbrother JM. 2003. Role of avian pathogenic Escherichia coli virulence factors in bacterial interaction with chicken heterophils and macrophages. Infect Immun 71:494-503.

58. Klemm P, Schembri M. 2004. Type 1 Fimbriae, Curli, and Antigen 43: Adhesion, Colonization, and Biofilm Formation. Ecosal Plus 1.

59. Eto DS, Jones TA, Sundsbak JL, Mulvey MA. 2007. Integrin-mediated host cell invasion by type 1-piliated uropathogenic Escherichia coli. PLoS Pathog 3:e100.

60. Anderson GG, Palermo JJ, Schilling JD, Roth R, Heuser J, Hultgren SJ. 2003. Intracellular bacterial biofilm-like pods in urinary tract infections. Science 301:105-7.

61. Justice SS, Hung C, Theriot JA, Fletcher DA, Anderson GG, Footer MJ, Hultgren SJ. 2004. Differentiation and developmental pathways of uropathogenic Escherichia coli in urinary tract pathogenesis. Proc Natl Acad Sci U S A 101:1333-8.

62. Nagamatsu K, Hannan TJ, Guest RL, Kostakioti M, Hadjifrangiskou M, Binkley J, Dodson K, Raivio TL, Hultgren SJ. 2015. Dysregulation of Escherichia coli α-hemolysin expression alters the course of acute and persistent urinary tract infection. Proc Natl Acad Sci U S A 112:E871-80.

63. Mulvey MA, Schilling JD, Martinez JJ, Hultgren SJ. 2000. Bad bugs and beleaguered bladders: interplay between uropathogenic Escherichia coli and innate host defenses. Proc Natl Acad Sci U S A 97:8829-35.

64. Mysorekar IU, Hultgren SJ. 2006. Mechanisms of uropathogenic Escherichia coli persistence and eradication from the urinary tract. Proc Natl Acad Sci U S A 103:14170-5.

65. O'Brien VP, Hannan TJ, Yu L, Livny J, Roberson ED, Schwartz DJ, Souza S, Mendelsohn CL, Colonna M, Lewis AL, Hultgren SJ. 2016. A mucosal imprint left by prior Escherichia coli bladder infection sensitizes to recurrent disease. Nat Microbiol 2:16196.

66. Schmiemann G, Kniehl E, Gebhardt K, Matejczyk MM, Hummers-Pradier E. 2010. The diagnosis of urinary tract infection: a systematic review. Dtsch Arztebl Int 107:361-7.

67. Abraham SN, Miao Y. 2015. The nature of immune responses to urinary tract infections. Nat Rev Immunol 15:655-63.

68. Gupta K, Hooton TM, Miller L, Committee UUIG. 2011. Managing uncomplicated urinary tract infection--making sense out of resistance data. Clin Infect Dis 53:1041-2.

69. Coque TM, Novais A, Carattoli A, Poirel L, Pitout J, Peixe L, Baquero F, Cantón R, Nordmann P. 2008. Dissemination of clonally related Escherichia coli strains expressing extended-spectrum beta-lactamase CTX-M-15. Emerg Infect Dis 14:195-200.

70. Nicolas-Chanoine MH, Blanco J, Leflon-Guibout V, Demarty R, Alonso MP, Canica MM, Park YJ, Lavigne JP, Pitout J, Johnson JR. 2008. Intercontinental emergence of Escherichia coli clone O25:H4-ST131 producing CTX-M-15. J Antimicrob Chemother 61:273-81.

71. Sadeyen JR, Kaiser P, Stevens MP, Dziva F. 2015. A cyclophosphamide-sensitive cell compartment is essential for homologous protection conferred by licensed vaccines for the control of avian pathogenic Escherichia coli in chickens. Vaccine 33:3624-7.

72. Kakkanat A, Totsika M, Schaale K, Duell BL, Lo AW, Phan MD, Moriel DG, Beatson SA, Sweet MJ, Ulett GC, Schembri MA. 2015. The role of H4 flagella in Escherichia coli ST131 virulence. Sci Rep 5:16149.

73. McGann P, Snesrud E, Maybank R, Corey B, Ong AC, Clifford R, Hinkle M, Whitman T, Lesho E, Schaecher KE. 2016. Escherichia coli Harboring mcr-1 and blaCTX-M on a Novel IncF Plasmid: First Report of mcr-1 in the United States. Antimicrob Agents Chemother 60:4420-1.

74. Lima Barbieri N, Nielsen DW, Wannemuehler Y, Cavender T, Hussein A, Yan SG, Nolan LK, Logue CM. 2017. mcr-1 identified in Avian Pathogenic Escherichia coli (APEC). PLoS One 12:e0172997.

75. Blaser MJ, Falkow S. 2009. What are the consequences of the disappearing human microbiota? Nat Rev Microbiol 7:887-94.

76. Doumith M, Day M, Ciesielczuk H, Hope R, Underwood A, Reynolds R, Wain J, Livermore DM, Woodford N. 2015. Rapid identification of major Escherichia coli sequence types causing urinary tract and bloodstream infections. J Clin Microbiol 53:160-6.

77. Gao Q, Zhang D, Ye Z, Zhu X, Yang W, Dong L, Gao S, Liu X. 2017. Virulence traits and pathogenicity of uropathogenic Escherichia coli isolates with common and uncommon O serotypes. Microb Pathog 104:217-224.

78. Anderson GG, Goller CC, Justice S, Hultgren SJ, Seed PC. 2010. Polysaccharide capsule and sialic acid-mediated regulation promote biofilm-like intracellular bacterial communities during cystitis. Infect Immun 78:963-75.

79. Schreiber HL, Conover MS, Chou WC, Hibbing ME, Manson AL, Dodson KW, Hannan TJ, Roberts PL, Stapleton AE, Hooton TM, Livny J, Earl AM, Hultgren SJ. 2017. Bacterial virulence phenotypes of Escherichia coli and host susceptibility determine risk for urinary tract infections. Sci Transl Med 9.

80. Svenson SB, Hultberg H, Källenius G, Korhonen TK, Möllby R, Winberg J. 1983. P-fimbriae of pyelonephritogenic Escherichia coli: identification and chemical characterization of receptors. Infection 11:61-7.

81. Dodson KW, Jacob-Dubuisson F, Striker RT, Hultgren SJ. 1993. Outer-membrane PapC molecular usher discriminately recognizes periplasmic chaperone-pilus subunit complexes. Proc Natl Acad Sci U S A 90:3670-4.

82. Schilling JD, Mulvey MA, Hultgren SJ. 2001. Structure and function of Escherichia coli type 1 pili: new insight into the pathogenesis of urinary tract infections. J Infect Dis 183 Suppl 1:S36-40.

83. Barnhart MM, Chapman MR. 2006. Curli biogenesis and function. Annu Rev Microbiol 60:131-47.

84. Knöbl T, Baccaro MR, Moreno AM, Gomes TA, Vieira MA, Ferreira CS, Ferreira AJ. 2001. Virulence properties of Escherichia coli isolated from ostriches with respiratory disease. Vet Microbiol 83:71-80.

85. Johnson TJ, Siek KE, Johnson SJ, Nolan LK. 2006. DNA sequence of a ColV plasmid and prevalence of selected plasmid-encoded virulence genes among avian Escherichia coli strains. J Bacteriol 188:745-58.

86. Lloyd AL, Rasko DA, Mobley HL. 2007. Defining genomic islands and uropathogen-specific genes in uropathogenic Escherichia coli. J Bacteriol 189:3532-46.

87. Wiles TJ, Kulesus RR, Mulvey MA. 2008. Origins and virulence mechanisms of uropathogenic Escherichia coli. Exp Mol Pathol 85:11-9.

88. Zhu L, Pearce D, Kim KS. 2010. Prevention of Escherichia coli K1 penetration of the blood-brain barrier by counteracting the host cell receptor and signaling molecule involved in E. coli invasion of human brain microvascular endothelial cells. Infect Immun 78:3554-9.

89. Nazemi A, Mirinargasi M, Merikhi N, Sharifi SH. 2011. Distribution of Pathogenic Genes aatA, aap, aggR, among Uropathogenic Escherichia coli (UPEC) and Their Linkage with StbA Gene. Indian J Microbiol 51:355-8.

90. Spurbeck RR, Stapleton AE, Johnson JR, Walk ST, Hooton TM, Mobley HL. 2011. Fimbrial Profiles Predict Virulence of Uropathogenic E. coli Strains: Contribution of Ygi and Yad Fimbriae. Infect Immun.

91. Logue CM, Doetkott C, Mangiamele P, Wannemuehler YM, Johnson TJ, Tivendale KA, Li G, Sherwood JS, Nolan LK. 2012. Genotypic and phenotypic traits that distinguish neonatal meningitis-associated Escherichia coli from fecal E. coli isolates of healthy human hosts. Appl Environ Microbiol 78:5824-30.

92. Zhu Ge X, Jiang J, Pan Z, Hu L, Wang S, Wang H, Leung FC, Dai J, Fan H. 2014. Comparative genomic analysis shows that avian pathogenic Escherichia coli isolate IMT5155 (O2:K1:H5; ST complex 95, ST140) shares close relationship with ST95 APEC O1:K1 and human ExPEC O18:K1 strains. PLoS One 9:e112048.

93. Huja S, Oren Y, Trost E, Brzuszkiewicz E, Biran D, Blom J, Goesmann A, Gottschalk G, Hacker J, Ron EZ, Dobrindt U. 2015. Genomic avenue to avian colisepticemia. MBio 6.

94. Wang S, Bao Y, Meng Q, Xia Y, Zhao Y, Wang Y, Tang F, ZhuGe X, Yu S, Han X, Dai J, Lu C. 2015. IbeR facilitates stress-resistance, invasion and pathogenicity of avian pathogenic Escherichia coli. PLoS One 10:e0119698.

95. Wijetunge DS, Gongati S, DebRoy C, Kim KS, Couraud PO, Romero IA, Weksler B, Kariyawasam S. 2015. Characterizing the pathotype of neonatal meningitis causing Escherichia coli (NMEC). BMC Microbiol 15:211.

96. Welch RA, Burland V, Plunkett G, 3rd, Redford P, Roesch P, Rasko D, Buckles EL, Liou SR, Boutin A, Hackett J, Stroud D, Mayhew GF, Rose DJ, Zhou S, Schwartz DC, Perna NT, Mobley HL, Donnenberg MS, Blattner FR. 2002. Extensive mosaic structure revealed by the complete genome sequence of uropathogenic Escherichia coli. Proc Natl Acad Sci U S A 99:17020-4.

97. Chen SL, Hung CS, Xu J, Reigstad CS, Magrini V, Sabo A, Blasiar D, Bieri T, Meyer RR, Ozersky P, Armstrong JR, Fulton RS, Latreille JP, Spieth J, Hooton TM, Mardis ER, Hultgren SJ, Gordon JI. 2006. Identification of genes subject to positive selection in

uropathogenic strains of Escherichia coli: a comparative genomics approach. Proc Natl Acad Sci U S A 103:5977-82.

98. Henderson JP, Crowley JR, Pinkner JS, Walker JN, Tsukayama P, Stamm WE, Hooton TM, Hultgren SJ. 2009. Quantitative metabolomics reveals an epigenetic blueprint for iron acquisition in uropathogenic Escherichia coli. PLoS Pathog 5:e1000305.

99. Cassat JE, Skaar EP. 2013. Iron in infection and immunity. Cell Host Microbe 13:509-19.

100. Alteri CJ, Smith SN, Mobley HL. 2009. Fitness of Escherichia coli during urinary tract infection requires gluconeogenesis and the TCA cycle. PLoS Pathog 5:e1000448.

101. Hadjifrangiskou M, Kostakioti M, Chen SL, Henderson JP, Greene SE, Hultgren SJ. 2011. A central metabolic circuit controlled by QseC in pathogenic Escherichia coli. Mol Microbiol 80:1516-29.

102. Floyd KA, Moore JL, Eberly AR, Good JA, Shaffer CL, Zaver H, Almqvist F, Skaar EP, Caprioli RM, Hadjifrangiskou M. 2015. Adhesive fiber stratification in uropathogenic Escherichia coli biofilms unveils oxygen-mediated control of type 1 pili. PLoS Pathog 11:e1004697.

103. Floyd KA, Mitchell CA, Eberly AR, Colling SJ, Zhang EW, DePas W, Chapman MR, Conover M, Rogers BR, Hultgren SJ, Hadjifrangiskou M. 2016. The UbiI (VisC) Aerobic Ubiquinone Synthase Is Required for Expression of Type 1 Pili, Biofilm Formation, and Pathogenesis in Uropathogenic Escherichia coli. J Bacteriol 198:2662-72.

104. Shepherd M, Achard ME, Idris A, Totsika M, Phan MD, Peters KM, Sarkar S, Ribeiro CA, Holyoake LV, Ladakis D, Ulett GC, Sweet MJ, Poole RK, McEwan AG, Schembri MA. 2016. The cytochrome bd-I respiratory oxidase augments survival of multidrug-resistant Escherichia coli during infection. Sci Rep 6:35285.

105. Tatum EL, Lederberg J. 1947. Gene Recombination in the Bacterium Escherichia coli. J Bacteriol 53:673-84.

106. Abana CM, Brannon JR, Ebbott RA, Dunigan TL, Guckes KR, Fuseini H, Powers J, Rogers BR, Hadjifrangiskou M. 2017. Characterization of blue light irradiation effects on pathogenic and nonpathogenic Escherichia coli. Microbiologyopen.

107. Behr S, Kristoficova I, Witting M, Breland EJ, Eberly AR, Sachs C, Schmitt-Kopplin P, Hadjifrangiskou M, Jung K. 2017. Identification of a High-Affinity Pyruvate Receptor in Escherichia coli. Sci Rep 7:1388.

108. van Elsas JD, Semenov AV, Costa R, Trevors JT. 2011. Survival of Escherichia coli in the environment: fundamental and public health aspects. ISME J 5:173-83.

109. Gorden J, Small PL. 1993. Acid resistance in enteric bacteria. Infect Immun 61:364-7.

110. Wagenlehner FM, Naber KG. 2006. Treatment of bacterial urinary tract infections: presence and future. Eur Urol 49:235-44.

111. (CDC) CfDCaP. 2013. Antibiotic Resistance Threats in the United States, 2013.

112. Murima P, McKinney JD, Pethe K. 2014. Targeting bacterial central metabolism for drug development. Chem Biol 21:1423-32.

113. Cusumano CK, Hultgren SJ. 2009. Bacterial adhesion--a source of alternate antibiotic targets. IDrugs 12:699-705.

114. Cegelski L, Marshall GR, Eldridge GR, Hultgren SJ. 2008. The biology and future prospects of antivirulence therapies. Nat Rev Microbiol 6:17-27.

115. Clatworthy AE, Pierson E, Hung DT. 2007. Targeting virulence: a new paradigm for antimicrobial therapy. Nat Chem Biol 3:541-8.

116. Mitrophanov AY, Groisman EA. 2008. Signal integration in bacterial two-component regulatory systems. Genes Dev 22:2601-11.

117. Grant SS, Hung DT. 2013. Persistent bacterial infections, antibiotic tolerance, and the oxidative stress response. Virulence 4:273-83.

118. Hood MI, Skaar EP. 2012. Nutritional immunity: transition metals at the pathogen-host interface. Nat Rev Microbiol 10:525-37.

119. Porcheron G, Garénaux A, Proulx J, Sabri M, Dozois CM. 2013. Iron, copper, zinc, and manganese transport and regulation in pathogenic Enterobacteria: correlations between strains, site of infection and the relative importance of the different metal transport systems for virulence. Front Cell Infect Microbiol 3:90.

120. Chung HJ, Bang W, Drake MA. 2006. Stress Response of E*scherichia coli*. Comprehensive Reviews in Food Science and Food Safety 5:52-64.

121. Lux R, Shi W. 2005. A novel bacterial signalling system with a combination of a Ser/Thr kinase cascade and a His/Asp two-component system. Mol Microbiol 58:345-8.

122. Stock JB, Ninfa AJ, Stock AM. 1989. Protein phosphorylation and regulation of adaptive responses in bacteria. Microbiol Rev 53:450-90.

123. Stock AM, Robinson VL, Goudreau PN. 2000. Two-component signal transduction. Annu Rev Biochem 69:183-215.

124. Bijlsma JJ, Groisman EA. 2003. Making informed decisions: regulatory interactions between two-component systems. Trends Microbiol 11:359-66.

125. Hoch JA. 2000. Two-component and phosphorelay signal transduction. Curr Opin Microbiol 3:165-70.

126. Fabret C, Feher VA, Hoch JA. 1999. Two-component signal transduction in Bacillus subtilis: how one organism sees its world. J Bacteriol 181:1975-83.

127. Bourret RB, Hess JF, Simon MI. 1990. Conserved aspartate residues and phosphorylation in signal transduction by the chemotaxis protein CheY. Proc Natl Acad Sci U S A 87:41-5.

128. Bourret RB, Hess JF, Borkovich KA, Pakula AA, Simon MI. 1989. Protein phosphorylation in chemotaxis and two-component regulatory systems of bacteria. J Biol Chem 264:7085-8.

129. Ninfa AJ, Ninfa EG, Lupas AN, Stock A, Magasanik B, Stock J. 1988. Crosstalk between bacterial chemotaxis signal transduction proteins and regulators of transcription of the Ntr regulon: evidence that nitrogen assimilation and chemotaxis are controlled by a common phosphotransfer mechanism. Proc Natl Acad Sci U S A 85:5492-6.

130. Igo MM, Slauch JM, Silhavy TJ. 1990. Signal transduction in bacteria: kinases that control gene expression. New Biol 2:5-9.

131. Grebe TW, Stock JB. 1999. The histidine protein kinase superfamily. Adv Microb Physiol 41:139-227.

132. Cheung J, Hendrickson WA. 2010. Sensor domains of two-component regulatory systems. Curr Opin Microbiol 13:116-23.

133. Dethlefsen L, Huse S, Sogin ML, Relman DA. 2008. The pervasive effects of an antibiotic on the human gut microbiota, as revealed by deep 16S rRNA sequencing. PLoS Biol 6:e280.

134. Song L, Sudhakar P, Wang W, Conrads G, Brock A, Sun J, Wagner-Döbler I, Zeng AP. 2012. A genome-wide study of two-component signal transduction systems in eight newly sequenced mutans streptococci strains. BMC Genomics 13:128.

135. Galperin MY. 2006. Structural classification of bacterial response regulators: diversity of output domains and domain combinations. J Bacteriol 188:4169-82.

136. McCleary WR, Stock JB. 1994. Acetyl phosphate and the activation of two-component response regulators. J Biol Chem 269:31567-72.

137. Capra EJ, Laub MT. 2012. Evolution of two-component signal transduction systems. Annu Rev Microbiol 66:325-47.

138. Cai W, Wannemuehler Y, Dell'anna G, Nicholson B, Barbieri NL, Kariyawasam S, Feng Y, Logue CM, Nolan LK, Li G. 2013. A novel two-component signaling system

facilitates uropathogenic Escherichia coli's ability to exploit abundant host metabolites. PLoS Pathog 9:e1003428.

139. Loui C, Chang AC, Lu S. 2009. Role of the ArcAB two-component system in the resistance of Escherichia coli to reactive oxygen stress. BMC Microbiol 9:183.

140. Sacco SA, Adolfsen KJ, Brynildsen MP. 2017. An integrated network analysis identifies how ArcAB enables metabolic oscillations in the nitric oxide detoxification network of Escherichia coli. Biotechnol J.

141. Gunsalus RP, Park SJ. 1994. Aerobic-anaerobic gene regulation in Escherichia coli: control by the ArcAB and Fnr regulons. Res Microbiol 145:437-50.

142. Georgellis D, Kwon O, Lin EC. 2001. Quinones as the redox signal for the arc two-component system of bacteria. Science 292:2314-6.

143. Morales EH, Collao B, Desai PT, Calderón IL, Gil F, Luraschi R, Porwollik S, McClelland M, Saavedra CP. 2013. Probing the ArcA regulon under aerobic/ROS conditions in Salmonella enterica serovar Typhimurium. BMC Genomics 14:626.

144. Jiang F, An C, Bao Y, Zhao X, Jernigan RL, Lithio A, Nettleton D, Li L, Wurtele ES, Nolan LK, Lu C, Li G. 2015. ArcA Controls Metabolism, Chemotaxis, and Motility Contributing to the Pathogenicity of Avian Pathogenic Escherichia coli. Infect Immun 83:3545-54.

145. Pernestig AK, Melefors O, Georgellis D. 2001. Identification of UvrY as the cognate response regulator for the BarA sensor kinase in Escherichia coli. J Biol Chem 276:225-31.

146. Pernestig AK, Georgellis D, Romeo T, Suzuki K, Tomenius H, Normark S, Melefors O. 2003. The Escherichia coli BarA-UvrY two-component system is needed for efficient switching between glycolytic and gluconeogenic carbon sources. J Bacteriol 185:843-53.

147. Suzuki K, Wang X, Weilbacher T, Pernestig AK, Melefors O, Georgellis D, Babitzke P, Romeo T. 2002. Regulatory circuitry of the CsrA/CsrB and BarA/UvrY systems of Escherichia coli. J Bacteriol 184:5130-40.

148. Tomenius H, Pernestig AK, Jonas K, Georgellis D, Möllby R, Normark S, Melefors O. 2006. The Escherichia coli BarA-UvrY two-component system is a virulence determinant in the urinary tract. BMC Microbiol 6:27.

149. Palaniyandi S, Mitra A, Herren CD, Lockatell CV, Johnson DE, Zhu X, Mukhopadhyay S. 2012. BarA-UvrY two-component system regulates virulence of uropathogenic E. coli CFT073. PLoS One 7:e31348.

150. Lasaro M, Liu Z, Bishar R, Kelly K, Chattopadhyay S, Paul S, Sokurenko E, Zhu J, Goulian M. 2014. Escherichia coli isolate for studying colonization of the mouse intestine and its application to two-component signaling knockouts. J Bacteriol 196:1723-32.

151. Pogliano J, Lynch AS, Belin D, Lin EC, Beckwith J. 1997. Regulation of Escherichia coli cell envelope proteins involved in protein folding and degradation by the Cpx two-component system. Genes Dev 11:1169-82.

152. Raivio TL, Silhavy TJ. 1997. Transduction of envelope stress in Escherichia coli by the Cpx two-component system. J Bacteriol 179:7724-33.

153. Otto K, Silhavy TJ. 2002. Surface sensing and adhesion of Escherichia coli controlled by the Cpx-signaling pathway. Proc Natl Acad Sci U S A 99:2287-92.

154. DiGiuseppe PA, Silhavy TJ. 2003. Signal detection and target gene induction by the CpxRA two-component system. J Bacteriol 185:2432-40.

155. Hung DL, Raivio TL, Jones CH, Silhavy TJ, Hultgren SJ. 2001. Cpx signaling pathway monitors biogenesis and affects assembly and expression of P pili. Embo J 20:1508-18.

156. Lee YM, DiGiuseppe PA, Silhavy TJ, Hultgren SJ. 2004. P pilus assembly motif necessary for activation of the CpxRA pathway by PapE in Escherichia coli. J Bacteriol 186:4326-37.

157. Isaac DD, Pinkner JS, Hultgren SJ, Silhavy TJ. 2005. The extracytoplasmic adaptor protein CpxP is degraded with substrate by DegP. Proc Natl Acad Sci U S A 102:17775-9.

158. Raivio TL, Leblanc SK, Price NL. 2013. The Escherichia coli Cpx envelope stress response regulates genes of diverse function that impact antibiotic resistance and membrane integrity. J Bacteriol 195:2755-67.

159. Hou B, Meng XR, Zhang LY, Tan C, Jin H, Zhou R, Gao JF, Wu B, Li ZL, Liu M, Chen HC, Bi DR, Li SW. 2014. TolC promotes ExPEC biofilm formation and curli production in response to medium osmolarity. Biomed Res Int 2014:574274.

160. Debnath I, Norton JP, Barber AE, Ott EM, Dhakal BK, Kulesus RR, Mulvey MA. 2013. The Cpx stress response system potentiates the fitness and virulence of uropathogenic Escherichia coli. Infect Immun 81:1450-9.

161. Schwan WR. 2009. Survival of uropathogenic Escherichia coli in the murine urinary tract is dependent on OmpR. Microbiology 155:1832-9.

162. Hall MN, Silhavy TJ. 1981. Genetic analysis of the ompB locus in Escherichia coli K-12. J Mol Biol 151:1-15.

163. Igo MM, Silhavy TJ. 1988. EnvZ, a transmembrane environmental sensor of Escherichia coli K-12, is phosphorylated in vitro. J Bacteriol 170:5971-3.

164. Forst S, Delgado J, Inouye M. 1989. Phosphorylation of OmpR by the osmosensor EnvZ modulates expression of the ompF and ompC genes in Escherichia coli. Proc Natl Acad Sci U S A 86:6052-6.

165. Cai SJ, Inouye M. 2002. EnvZ-OmpR interaction and osmoregulation in Escherichia coli. J Biol Chem 277:24155-61.

166. Gally DL, Leathart J, Blomfield IC. 1996. Interaction of FimB and FimE with the fim switch that controls the phase variation of type 1 fimbriae in Escherichia coli K-12. Mol Microbiol 21:725-38.

167. Helena Mäkelä P, Sarvas M, Calcagno S, L ounatmaa K. 1978. Isolation and genetic characterization of polymyxin ‐ resistant mutants of Salmonella. *FEMS Microbiology Letters 3*:323-326.

168. Roland KL, Martin LE, Esther CR, Spitznagel JK. 1993. Spontaneous pmrA mutants of Salmonella typhimurium LT2 define a new two-component regulatory system with a possible role in virulence. J Bacteriol 175:4154-64.

169. Groisman EA, Kayser J, Soncini FC. 1997. Regulation of polymyxin resistance and adaptation to low-Mg2+ environments. J Bacteriol 179:7040-5.

170. Wösten MM, Kox LF, Chamnongpol S, Soncini FC, Groisman EA. 2000. A signal transduction system that responds to extracellular iron. Cell 103:113-25.

171. Chen HD, Groisman EA. 2013. The biology of the PmrA/PmrB two-component system: the major regulator of lipopolysaccharide modifications. Annu Rev Microbiol 67:83-112.

172. Froelich JM, Tran K, Wall D. 2006. A pmrA constitutive mutant sensitizes Escherichia coli to deoxycholic acid. J Bacteriol 188:1180-3.

173. Gunn JS, Ryan SS, Van Velkinburgh JC, Ernst RK, Miller SI. 2000. Genetic and functional analysis of a PmrA-PmrB-regulated locus necessary for lipopolysaccharide modification, antimicrobial peptide resistance, and oral virulence of Salmonella enterica serovar typhimurium. Infect Immun 68:6139-46.

174. Warner DM, Duval V, Levy SB. 2013. The contribution of PmrAB to the virulence of a clinical isolate of Escherichia coli. Virulence 4:634-7.

175. Kato A, Mitrophanov AY, Groisman EA. 2007. A connector of two-component regulatory systems promotes signal amplification and persistence of expression. Proc Natl Acad Sci U S A 104:12063-8.

176. Winfield MD, Groisman EA. 2004. Phenotypic differences between Salmonella and Escherichia coli resulting from the disparate regulation of homologous genes. Proc Natl Acad Sci U S A 101:17162-7.

177. Kostakioti M, Hadjifrangiskou M, Pinkner JS, Hultgren SJ. 2009. QseC-mediated dephosphorylation of QseB is required for expression of genes associated with virulence in uropathogenic Escherichia coli. Mol Microbiol 73:1020-31.

178. Sperandio V, Torres AG, Kaper JB. 2002. Quorum sensing Escherichia coli regulators B and C (QseBC): a novel two-component regulatory system involved in the regulation of flagella and motility by quorum sensing in E. coli. Mol Microbiol 43:809-21.

179. Clarke MB, Hughes DT, Zhu C, Boedeker EC, Sperandio V. 2006. The QseC sensor kinase: a bacterial adrenergic receptor. Proc Natl Acad Sci U S A 103:10420-5.

180. Hughes DT, Clarke MB, Yamamoto K, Rasko DA, Sperandio V. 2009. The QseC adrenergic signaling cascade in Enterohemorrhagic E. coli (EHEC). PLoS Pathog 5:e1000553.

181. Laub MT, Goulian M. 2007. Specificity in two-component signal transduction pathways. Annu Rev Genet 41:121-45.

182. Noriega CE, Lin HY, Chen LL, Williams SB, Stewart V. 2010. Asymmetric cross-regulation between the nitrate-responsive NarX-NarL and NarQ-NarP two-component regulatory systems from Escherichia coli K-12. Mol Microbiol 75:394-412.

183. Siryaporn A, Goulian M. 2008. Cross-talk suppression between the CpxA-CpxR and EnvZ-OmpR two-component systems in E. coli. Mol Microbiol 70:494-506.

184. Kato A, Groisman EA. 2004. Connecting two-component regulatory systems by a protein that protects a response regulator from dephosphorylation by its cognate sensor. Genes Dev 18:2302-13.

185. Mike LA, Choby JE, Brinkman PR, Olive LQ, Dutter BF, Ivan SJ, Gibbs CM, Sulikowski GA, Stauff DL, Skaar EP. 2014. Two-component system cross-regulation integrates Bacillus anthracis response to heme and cell envelope stress. PLoS Pathog 10:e1004044.

186. Guckes KR, Kostakioti M, Breland EJ, Gu AP, Shaffer CL, Martinez CR, 3rd, Hultgren SJ, Hadjifrangiskou M. 2013. Strong cross-system interactions drive the activation of the QseB response regulator in the absence of its cognate sensor. Proc Natl Acad Sci U S A.

187. Kraxenberger T, Fried L, Behr S, Jung K. 2012. First insights into the unexplored two-component system YehU/YehT in Escherichia coli. J Bacteriol 194:4272-84.

188. Fried L, Behr S, Jung K. 2013. Identification of a target gene and activating stimulus for the YpdA/YpdB histidine kinase/response regulator system in Escherichia coli. J Bacteriol 195:807-15.

189. Maslennikov I, Klammt C, Hwang E, Kefala G, Okamura M, Esquivies L, Mörs K, Glaubitz C, Kwiatkowski W, Jeon YH, Choe S. 2010. Membrane domain structures of three classes of histidine kinase receptors by cell-free expression and rapid NMR analysis. Proc Natl Acad Sci U S A 107:10902-7.

190. Bader MW, Sanowar S, Daley ME, Schneider AR, Cho U, Xu W, Klevit RE, Le Moual H, Miller SI. 2005. Recognition of antimicrobial peptides by a bacterial sensor kinase. Cell 122:461-72.

191. Ng WL, Bassler BL. 2009. Bacterial quorum-sensing network architectures. Annu Rev Genet 43:197-222.

192. Kenney LJ. 1997. Kinase activity of EnvZ, an osmoregulatory signal transducing protein of Escherichia coli. Arch Biochem Biophys 346:303-11.

193. Matamouros S, Hager KR, Miller SI. 2015. HAMP Domain Rotation and Tilting Movements Associated with Signal Transduction in the PhoQ Sensor Kinase. MBio 6:e00616-15.

194. Snyder WB, Davis LJ, Danese PN, Cosma CL, Silhavy TJ. 1995. Overproduction of NlpE, a new outer membrane lipoprotein, suppresses the toxicity of periplasmic LacZ by activation of the Cpx signal transduction pathway. J Bacteriol 177:4216-23.

195. Vogt SL, Raivio TL. 2012. Just scratching the surface: an expanding view of the Cpx envelope stress response. FEMS Microbiol Lett 326:2-11.

196. Igo MM, Ninfa AJ, Stock JB, Silhavy TJ. 1989. Phosphorylation and dephosphorylation of a bacterial transcriptional activator by a transmembrane receptor. Genes Dev 3:1725-34.

197. Laub MT, Biondi EG, Skerker JM. 2007. Phosphotransfer profiling: systematic mapping of two-component signal transduction pathways and phosphorelays. Methods Enzymol 423:531-48.

198. Gao R, Stock AM. 2009. Biological insights from structures of two-component proteins. Annu Rev Microbiol 63:133-54.

199. Gao R, Stock AM. 2010. Molecular strategies for phosphorylation-mediated regulation of response regulator activity. Curr Opin Microbiol 13:160-7.

200. Shin D, Lee EJ, Huang H, Groisman EA. 2006. A positive feedback loop promotes transcription surge that jump-starts Salmonella virulence circuit. Science 314:1607-9.

201. Yeo WS, Zwir I, Huang HV, Shin D, Kato A, Groisman EA. 2012. Intrinsic negative feedback governs activation surge in two-component regulatory systems. Mol Cell 45:409-21.

202. Matsubara M, Kitaoka SI, Takeda SI, Mizuno T. 2000. Tuning of the porin expression under anaerobic growth conditions by his-to-Asp cross-phosphorelay through both the EnvZ-osmosensor and ArcB-anaerosensor in Escherichia coli. Genes Cells 5:555-69.

203. Howell A, Dubrac S, Noone D, Varughese KI, Devine K. 2006. Interactions between the YycFG and PhoPR two-component systems in Bacillus subtilis: the PhoR kinase phosphorylates the non-cognate YycF response regulator upon phosphate limitation. Mol Microbiol 59:1199-215.

204. Rabin RS, Stewart V. 1993. Dual response regulators (NarL and NarP) interact with dual sensors (NarX and NarQ) to control nitrate- and nitrite-regulated gene expression in Escherichia coli K-12. J Bacteriol 175:3259-68.

205. Drepper T, Wiethaus J, Giaourakis D, Gross S, Schubert B, Vogt M, Wiencek Y, McEwan AG, Masepohl B. 2006. Cross-talk towards the response regulator NtrC controlling nitrogen metabolism in Rhodobacter capsulatus. FEMS Microbiol Lett 258:250-6.

206. Mika F, Hengge R. 2005. A two-component phosphotransfer network involving ArcB, ArcA, and RssB coordinates synthesis and proteolysis of sigmaS (RpoS) in E. coli. Genes Dev 19:2770-81.

207. Stauff DL, Skaar EP. 2009. Bacillus anthracis HssRS signalling to HrtAB regulates haem resistance during infection. Mol Microbiol 72:763-78.

208. Bearson BL, Bearson SM. 2008. The role of the QseC quorum-sensing sensor kinase in colonization and norepinephrine-enhanced motility of Salmonella enterica serovar Typhimurium. Microb Pathog 44:271-8.

209. Bearson BL, Bearson SM, Lee IS, Brunelle BW. 2010. The Salmonella enterica serovar Typhimurium QseB response regulator negatively regulates bacterial motility and swine colonization in the absence of the QseC sensor kinase. Microb Pathog 48:214-9.

210. Wu H, Mao F, Olman V, Xu Y. 2007. Hierarchical classification of functionally equivalent genes in prokaryotes. Nucleic Acids Res 35:2125-40.

211. Kaye KS, Pogue JM, Tran TB, Nation RL, Li J. 2016. Agents of Last Resort: Polymyxin Resistance. Infect Dis Clin North Am 30:391-414.

212. Murphy KC, Campellone KG. 2003. Lambda Red-mediated recombinogenic engineering of enterohemorrhagic and enteropathogenic E. coli. BMC Mol Biol 4:11.

213. Clarke MB, Sperandio V. 2005. Transcriptional autoregulation by quorum sensing Escherichia coli regulators B and C (QseBC) in enterohaemorrhagic E. coli (EHEC). Mol Microbiol 58:441-55.

214. Nelson DL, Kennedy EP. 1971. Magnesium transport in Escherichia coli. Inhibition by cobaltous ion. J Biol Chem 246:3042-9.

215. Kato A, Chen HD, Latifi T, Groisman EA. 2012. Reciprocal control between a bacterium's regulatory system and the modification status of its lipopolysaccharide. Mol Cell 47:897-908.

216. Wosten MM, Kox LF, Chamnongpol S, Soncini FC, Groisman EA. 2000. A signal transduction system that responds to extracellular iron. Cell 103:113-25.

217. Perez JC, Groisman EA. 2007. Acid pH activation of the PmrA/PmrB two-component regulatory system of Salmonella enterica. Mol Microbiol 63:283-93.

218. Gunn JS, Miller SI. 1996. PhoP-PhoQ activates transcription of pmrAB, encoding a two-component regulatory system involved in Salmonella typhimurium antimicrobial peptide resistance. J Bacteriol 178:6857-64.

219. Kox LF, Wosten MM, Groisman EA. 2000. A small protein that mediates the activation of a two-component system by another two-component system. EMBO J 19:1861-72.

220. Minagawa S, Ogasawara H, Kato A, Yamamoto K, Eguchi Y, Oshima T, Mori H, Ishihama A, Utsumi R. 2003. Identification and molecular characterization of the Mg2+ stimulon of Escherichia coli. J Bacteriol 185:3696-702.

221. Kostakioti M, Hadjifrangiskou M, Cusumano CK, Hannan TJ, Janetka JW, Hultgren SJ. 2012. Distinguishing the contribution of type 1 pili from that of other QseB-misregulated factors when QseC is absent during urinary tract infection. Infect Immun 80:2826-34.

222. Lee LJ, Barrett JA, Poole RK. 2005. Genome-wide transcriptional response of chemostat-cultured Escherichia coli to zinc. J Bacteriol 187:1124-34.

223. Zhou L, Lei XH, Bochner BR, Wanner BL. 2003. Phenotype microarray analysis of Escherichia coli K-12 mutants with deletions of all two-component systems. J Bacteriol 185:4956-72.

224. Chen HD, Jewett MW, Groisman EA. 2011. Ancestral genes can control the ability of horizontally acquired loci to confer new traits. PLoS Genet 7:e1002184.

225. Merighi M, Septer AN, Carroll-Portillo A, Bhatiya A, Porwollik S, McClelland M, Gunn JS. 2009. Genome-wide analysis of the PreA/PreB (QseB/QseC) regulon of Salmonella enterica serovar Typhimurium. BMC Microbiol 9:42.

226. Kato A, Latifi T, Groisman EA. 2003. Closing the loop: the PmrA/PmrB two-component system negatively controls expression of its posttranscriptional activator PmrD. Proc Natl Acad Sci U S A 100:4706-11.

227. Tamayo R, Prouty AM, Gunn JS. 2005. Identification and functional analysis of Salmonella enterica serovar Typhimurium PmrA-regulated genes. FEMS Immunol Med Microbiol 43:249-58.

228. Miller SI, Kukral AM, Mekalanos JJ. 1989. A two-component regulatory system (phoP phoQ) controls Salmonella typhimurium virulence. Proc Natl Acad Sci U S A 86:5054-8.

229. Schröder I, Wolin CD, Cavicchioli R, Gunsalus RP. 1994. Phosphorylation and dephosphorylation of the NarQ, NarX, and NarL proteins of the nitrate-dependent two-component regulatory system of Escherichia coli. J Bacteriol 176:4985-92.

230. Guckes KR, Breland EJ, Zhang EW, Hanks SC, Gill NK, Algood HM, Schmitz JE, Stratton CW, Hadjifrangiskou M. 2017. Signaling by two-component system noncognate partners promotes intrinsic tolerance to polymyxin B in uropathogenic Escherichia coli. Sci Signal 10.

231. West AH, Stock AM. 2001. Histidine kinases and response regulator proteins in two-component signaling systems. Trends Biochem Sci 26:369-76.

232. Mizuno T. 1997. Compilation of all genes encoding two-component phosphotransfer signal transducers in the genome of Escherichia coli. DNA Res 4:161-8.

233. Zschiedrich CP, Keidel V, Szurmant H. 2016. Molecular Mechanisms of Two-Component Signal Transduction. J Mol Biol 428:3752-75.

234. Khetrapal V, Mehershahi K, Rafee S, Chen S, Lim CL, Chen SL. 2015. A set of powerful negative selection systems for unmodified Enterobacteriaceae. Nucleic Acids Res 43:e83.

235. Wright KJ, Seed PC, Hultgren SJ. 2005. Uropathogenic Escherichia coli flagella aid in efficient urinary tract colonization. Infect Immun 73:7657-68.

236. Capra EJ, Perchuk BS, Skerker JM, Laub MT. 2012. Adaptive mutations that prevent crosstalk enable the expansion of paralogous signaling protein families. Cell 150:222-32.

237. Barák I, Muchová K. 2013. The role of lipid domains in bacterial cell processes. Int J Mol Sci 14:4050-65.

238. López D, Kolter R. 2010. Functional microdomains in bacterial membranes. Genes Dev 24:1893-902.

239. Skerker JM, Perchuk BS, Siryaporn A, Lubin EA, Ashenberg O, Goulian M, Laub MT. 2008. Rewiring the specificity of two-component signal transduction systems. Cell 133:1043-54.

240. Buelow DR, Raivio TL. 2010. Three (and more) component regulatory systems - auxiliary regulators of bacterial histidine kinases. Mol Microbiol 75:547-66.

241. Jung K, Fried L, Behr S, Heermann R. Histidine kinases and response regulators in networks. Curr Opin Microbiol 15:118-24.

242. Goryshin IY, Jendrisak J, Hoffman LM, Meis R, Reznikoff WS. 2000. Insertional transposon mutagenesis by electroporation of released Tn5 transposition complexes. Nat Biotechnol 18:97-100.

243. Ream DC, Bankapur AR, Friedberg I. 2015. An event-driven approach for studying gene block evolution in bacteria. Bioinformatics 31:2075-83.

244. Anderson RP, Roth JR. 1977. Tandem genetic duplications in phage and bacteria. Annu Rev Microbiol 31:473-505.

245. Starlinger P. 1977. DNA rearrangements in procaryotes. Annu Rev Genet 11:103-26.

246. Bratlie MS, Johansen J, Sherman BT, Huang dW, Lempicki RA, Drabløs F. 2010. Gene duplications in prokaryotes can be associated with environmental adaptation. BMC Genomics 11:588.

247. Rajan KS, Davis JM, Colburn RW. 1971. Metal chelates in the storage and transport of neurotransmitters: interactions of metal ions with biogenic amines. J Neurochem 18:345-64.

248. Lukjancenko O, Wassenaar TM, Ussery DW. 2010. Comparison of 61 sequenced Escherichia coli genomes. Microb Ecol 60:708-20.

249. Povolotsky TL, Hengge R. 2015. Genome-based comparison of c-di-GMP signaling in pathogenic and commensal Escherichia coli strains. J Bacteriol.

250. Joensen KG, Tetzschner AM, Iguchi A, Aarestrup FM, Scheutz F. 2015. Rapid and Easy In Silico Serotyping of Escherichia coli Isolates by Use of Whole-Genome Sequencing Data. J Clin Microbiol 53:2410-26.

251. Breland EJ, Zhang EW, Bermudez T, Martinez CR, Hadjifrangiskou M. 2017. The histidine residue of QseC is required for canonical signaling between QseB and PmrB in uropathogenic Escherichia coli. J Bacteriol.

252. Sandegren L, Andersson DI. 2009. Bacterial gene amplification: implications for the evolution of antibiotic resistance. Nat Rev Microbiol 7:578-88.

253. Reigstad CS, Hultgren SJ, Gordon JI. 2007. Functional genomic studies of uropathogenic Escherichia coli and host urothelial cells when intracellular bacterial communities are assembled. J Biol Chem 282:21259-67.

254. Curtis MM, Russell R, Moreira CG, Adebesin AM, Wang C, Williams NS, Taussig R, Stewart D, Zimmern P, Lu B, Prasad RN, Zhu C, Rasko DA, Huntley JF, Falck JR, Sperandio V. 2014. QseC inhibitors as an antivirulence approach for Gram-negative pathogens. MBio 5:e02165.

255. Rasko DA, Moreira CG, Li de R, Reading NC, Ritchie JM, Waldor MK, Williams N, Taussig R, Wei S, Roth M, Hughes DT, Huntley JF, Fina MW, Falck JR, Sperandio V. 2008. Targeting QseC signaling and virulence for antibiotic development. Science 321:1078-80.

256. Hirakawa H, Inazumi Y, Masaki T, Hirata T, Yamaguchi A. 2005. Indole induces the expression of multidrug exporter genes in Escherichia coli. Mol Microbiol 55:1113-26.